DEVELOPMENT OF A NOVEL IN VITRO MODEL TO STUDY THE TRYPTIC: ENDOTHELIAL CELLS, MONOCYTES AND FLOW

By

Alexis S. Turjman

M.S. in Mechanical Engineering and Materials Science
from Arts & Métiers ParisTech, 2009

SUBMITTED TO THE DEPARTMENT OF MATERIALS SCIENCE AND ENGINEERING
IN PARTIAL FULFILLMENT OF THE REQUIREMENTS FOR THE DEGREE
OF

DOCTOR OF PHILOSOPHY
AT THE
MASSACHUSETTS INSTITUTE OF TECHNOLOGY

SEPTEMBER 2014

Signature redacted

Signature of author.....
Department of Materials Science and Engineering
August 12, 2014

Signature redacted

Certified by.....
Elazer R. Edelman, M.D., PhD.
Thomas and Virginia Cabot Professor of Health Sciences and Technology, MIT
Thesis supervisor

Signature redacted

Certified by.....
Guillermo García-Cardeña, PhD.
Associate Professor of Pathology, Harvard Medical School
Thesis supervisor

Signature redacted

Accepted by.....
Gerbrand Ceder
R. P. Simmons Professor of Materials Science and Engineering, MIT
Chair, Departmental Committee on Graduate Students

DEVELOPMENT OF A NOVEL IN VITRO MODEL TO STUDY THE TRYPTIC: ENDOTHELIAL CELLS, MONOCYTES AND FLOW

By

Alexis S. Turjman

Submitted to the Department of Materials Science and Engineering on August 5, 2014 in Partial Fulfillment of the Requirements for the Degree of Doctor of Philosophy in Materials Science and Engineering.

Advisors: Elazer R. Edelman, Thomas and Virginia Cabot Professor of Health Sciences and Technology, MIT.

Guillermo García-Cardeña, Associate Professor of Pathology, Harvard Medical School

Thesis committee:

1. Michael J. Cima, David H. Koch Professor of Engineering, Sumitomo Electric Industries Professor of Engineering, MIT.
2. Darrell J. Irvine, Professor of Materials Science and Engineering & Biological Engineering, MIT.

ABSTRACT

This thesis describes the development of a novel in vitro model of monocytes transmigration under flow and use in the study of early molecular events of atherogenesis. In this work, we focused on how endothelial dysfunction, specifically mediated by disturbed flow from atherosusceptible regions of the vasculature, is both communicated to recruited monocytes as they reside in the subendothelial matrix, and how reciprocally, monocytes may exacerbate the endothelial dysfunctional state.

We built and integrated our *in vitro* model to a unique flow apparatus that can precisely replicate atheroprone and atheroprotective shear stress waveforms. We carefully characterized the model that relies on a fibronectin-coated collagenous matrix seeded with a confluent monolayer of endothelial cells co-cultured with THP-1 monocytes under flow. We used the model to draw biological insight from endothelial:monocyte co-cultures under flow. We found that monocytes preferentially accumulate on endothelial monolayers exposed to atheroprone flow. We also observed the upregulation of IL-1β in endothelial cells exposed to atheroprone flow when co-cultured with monocytes but not in endothelial cells alone, in each of three independent experiments; yet the aggregated results are not statistically relevant due to variability.

Flow-driven dysfunctional endothelium recruits and interacts with monocytes that soon after transmigration become dysfunctional foam cells. Our novel *in vitro* model that congregates endothelial cells, monocytes and flow responds to the pressing need to understand the interplay between these protagonist cells during

atherogenesis, and allowed us to define further monocyte- and flow-mediated transition of endothelium from normal to dysfunctional to diseased states. Harnessing the power of a versatile platform of transmigration under flow may foster the discovery of novel targets for atherogenesis and the development of original therapeutic strategies.

To my parents, Carole and Francis,
and my brother, Clément.

ACKNOWLEDGEMENTS

I express my deepest gratitude and appreciation to my mentors and research advisors Dr. Elazer R. Edelman and Dr. Guillermo García-Cardeña for their exceptional guidance, for sharing their exquisite knowledge with patience and building with me an exciting project at the frontier of vascular biology and engineering. I also want to thank them for their kindness, openness and understanding throughout the program. Both Elazer and Guillermo are bright scholars with exceptional minds and incredibly broad knowledge in biology and medicine but more importantly great family men. Each one in their own way has shaped my vision of the field and has helped me grow as a scientist, yet, it is their many teachings about life, wisdom and moral compass that helped me grow as a person and will remain the most profoundly anchored inside me. For all of these reasons, I am forever indebted to them and I wish that one day I can resemble them.

I want to genuinely thank the other members of my thesis committee, namely Dr. Michael Cima and Dr. Darrell Irvine, for keeping me focused on my goals and bringing their invaluable perspective to the project. Their continued encouragements and technical expertise has catalyzed the refinement of my thesis subject and sped up the research. In addition, Darrell and Michael are generous people with whom it is always possible to have a good laugh, which makes working with them a real pleasure.

Next, I want to acknowledge the outstanding teaching of my professors in the Department of Materials Science and Engineering: Dr. Gerbrand Ceder whose great sense of humor is only second to his mastery of thermodynamics and quantum mechanics, Dr. Michael Demkowicz who knows how to communicate his passion for the rigorous application of mechanics to students and Dr. Samuel Allen. I also would like to thank Dr. Michael Gimbrone (always ready to suggest a good Italian restaurant in Boston!) and Dr. Roger Kamm who both provided encouragements and with whom I had fascinating scientific discussions. I thank Dr. Ajay Wakhloo and Dr. Lionel Collet for their support.

This project would not have been possible without the support of my colleagues and friends. The Edelman and García-Cardeña laboratories are stimulating environments that foster scientific discovery through collaborative work and camaraderie. I dearly thank Ayumi Miyakawa for her caring mentorship inside and outside the laboratory and for training me as a vascular biologist. Ayumi is one of the kindest and most generous person I have met during my Ph.D. and an extraordinary woman who I am proud to be friends with. I thank Joseph Frances and Konstantinos Koskinas for their "big-brother's" advice and continued friendship. I am grateful for the patient training and scientific advice from Andrew Koo, William Adams and Hiroshi Kohara. I also want to fondly thank my cheerful lab mates Pauline De Jong, Bendix Slegtenhorst and Floris Voskuil for teaching me rudimentary Dutch and sharing their love for pannekoeken, stroopwafel and ice-skating. I also thank Kumaran Kolandaivelu Vijaya Kolachalama, Juliana Dreyfuss,

Laura Indolfi, and Tarek Shazly. In addition I wish to thank people who made our lives at the laboratory a safe and efficient place: Melissa St-Pierre, Yuzhi Zhang, Kay Case, Vannessa Davis and Luz Montilla. The 7th floor at NRB would not be the same without παππούς, the famous and affectionate George Stavrakis who grumpiness is second to none. We shared amazing moments of laughter.

As life outside the laboratory is at least as important as life inside the laboratory, my friends' support was instrumental in keeping a balanced life and good spirit. In this regard, I must say ευχαριστώ πολύ to the Scrivanos family especially Peter, Nectaria, George, Spiros and their parents for providing a home far away from home, feeding me with delicious Greek food and inviting me to many joyous celebrations. Peter is an extraordinary friend: he is a truly gifted person with a big heart. Only him would make me laugh so hard that I could forget any bad day or experiment that failed. Philipp Robbel and Hussam Busfar are also two exceptional friends. They are loyal and cheerful friends who brought much excitement to my life and with whom I share the best memories. All four of us had the best time at Liberty (almost to the point that I should give credit to Liberty for my well-being...). My dear friends Thibault Prévost-Monfort, Jonathan-Lionel Kluberg, Maxime "Maxou" Cohen, Audren Cloitre, Michael "Michel" Chemama, Elizabeth Rapoport, Jonah Bernstein, Alexandre "Boubou" Bouaziz, David "DPZ" Puyraimond-Zemmour, Luis Voloch, Gal Shulkind, Eleni and Yiannis Granas, Eleni and Ioannis Zervantonakis, Sacha and Ora Zyto, Veronica Azcutia Criado, Eva Ieronimaki and Spyros Zoumpoulis, Sara Agosta, Egle Spano and so many others are invaluable people that I keep close to my heart. I will not forget our many celebrations together and your sincere affection and enthusiastic support. I must thank the Panamanians at large for inviting me to so many Shabbat dinners and parties in Etna: you rock, chuchonitos; their kindness and generosity is infinite. The list of people is too long to spell out entirely but I want to thank in particular Jaime Cohen and his family for their encouragements and treating me graciously while in Panama. The help, advice and cheers from Jacques Bojin and David Znaty were a real motivation to come to MIT. Last, I need to thank Rabbis Dov Berish Ganz, Aaron Hamaoui, Hirschy Zarchi and Shmuel Posner and their families for their spiritual guidance and for always opening their doors during Jewish Holidays.

As always in my life, everything circles back to my family: my mom Carole, my dad Francis and my brother Clément. They deserve my deepest gratitude for their unconditional support and love. They have educated me with righteous moral values and covered me with affection. I thank them for being by my side during the tough times as well as the festive moments of my life. This work is dedicated to them; I could not have done it without them. I address a special and loving thank you to my grandmother *"Mamie Suzy"* who brightened my day so many times by calling me and sending me periodically packages filled with homemade pastries, presents or tomato-sauce tuna cans that I could not find at the local grocery store!

TABLE OF CONTENTS

TABLE OF FIGURES

1 Introduction

1.1 Arterial structure and function

1.1.1 Physiology of the cell

Cells are living organisms that are delimited into space by a membrane and perform certain functions such as self-replication, energy generation, the performance of various chemical reactions using and producing compounds. They are the building units of complex organisms and require energy in order to maintain a viable state. Energy in organisms is drawn from catabolism and cell respiration, the breakdown and oxidation of large molecules of the chemical reactions of catabolism. These biochemical reactions provide the cell with the energy needed to perform cellular functions, maintain its integrity and respond to environmental cues.

1.1.2 Carriage of oxygen and nutrient and disposal of by products

During development, complex organisms accrue their number of cells through cell division, grow in size and in mass. Although the delivery of nutrients and oxygen can be achieved through diffusion until a certain size, the critical value of ~200 μm [1, 2] is quickly attained and diffusion-based growth is no longer compatible with the metabolism of the organism that transitions to a convection plus diffusion mechanism: this is the role of the circulatory system. As an order of magnitude, the body of an adult human is constituted of about 100 trillion cells, which all depend on a convoluted network of arteries and veins to provide critical nutrients and oxygen to the tissue while remove waste.

1.1.3 Morphology of the vessels

Microstructure Large arteries are tubes composed of three coaxial layers that assume a myriad of roles in the sustenance of life. One of the most important and obvious ones is to contain and channel the blood to the various organs, but this obvious function has been gradually overshadowed by the more complex and global machinery that probes the biochemical and hemodynamic environments and, adapt and repairs the circulatory system, as vascular research

advanced. The three layers of the large and medium size arteries are: 1) the *tunica intima* 2) the *tunica media* and 3) the *adventitia* (Figure 1.1).

The *tunica intima* is a one-cell thick layer that lines the inner surface of blood vessel and is composed of tightly linked adjacent endothelial cells that pave the vessel wall. The endothelial cells sit on the basement membrane, extracellular matrix and the internal elastic lamina that circumscribes the intima from the media. The *tunica media* is a muscular layer composed essentially of phalanges of smooth muscle cells grouped in packets surrounded by connective tissue that control the tone of the vessel. Under stimulation with nitric oxide (NO), prostacyclin or prostaglandins, the media can relax within seconds and allow vasodilation when tissues need increased blood flow. The third and outmost layer of arteries is the *tunica adventitia* that is mainly composed of collagen and fibroblasts and that anchors the artery to the surrounding tissue of the viscera. The *adventitia* is separated from the *media* by the external elastic lamina. The cells of large vessels themselves need perfusion, supplied by the vasa vasorum, literally "vessels of the vessels". The *vasa vasorum* either originates from the outer tunic in which case it is referred to *vasa vasorum externa*, or inner tunic, giving rise to the *vasa vasorum interna*. In addition to capillaries, the vessels are innervated by the *nervi vascularis*.

As we will see in later in this Chapter, the microenvironment of the cells, especially the endothelial cells has profound implications on its state and phenotype. The extracellular matrix separating the endothelium from the media is composed of several major macromolecules such as elastin and collagen. The internal elastic lamina of the aorta is dominated by collagen type III and I. Yet, the extracellular matrix of vessels is a dynamic interface modulated by many environmental cues that affect the state of the surroundings cells. This is extremely relevant to the study of cardiovascular diseases because as the lesion develops, the microstructure of the vessel is remodeled. Throughout the pathogenesis of atherosclerosis the composition, abundance and structure of the extracellular matrix changes; endothelial cells are sensitive to these changes, which influence their state.

Exchanges The blood is the fluid used by the human body to carry the oxygen and the nutrients necessary to the cell functions. The exchanges between the blood and the tissue are mainly carried through diffusion. Hence to be most efficient, the interface between blood and tissue should be maximal. The surface-to-volume ratio of a cylinder of radius R and height h is $2\pi*R*h/(\pi*R\hat{}2*h)$, which varies with the inverse of the radius of the cylinder. Thus vessels with large surface-to-volume ratios are particularly suited for this task since they provide a high interfacial density. Theses vessels are called the capillaries and are composed of endothelial cells surrounded by pericytes. They are typically in the range of 5 to 10 μm in diameter. This is small enough that the erythrocytes that carry oxygen have to deform when going through the capillaries. The network of capillaries is highly parallel meaning that large arteries branch out many times before becoming capillaries and connecting to the venous circulation. The development of a parallel circulatory system is supported by energy and safety considerations. Indeed, if the circulatory system was linear then any disruption of the flow would cause all tissues and organs distal to the blockage to suffer from ischemia. The analogy with the design of the electrical grid illustrates well the point. The electrical grid is designed in parallel from the power source to avoid massive disruption of service, similarly, a semi-parallel vascular network secures the supply of blood to parallel patent branches even if one of them is occluded.

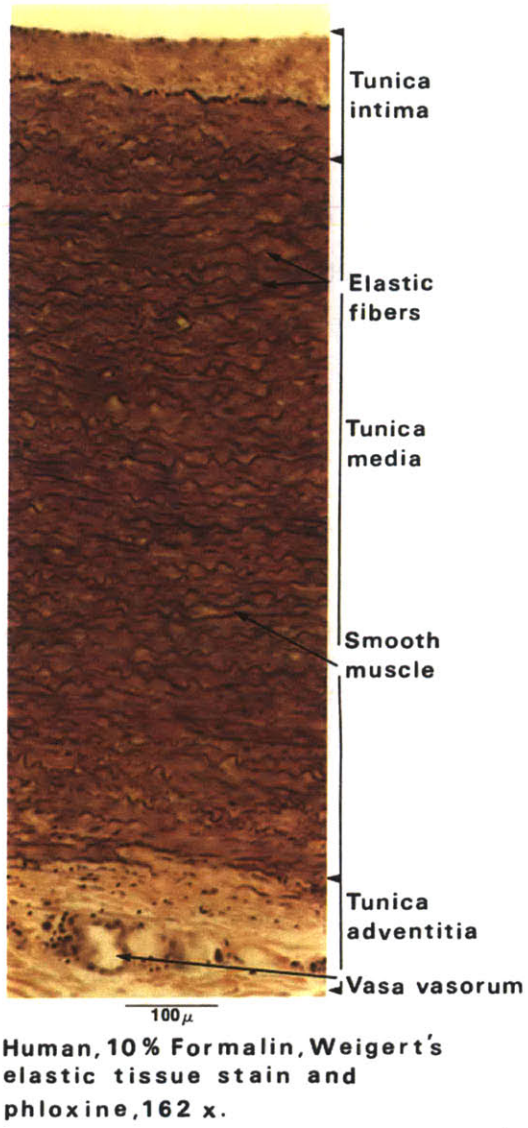

Figure 1.1: Ultrastructure of the human aorta.

Histological section showing the trilaminate architecture of the human aorta. From the lumen to the periphery, three tunics can be delineated: the intima, the media and the adventitia [3].

1.1.4 Distinct hemodynamic environments throughout the body

The circulatory system is a complex network of vessels that branch out at numerous bifurcations creating variable hemodynamic profiles throughout the body. In the previous paragraphs, we explained some of the evolutionary reasons that lead to this complex circuitry. Here we combine this list and summarize.

Humans have developed with one organ, the heart, to propel blood – a liquid – to the organs. As the vast majority of animals, humans have a high degree of bilateral symmetry – however some internal organs such as the heart, liver or digestive track are not symmetrical with respect to the sagittal plane – and their delivery system of oxygen and nutrients is based on convection and diffusion. Those two considerations, combined to the safety advantages of a parallel circulatory system over a linear one, have forced the evolution towards an anatomy dominated by a central vessel, the aorta, that ramifies into large arteries, medium arteries and capillaries to irrigates organs.

Characteristics of flows Flowing blood applies three types of stress on the vascular bed: pressure, which acts normal to the lumen and can affect the physiology of the endothelium and the tension of the smooth muscle cells (SMC) creating at the same time cyclic stress due to the increase in diameter of the vessel during the cardiac cycle, and wall shear stress or endothelial shear stress. Wall shear stress corresponds to the force per unit area applied by the blood in a direction tangential to the wall; it is also defined as the product of viscosity, the friction between layers of the flow with different velocities, and shear rate (Figure 1.2). In general and when parabolic flow dominates blood flow can be considered as a series of parallel flow lines whose velocity is maximal at the centerline and zero at the walls. The change in velocity follows inversely, maximum at the walls and zero at the centerline. Shear rate describes the rate by which the velocity changes as a distance from the wall. Wall shear stress and rate computed from the derivation of velocities throughout the fluid domain are particularly interesting in the study of vascular diseases as endothelial cells respond to variations in wall shear stress, eliciting different phenotypes and biological processes.

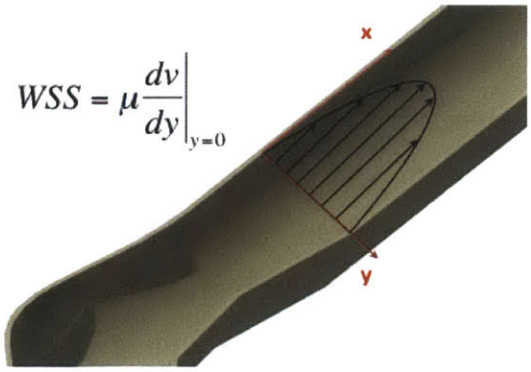

Figure 1.2: Physical definition of wall shear stress

Blood flood applies two types of stress on the vessels; pressure directed perpendicular to the vessel wall and wall shear stress that is tangential to the wall and is the consequence of frictional forces of the fluid onto the surface due to viscosity. The diagram illustrates the calculation of wall shear stress (WSS). It shows a typical velocity profile for a straight vascular segment. The slope of the tangent of the velocity distribution at the origin (grey line) is proportional to the WSS. Flows that are highly variable in velocity close to the wall have a high wall shear stress, whereas shallow velocity distributions will correspond to low WSS. Of notice, WSS is a dynamic value that evolves with time similarly to velocities during the cardiac cycle.

Means of quantifying flow parameters Computational fluid dynamics (CFD) is one of the major techniques used to quantify the motion, frictional forces and other characteristics of flows. Compared to direct measurements CFD has the advantage of being non-invasive and once the geometry and boundary conditions are measured the computational time does not require the patient to be present. CFD emerged in the 1930s as a branch of fluid mechanics to solve problems too complex for analytical solutions. CFD is based on the strategic partition of a fluid domain into small elements, usually tetrahedrons or hexahedrons. The equations that define fluid mechanics in each element provide neighboring elements with boundary conditions for their equations of state and when coupled, provide an integrated view of the fluid dynamics of the system. The quality of the results depend on many parameters including the partitioning strategy and number of

elements used to divide the fluid domain, the original boundary conditions, the algorithm used to solve the equations and the time steps between each calculation, in the case of a time-dependent simulation. As discussed in detail later in this section, the geometry of the vasculature, the fluid boundary conditions, the constitutive laws describing the vessel rigidity and blood, collectively determine the degree of precision of the solution and extra care should be taken to generate a solution that matches the level of understanding of the biological phenomenon studied.

Parameters and sensitivity of flow simulation in biology The overall relevance of CFD depends on the definition of the boundary conditions: the geometry describing the arterial wall, the inflow and outflow conditions and the model used to describe the behavior of the blood. CFD is a tool and one should not expect that the precision of the simulation will be greater than the precision of the input values or constitutive models. The CFD procedure to model flow in a vessel begins with the reconstruction of the geometry of the lumen obtained from a range of medical imaging modalities. The gold standard is rotational angiography, which produces a series of contrast maps defining the fluid volume. Angiography is often used in concert with iodine-based contrast agents that increase the quality and contrast of the images. Software is used to segment and stack together sequential images, and then clean and smooth the volume. The most delicate steps in setting up a CFD analysis are adequately meshing the fluid domain and prescribing the fluid boundary conditions. See the example of a mesh used to compute the flow characteristics in branches of the internal carotid artery (ICA, Figure 1.3). An ideal mesh should be fine enough such that increasing the number of elements does not affect the solution of the problem. Detailed procedures and information are available in Finite element procedure by K. J. Bathe [4].The precision and relevance of the waveforms/flow rates imposed at inlets and outlets are the subject of debate. Options include phase-contrast MRI, Doppler or intravascular ultrasound (IVUS) velocimetry. MRI gives the most precise information as it yields a map of velocities in a section of the vessel. Practically, phase-contrast MRI can difficult to obtain in a

clinical setting because it often extends the diagnostic time, so it is not always available. Alternatively, one can compute the Womersley profiles at the inlet from the waveform of the flow rate, which correspond to the analytic solution for this specific waveform in a straight pipe of the same diameter than the inlet.

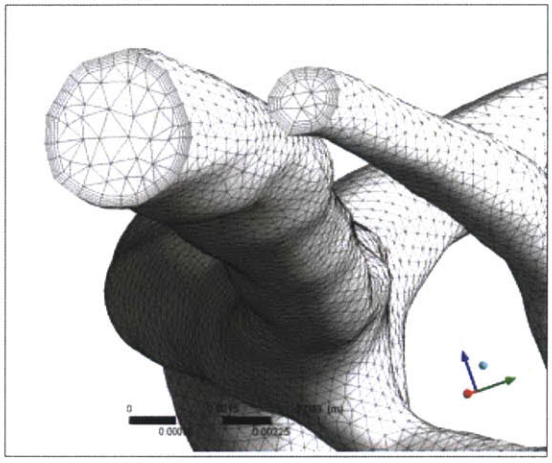

Figure 1.3: Meshing of a reconstructed artery before CFD analysis.

Example of meshed volume with tetrahedron, pentahedron and hexahedron elements. Sequential images of the bifurcation of the ICA were acquired with angiography, segmented and reconstructed. The volume was meshed with ANSYS Fluent (Canonsburg, PA).

The reconstruction of the arterial geometry is crucial as real images rarely delineate a clean border between tissue and blood; thus, image segmentation and smoothing is left to the judgment of the operator. This is all the more important as such considerations freeze the geometry, impacting subsequent results. If the artery is distensible, the use of a model that correctly takes into account the deformation of the vessel during the cardiac cycle is important. For the in vitro model that we will describe later, we used flow waveforms derived from 1) the carotid sinus and 2) a straight segment of the internal carotid artery. To account for the deformation the vessel, the vessel was modeled with a nonlinear, isotropic, hyperelastic material. This class of computational simulations that takes both into account the dynamics of the fluid and the boundaries are called Fluid Structure Interaction (FSI) models. The

solving algorithm not only iterates on the equations ruling fluid dynamics but also considers the fluid forces deforming the walls of the model and adjusts the geometry and iterates back on the equations of fluid mechanics. FSI is currently the most accurate way to derive flow parameters such as the velocity vector field, shear stress or shear gradient.

Fluid boundary conditions include evaluation of the flow inlets and outlets. Classically, inlets are set to drive the simulation by specifying the velocity or flow rate in a cross-section, while outlets insure the continuity of the flow through setting the exit pressure. Ideally, phase contrast-MRI at the inlet and pressure measurements at the outlet, in the same patient, should be used for maximal precision. Yet, phase contrast-MRI is not a panacea, it is highly dependent on the parameters specified for acquisition and the range of velocities that can be tracked is limited. Thus, heterogeneous flows have larger uncertainty and may require extrapolation of the velocity distribution near the wall. Fortunately, the characteristics of the flow change as it develops in the vasculature, decreasing its dependence on the boundary condition away from the inlet; consequently, it is key to keep enough length before the region of interest.

Blood is a viscous fluid, described with classical Newtonian physics, but more appropriately considered with more complex models [5]. Carreau-Yasuda or Casson approximations offer a more general framework, allowing viscosity to vary with the shear rate [6]. Rheological effects can be important depending on the geometry. Newtonian models can degrade the results of the simulation, while Casson models do not significantly burden computational cost.

The trend in CFD is to bring additional physiological relevance and complexity to the models and boundary conditions, in particular, to circumvent the rigid wall assumption. FSI takes into account a model of deformation of the wall to constantly iterate on the mechanical model of the artery to make the geometry current – pulses of flow induce the dilation of the vasculature. The challenges that remain are to

obtain more precise and appropriate experimental data on the mechanics and patient-specific topology of the wall to drive the models proposed.

CFD is a valuable tool because of the dearth of adequate in vivo imaging that can reliably measure flow parameters such as WSS, but as a sensitive tool, requires careful selection of boundary conditions. General mechanistic processes, such as mechanotransduction, need only low precision and averages, as they seek to reach global conclusions. Case-specific problems, such as the destabilization of the atheromatous plaque or aneurysmal cavities, are in contrast highly dependent on the level of details. In conclusion, the precision of CFD should match the level of understanding required to derive mechanistic insight.

The hemodynamic stress applied to the vessel drastically change throughout the vasculature. The diagram in Figure 1.4 shows the computed average WSS in the aortic arch of a mouse [7]. The color-coded map highlights clearly the spatial variations in WSS, especially between the lower curvature of the arch or parts of the bifurcations (blue, low intensity) and the median or higher curvature (green/red, high intensity).

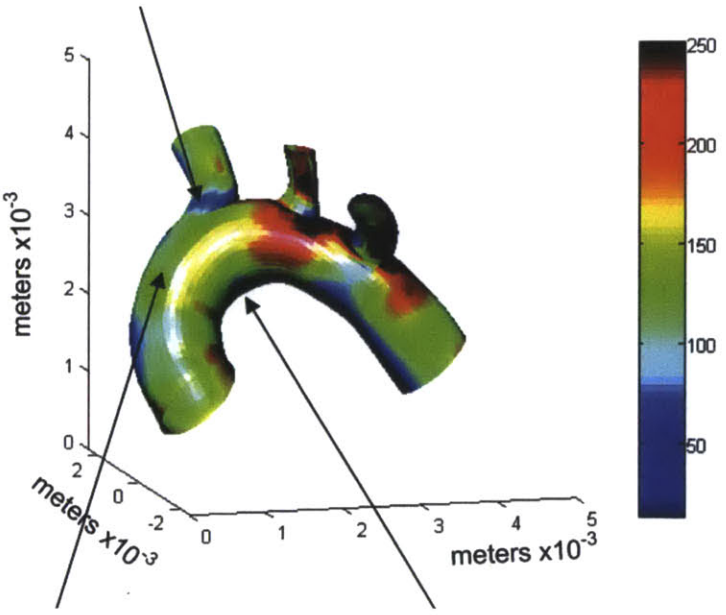

Figure 1.4: The lower curvature of the aorta and the adjacent branches are subjected to disturbed blood flow.

Map of the time-average intensity of wall shear stress in a mouse aorta quantified from CFD. The colors indicate the level of wall shear stress in dynes/cm^2. The arrows show regions of the arch with distinct flow patterns [7].

A similar observation can be made in the human vasculature: shear stress varies both spatially and with time. Figure 1.5 shows a CFD analysis of a healthy volunteer with no history of cardiovascular diseases. The map of WSS at the bifurcation of the common carotid illustrates the variations in intensity of the shear forces in straight segments of the carotid arteries compared to the carotid sinus.

The heterogeneity in hemodynamics are particularly important to the development of cardiovascular diseases such as atherosclerosis because endothelial cells are prime sensors and responders to fluid forces. In the following sections, we will give some background on the endothelium and its multiple functions, notably in relationship to flow and leukocytes and we will explain how it relates to atherogenesis.

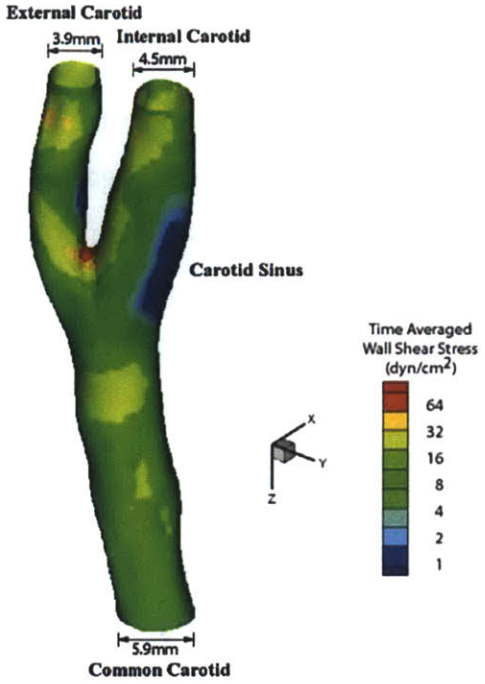

Figure 1.5: CFD analysis of the wall shear stress in the human carotid artery.

CFD analysis of the WSS of the carotid of a healthy male. Similar to the previous figure, this diagram shows a clear heterogeneity in the level of WSS between the straight parts of the arteries i.e. common carotid and internal and external carotids, and the carotid sinus (adapted from [8])

1.2 Endothelial cells

1.2.1 Discovery

Three British scientists, Henry Hyde Salter, Robert Bentley Todd and Sir William Browman, first observed and isolated the endothelial cells. The trio isolated for the first time in 1852 what they named *epithelial particles* – pointy and elongated cells with a large nucleus that align with the axis of the vessel – from the aortae of an ox and horse and published there work in *Physiological Anatomy and Physiology of Man* in 1856. Yet, Wilhelm His is credited for coining the term "endothelium" as he posited in 1865 that epithelium and endothelium have different functions and origins.

1.2.2 Characteristics

Endothelial cells pave the innermost layer of vessels as they form a monolayer that plays multiple roles in vascular homeostasis. The appearance of the endothelium is often compared to cobblestone as the cells form a confluent monolayer made from elongated cells. Each individual endothelial cell measures around 10 μm in length, by 3 μm in width and 0.5-1 μm in thickness [9] (endothelial cells are sensitive to mechanical forces such as flow, which accentuate their elongated shape as they align with the direction of the flow) and is connected to its neighboring cells by junctional molecules. The endothelium is found in three different configurations: 1) "continuous" like in most of the vasculature of large vessels or in the brain-blood barrier (central nervous system) that strictly regulates insudation of plasma molecules and circulating cells, 2) "fenestrated", characterized by small disruptions (0.1-1 μm) between endothelial cells but an intact basement membrane, like in the kidney glomeruli or 3) "discontinuous" when disruptions occur in both, endothelial junctions cells and basement membrane e.g. in the liver, spleen or bone marrow. The state of the monolayer reflects the functional requirements of the local vascular bed in terms of permeation, filtration or secretion, yet fenestrations are also observed at bifurcations, loci of intense hemodynamics stresses and gradients [10, 11]. This is all the more important that vascular lesions often occur at branching points where fenestration allows for increased exchanges between lumen and tissue.

Endothelial cells possess the same set of major organelles than other cells: a plasma membrane that delimits a cytoplasm, a nucleus anchored to the cells membrane by an actin skeleton, endoplasmic reticula, ribosomes, Golgi apparatus, mitochondria as well as some endothelial-specific organelles such as the Weibel-Palade bodies that store granules of von Willebrand factor and P-selectin and vesiculo-vacuolar organelles (VVO). In addition, a network of polysaccharides covers the apical surface of endothelial cells, in the same way that the kelp covers the seafloor. The glycocalyx is 0.2-4.5 μm thick and is composed of three major glycosaminoglycans: heparin sulfate, chondroitin sulfate and hyaluronic acid that are attached to the

transmembrane proteins. This organelle that is a charged interface, plays a key role in regulating what binds to the endothelial surface.

1.2.3 Historical perspective of endothelial function in vascular homeostasis

1.2.3.1 The endothelium as a container

The human endothelium constitutes an impressive interfacial surface of about 350 m^2 [12], yet because of its feeble thickness it only accounts for a negligible ~110g compared to the ~70kg of body mass of an adult [9]. Until the 1950, the endothelium is mainly regarded as a coating or envelope that acts as a container for the blood. Part of the disinterest for the endothelial layer was due, in part, to the limited visualization tools available at the time. To put things into perspective with the technological advances at the time, the first electron microscope was made in 1926 but only commercialized at the end of the 30s. The other hurdle that muted investigational ardor was the unavailability of an *in vitro* model. As we will see in the next paragraphs, these two limitations were overcome in the following years.

1.2.3.2 Barrier function

In 1966, Lord Henry Florey published a seminal paper that challenged the assumption of the endothelium as an inert liner between the vascular space and the interstitium but rather recognized the variety of endothelial cells states and functions and conceptualized it as an active barrier that has a major role in transporting molecules from the blood to the underlying tissue. He concludes the article by writing:

> *"In the time available, I have been able to show you a little of the current knowledge of the morphology of cells which fifteen years ago were thought to form little more than a sheet of nucleated cellophane.*
>
> *The caveolae intracellulares, which are prominent in some but not all endothelium, may facilitate the passage of substances through*

endothelium even if they function only by furnishing a greater area through which diffusion may occur. The fine structure of the interendothelial junctions may hold the key to understanding how small quantities of plasma proteins may leak out of even the most impermeable blood-vessels." Lord H. Florey [13].

This paradigm shift – from a simple wrapper to an active barrier – was one of the motors for the nascent field of vascular biology because it opened a new field of investigation that would unveil the many characteristics and functions of endothelial cells, which emerged as the central actor of vascular health or disease. Yet, another discovery was missing before the field could really develop; a practical *in vitro* model of endothelial cell was required. This milestone was achieved in the 70s when Jaffe, Nachman, Becker and Minic [14] and Gimbrone, Cotran and Folkman [15] independently reported the isolation, prolonged culture and identification of Human Umbilical Cord Endothelial Cells (HUVEC).

These concurrent discoveries propelled the field to great extent and permitted its exponential growth. A PubMed search with the terms "endothelial cells" returned respectively 229 and 487 until 1965 and 1973 when the same query returns an astonishing 150,000+ publications when the time range is up to 2014. We know today, that the endothelium is involved in virtually all the diseases either directly or indirectly [16, 17]. In the next paragraphs, we briefly highlight the major functions performed by the endothelium and explain its involvement in atherosclerosis.

1.2.3.3 Active paracrine signaling

The endothelium regulates many of the processes that maintain homeostasis, such as controlling permeability, adjusting the vascular tone, providing an anti-thrombogenic surface to the blood, creating new vessels, namely angiogenesis or mounting an inflammatory response, by paracrine secretions. Here, we summarize the major proteins that mediate these endothelial functions.

1.2.3.3.1 Permeability

The first hypotheses of the endothelium seen as a permeable surface originate from functional studies by Starling in 1896 [18], followed by the exquisite drawings and insight by Ramon y Cajal (Museum Ramón y Cajal, Madrid; Spain), and later Kohn and Cowdry and Pappenheimer [19], who laid the foundations of modern views on endothelial functions. Many of the major advances on the ultrastructure of the endothelium and the vessels could not have happened without the technical prowess and deep scientific insight of Karnovsky [20, 21], notably through his drastic improvement of cytochemical analysis of intact tissue and avant-garde methods to prepare scanning electron microscope samples. Permeability is a physical trait of a barrier or interface that quantifies the amount of matter allowed to cross the barrier. In the context of the endothelium it is characterized by the propensity of the monolayer to let plasma components intravasate or *vice versa*. The exchanges occur principally either in between the cells, via the paracellular route, or through the cell itself, via transcellular mechanisms. Both molecules and cells can be channeled through the endothelium. For molecules such as cholesterol, caveolae, which are lipid raft invagination at the surface of endothelial cells, bundles of caveolae or vesicles can regulate their passage. Concomitantly, cellular junctions that anchor one cell to its neighbors, also regulate the passage of molecules between them by building pores. The junctional molecules include claudins, occuldins, nectins, junctional adhesion molecules and Vascular Endothelial-Cadherin (VE-Cadherin). The transport of plasma cells requires a different set of molecules and will be discussed later. During atherogenesis, the increase in endothelial permeability causes lipid insudation and accumulation in the subendothelial space that is characteristic of the beginning of the lesion.

Three classes of junctional molecules are the major regulator of permeability: 1) tight junctions, including junctional adhesion molecules (JAM), occulinds and claudins, 2) gap junctions, mainly the connexins and 3) adherens junctions such as VE-Cadherin. Several secreted factors including thrombin, bradykinin, histamine and Vascular Endothelial Growth Factor (VEGF) can disrupt the organization of cell

junctions and therefore increase permeability. On the contrary, molecules such as cyclic AMP (cAMP) can improve the endothelial barrier function [22].

1.2.3.3.2 Vascular tone

The vasculature controls blood pressure by dilating or constricting the lumen of the vessels in a process that we know now is tightly regulated by the endothelium. At the beginning of the 70s however, little was known about the effectors of vasodilation. To fill this void, many vascular biologists would try to understand what causes the relaxation or constriction of smooth muscle cells. The following 15 years of research produced quantum leaps in characterizing these mechanisms, in particular, the discovery of two puissant vasodilators: prostacyclin and nitric oxide (NO), profoundly transformed the field by the breadth of their implication in vascular homeostasis.

Two years after the establishment of HUVEC as a model for endothelial cells, Gimbrone and Alexander showed that the endothelium is a source for prostaglandin, a hormone-like lipid that has implications in vasodilation, platelet aggregation and permeability [23]. Later, Sir Moncada and colleagues isolated the most potent form of prostaglandin, prostacyclin (PGI_2) [24, 25] while Furchgott and Zawadzki showed that the endothelium was necessary to the vasomotility and discovered and characterized the Endothelium-Derived Relaxation Factor as the active substance[26]. Rich from the knowledge accumulated by the forefathers of modern vascular biology, we now know that cyclooxygenase (COX), especially COX-2, catalyzes the conversion of arachidonic acid into prostaglandins; in parallel, Nitric Oxide Synthase (NOS) – and for the matter of interest to us, endothelial NOS (eNOS) – catalyzes the synthesis of NO from L-arginine in endothelial cells [27, 28]. The scope of the biology of NO is extremely wide. It ranges from vasodilation to leukocyte adhesion and is also produced by the endothelium subjected to healthy flow.

1.2.3.3.3 Anti-thrombogenic surface

Healthy endothelium provides an anti-thrombogenic surface that prevents the aggregation of plasma cells on its surface and thus is responsible for keeping the vessel patent by acting on four major mechanisms: 1) the endothelium displays tissue factor pathway inhibitors that block Factor VIIa, a serine protease involved in the initiation of the coagulation cascade; 2) the heparin sulfate of the glycocalyx tethers anti-thrombin III that inhibit thrombin molecules, another serine protease that cleaves soluble fibrinogen into insoluble fibrin; 3) the display of cell surface thrombomodulin, which binds thrombin, change its substrate from fibrinogen to Protein C and activates Protein C. Activated Protein C cleaves factors of clot formation; 4) the sequestration of von Willebrand Factor (vWF) into Weibel-Palade Bodies (WPB) that prevents vWF to bind to Factor VIII, collagen or platelets. In endothelial cells, vWF is present as multimers of over 20,000 kDa that bundle in helical arrangements. This helical packing is responsible for the cigar shape of the mature WPB that contain vWF. Upon activation of the endothelial cells, for example with thrombin, histamine, epinephrine or vasopressin, the WBP vesicles release vWF in the plasma, which acts as a carrier for Factor XIII and triggers the coagulation cascade. Exocytosis proceeds through two mechanisms: 1) lingering-kiss exocytosis where WPB vesicles merge with the plasma membrane or 2) multi-granular exocytosis, where several WBP fuse together into secretory pods before releasing amalgamate vWF [29].

1.2.3.3.4 Angiogenesis

Angiogenesis is one of the major functions of the endothelium. It is the process leading to the formation of new vessel from existing ones. Several stimuli including hypoxia can trigger angiogenesis, which goal is to restore hemostasis by forming collaterals. The endothelium is equipped to sense disturbance in oxygen supply and hypoxia-inducible factor and can activate the angiogenic cascade if new vessel are needed for tissue perfusion. The main stimuli for angiogenesis are the VEGF family, the Fibroblast Growth Factor (FGF) family, Angiopoietin-2 and chemokines.

Angiogenesis is very relevant to myocardial infarction caused by the occlusion of coronary arteries because it provides new vessels to perfuse the heart. A complete review of angiogenesis can be found elsewhere [30].

1.2.3.3.5 Inflammation

Inflammation is a biological process triggered by harmful stimuli with the aim of eradicating it. It begins with acute inflammation, a rapid response of the vascular system, which builds up through the synergistic combination of leukocyte chemoattraction, activation, adhesion, and transmigration into the arterial wall. The successful removal of the noxious stimulus restores homeostasis and depending on the magnitude and intensity of the inflammation the initial vascular architecture is either recovered or replaced by connective scar tissue. If however the stimulus persists, inflammation becomes chronic and set a new set of interactions between endothelium and plasma cells.

The four cardinal signs of inflammation, *rubor* (redness), *calor* (feeling of heat), *dolor* (pain) and *tumor* (swelling), sometimes complemented by a fifth *mousquetaire, fonctio laesa* (loss of function; although not unique to inflammation) are the direct result of the alteration of the endothelial state and its interaction with the immune system. *Rubor* and *calor* are the consequences of vasodilation through an increase of cytosolic Ca^{2+} that mediates the release of PGI_2 via the COX pathway and NO. Additionally, the influx of Ca^{2+} and synergetic activation of the RHO-pathway phosphorylates myosin light chain, which results in the contraction of the actin cytoskeleton and promotes vascular leakiness. The increase in permeability of the vessel induces the leakage of plasma exudate, which accounts for the *tumor*. The secretions of inflammatory cytokines by leukocyte cause *dolor* [31].

The infiltration of leukocytes, in particular the early recruitment of neutrophils and monocytes, sustains inflammation by the secretion of the potent pro-inflammatory cytokines Tumor Necrosis Factor-α (TNF-α) and Interleukin-1 (IL-1) [32, 33]. These cytokines activate the master regulator NF-κB that in turn trigger the expression of myriad of pro-inflammatory mediators including COX2 involves in increased

permeability, chemokines such as Monocyte Chemoattractant Protein-1 (MCP-1) and Interleukin-8 (IL-8) that augment the affinity of the adhesions molecules for their cognate receptor, and adhesion molecules like Intercellular Cell Adhesion Molecule-1 (ICAM-1), Vascular Cell Adhesion Molecule-1 (VCAM-1), E-selectin that are directly responsible for the recruitment of leukocytes.

The recruitment of leukocytes is a complex process involving many molecules at the surface of the endothelium and leukocytes. Together, these molecules interact to signal and create bonds between the cells. Endothelial cells are quasi-immobile in the frame of reference of the body, whereas leukocytes are in motion, propelled by blood flow. In order to decrease their momentum, bonds have to be created with the vascular bed, which further allows leukocytes to change direction and intravasate despite fluid forces. Transmigration is described as a multiple step process consisting of capture, rolling, slow rolling during which leukocyte find the best "spot" to transmigrate, arrest of activated leukocytes, adhesion strengthening and spreading, crawling and finally the actual transmigration that can occur either paracellularly or transcellularly. At each step, various surface molecules are involved both on the endothelium and the leukocytes reviewed in great details by Ley and colleagues [34] (Figure 1.6).

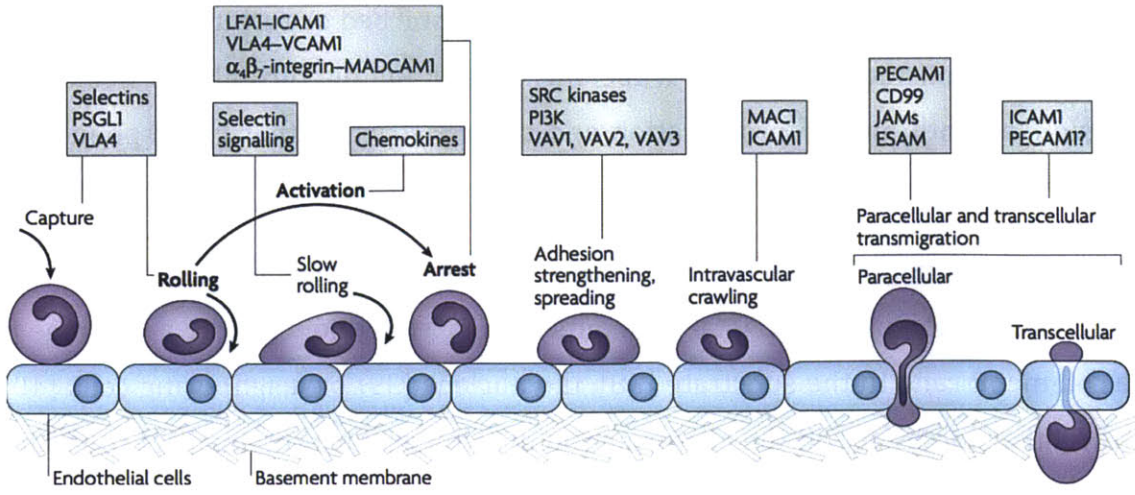

Figure 1.6: Summary of the transendothelial migration of leukocytes process.

Transmigration is a multiple-step process during which activated leukocytes are stopped before they can cross the endothelial barrier at determined loci such as cell junctions or thin cell membranes. PSGL1: P-selectin glycoprotein ligand-1; VLA4: Very Late Antigen 4; LFA1: Lymphocyte function-associated antigen 1; MADCAM1: mucosal vascular addressin cell-adhesion molecule 1; PI3K: phosphoinositide 3-kinase; MAC1: macrophage antigen 1; PECAM1: platelet/endothelial-cell adhesion molecule 1; JAMs: junctional adhesion molecules; ESAM: endothelial cell-selective adhesion molecule [34].

1.2.3.4 Mechanosensor

The endothelial monolayer is the center of command of vascular health and a fine sensor of its microenvironment. Its endothelial cells are the first line of exposure to luminal elements. Residing at the privileged vantage point at the frontier between vessel and blood on the one hand and smooth muscle from the opposing side, the endothelium is ideally suited to orchestrate the sensing of complex forces and flows, surveillance of circulating elements, and right of passage and defense of the vessel against these entities. Changes in endothelial connectivity, in endothelial cell shape and cytoskeleton are followed by dynamic alterations to the cell's secretome and with that regulation of state and environment [35, 36]. For example under laminar flow, endothelial cells become spindoidal and align with the flow but lose a preferential orientation and turn cuboidal under disturbed or turbulent flow due to F-actin reorganization [37], and while the former inhibit thrombosis, leukocyte adhesion, smooth muscle proliferation and vasoconstriction that latter phenotype promotes these processes.

The transmission of force to the cell is carried through intracellular tension created by the contraction of cytoskeletal filaments influenced by flow via the anchorage of the cell membrane to the substrate [38], the nucleus [39] or neighboring cells [40]. Intracellular forces act on the conformation of intracellular proteins [41] to modify the physiology of the cell and consequently the extracellular milieu, including the mechanical properties of the substrate, indirectly influences through this

mechanism, the biology of the cell [42]. Several mechanosensors have been identified at the apical and basal surfaces of the endothelium, such as ion channels [43], integrins [44], cell adhesion molecules [45], G-protein coupled receptors [46] or others cellular organelles [47] and can lead to the activation of inflammation mediators such as the master regulator Nuclear Factor-κB (NF-κB) or potent anti-inflammatory factor like Krüppel-Like Factor-2 [8] depending on the waveform applied to the cells. Further details on endothelial flow-mediated mechanotransduction are summarized in an exhaustive review by Davies [48].

1.3 Atherosclerosis

Atherosclerosis is the most prevalent disease in developed countries [49]. It slowly and often silently mutates into localized lesions of the large and medium vessels to culminate in myocardial infarction or stroke [50-52]. Together these two diseases claim a staggering 15 million lives in the U.S. each year despite the innumerable advances made in the understanding of the risk factors, the pathobiology of the disease, the general biology of vessels, and the deployment of a panel of small molecules to counteract the progression of the disease, and devices to prevent and protect patients during the acute phase [53, 54].

1.3.1 Incidence

The pathological evolution of atherosclerosis, namely plaque rupture or stenosis can causes myocardial infarction, *angina pectoris*, heart failure and stroke. All together cardiovascular diseases are the first cause of mortality in the world, especially in the Western world where cholesterol-rich diet promotes the disease. Eighty-three millions Americans have at least one cardiovascular disease and in 2010 alone, more than 1.3 million died because of cardiovascular maladies [53]. Despite great advances in our understanding of the pathogenesis of the disease and technological breakthroughs like the invention of stents, drug-eluding stents or cholesterol lowering drugs such as statins, the prevalence of atherosclerosis keeps rising notably in oriental countries adopting the Western diet. The conclusion of an acute cardiovascular event is often tragic: death and disabilities are still very frequent and

the colossal economic burden – $315+ billions in 2010, predicted to triple by 2030 – adds to the immense emotional strain [53]. The onus is on today's society to bend the macabre course of cardiovascular diseases. It is with this in mind that we have developed new tools to investigate atherosclerosis.

1.3.2 Historical perspective

With the earliest evidence of atherosclerotic lesions tracing back to Egyptian mummies and early histological data dating back to Gabrielle Falloppio's first reports of calcified arteries during the sixteenth century, the origin and mechanisms underlying atherosclerosis is a long-standing issue and the subject of intense speculation, hypotheses and investigation. Contrary to what is often read, the French pathologist Pierre Rayer and the British physician Joseph Hodgson were the first to postulate the inflammatory nature of atherosclerotic lesions, which to this day, still influences our modern vision of the disease. Rayer writes:

> *"Morbid ossification of the arteries [is] the result of the inflammation of their fibrous layer. It is accompanied by bright redness of its internal layer, [...] and frequently surrounded by a yellow matter, soft and solid, non transparent"*. P. Rayer [55].

Yet, another great scientist, the Prussian Rudolph Virchow, is credited with drawing the finest insight in the pathogenesis of atherosclerosis. In his 1856 treaty entitled "*Thrombose und Embolie. Gefässentzündung und septische Infektion*" [56], Virchow induced pulmonary embolism in dogs by seeding foreign material such as elderberry cores into their venous system, noting that the occlusion would induce thrombosis. He surmised that the consequences of thrombosis could be due to 1) irritation of the vessel, 2) coagulation of the blood or 3) interruption or disturbance of the flow. We now know that the concept is flipped on its head and that it is inflammation/endothelium dysfunction, blood coagulability and disturbed flow that are the three pillars of thrombosis, remembered as Virchow's Triad [57]. Nevertheless, Virchow's observations and analyses are brilliant and still shape our conception of atherogenesis. In 1858, two years after writing his opus on

thrombosis, he explains in lectures to the Pathological Institute of Berlin his agreement with the "old view" in which inflammation of the endothelium precedes the "fatty metamorphosis". He writes:

> *"The state of the matter here also is more or less very simply this, that two processes must be distinguished in the vessels, which are very analogous in their ultimate results ; first, the simple fatty metamorphosis, which sets in without any discoverable preliminary stage, and in which the existing histological elements pass directly into a state of fatty degeneration and are destroyed, so that a larger or smaller proportion of the constituents of the walls of the vessel perishes ; and, in the next place, a second series of changes, in which we can distinguish a stage of irritation preceding the fatty metamorphosis, comparable to the stage of swelling, cloudiness, and enlargement which we see in other inflamed parts. I have therefore felt no hesitation in siding with the old view in this matter, and in admitting an inflammation of the inner arterial coat to be the starting point of the so-called atheromatous degeneration ; and I have moreover endeavoured to show that this kind of inflammatory affection of the arterial coat, is in point of fact exactly the same as what is universally termed endocarditis, when it occurs in the parietes of the heart. There is no other difference between the two processes than that the one more frequently runs an acute, the other a chronic, course."* R. Virchow [58].

Another conceptual milestone was reached at the turn of the nineteenth century when Nikolai Anitschkow provided the first evidence linking dietary cholesterol to the development of atheroma in what is considered the germinal model of atherosclerosis in a rabbit [59, 60]. Yet, systemic elevated levels of cholesterol alone could not explain the confinement of inflammation and atheromatous lesions to specific regions of the vasculature, such as the lower curvature of the aortic arch, the carotid sinus or broadly bifurcations. Modern theories have emerged to attempt to reconcile the systemic and local components of atherogenesis, which gave rise to the

concept of flow-driven atheroprone endothelium. Under this framework, the endothelium is promoted to the rank of multifaceted and dynamic sensor, transducer and actuator of vascular homeostasis, which integrates a myriad of environmental factors like the local hemodynamics, the microenvironment or luminal factors.

1.3.3 Morphological description of atherosclerosis

1.3.3.1 Histology

Atherosclerotic lesions are local inflations of the vessel wall of large and mid-size arteries. The mature plaque is a complex amalgam of vascular cells, immune cells, cell debris, lipids and modified lipids, and connective tissue. Figure 1.7 shows the convoluted architecture of atheromatous lesions as observed and illustrated by Virchow, which bears impressive resemblance with a schematic of same type of lesion (Figure 1.8) but precedes it by 150 years. The major morphological characteristic of atherosclerosis is that it destroys the well-ordered trilaminate architecture of the vessel. The media is not confined anymore to the sub-basement membrane but instead crosses over to the intimal compartment. At the same time various immune cells including monocytes, their differentiated progeny the macrophages and the dendritic cells, neutrophils, mast cells and T-lymphocytes have invaded the sub-endothelial space and are floating in a lipid-rich, fibrous, extracellular matrix [61]. Ultimately either a thick protective fibrous cap build up on top of the plaque or erosion or even rupture causes massive thrombosis. Indeed, this remodeling is a dynamic process that occurs through years or even decades before symptoms brutally arise. In this work, we concentrate on the initiation of the lesional state, namely endothelial dysfunction and the recruitment and interaction with leukocytes.

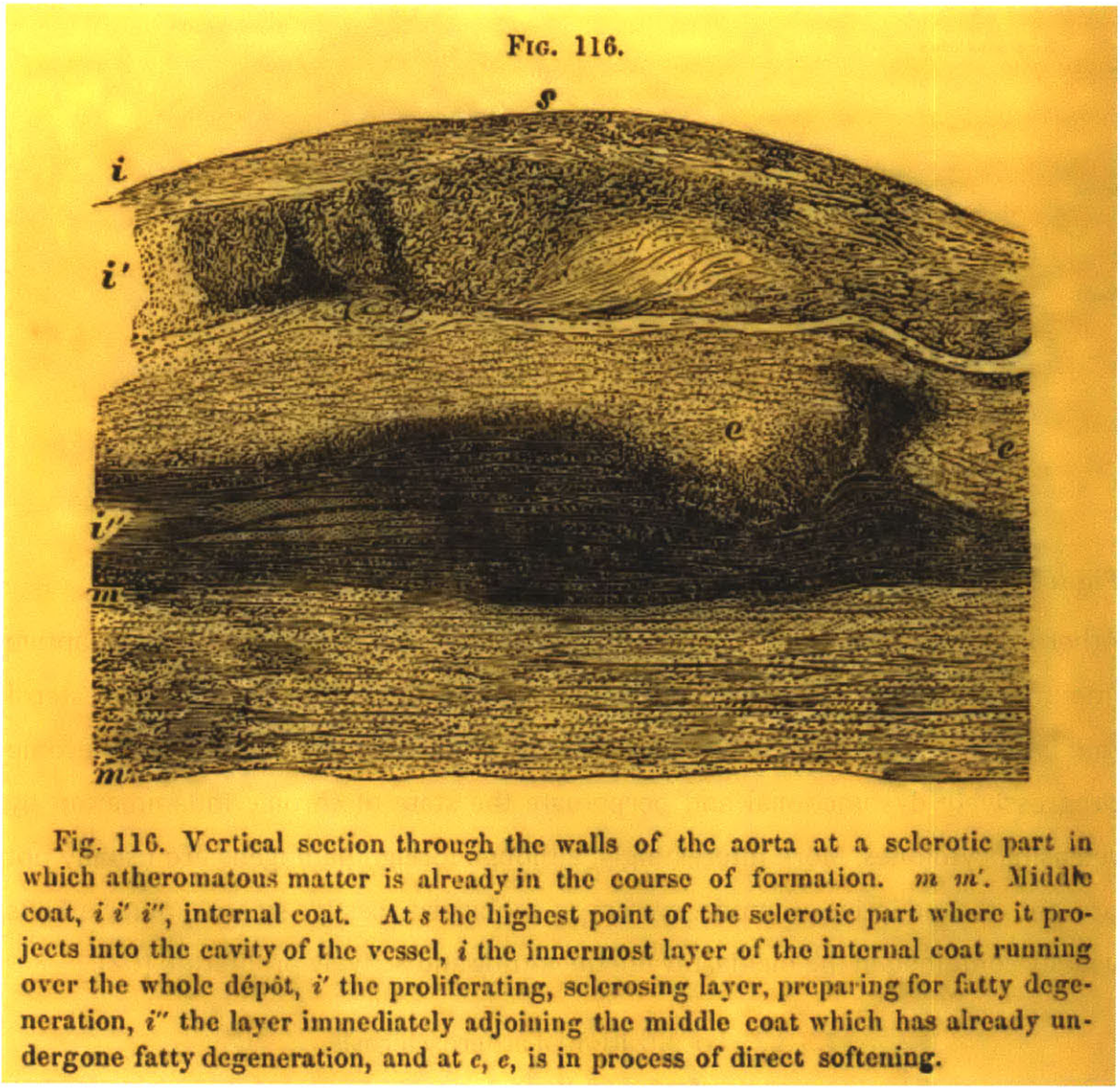

Fig. 116. Vertical section through the walls of the aorta at a sclerotic part in which atheromatous matter is already in the course of formation. *m m'*. Middle coat, *i i' i''*, internal coat. At *s* the highest point of the sclerotic part where it projects into the cavity of the vessel, *i* the innermost layer of the internal coat running over the whole dépôt, *i'* the proliferating, sclerosing layer, preparing for fatty degeneration, *i''* the layer immediately adjoining the middle coat which has already undergone fatty degeneration, and at *e*, *e*, is in process of direct softening.

Figure 1.7: Engraving on wood of one of the earliest histological section of an atherosclerotic lesion.

The intimal and medial layers are represented at the location of plaque formation. *i.* denotes the intima and probably a fibrous cap made of proliferative smooth muscle cells over the lipid laden cellular mass referred to as the fatty degeneration *i'*. *i''* shows the basement membrane on top of the medial layer *m* and *m'*. Interestingly, the author also detects the softening of regions *e* that is probably ascribable to the remodeling of the wall by proteases released by immune cells [58].

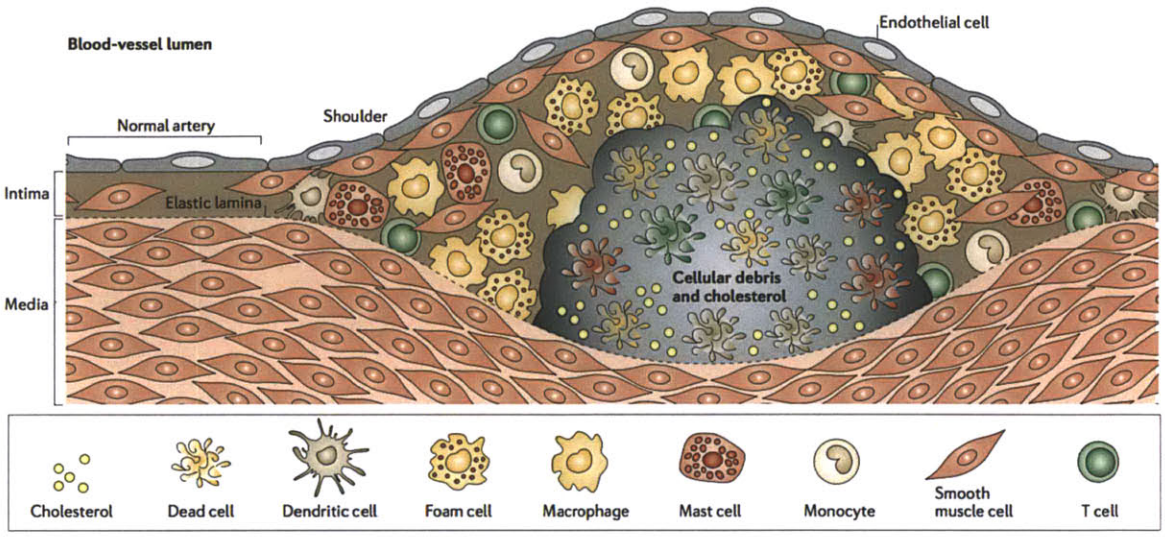

Figure 1.8: The inflammatory cascade in atherosclerosis.

Atherosclerotic lesions contain immune cells from both the innate and adaptive immune system as well as debris. The extracellular matrix is filled with cholesterol that is uptaken by macrophages. The lipid-laden macrophages or foam cells become progressively dysfunctional and perpetuate the state of chronic inflammation by releasing cytokines. More interestingly, although foreign pathogens are usually not present, the adaptive immune system is mobilized. Lastly, smooth muscle cells usually contained in the media, invade the intima and actively proliferate [62].

1.3.3.2 Localization of atherosclerosis

One of the fascinating features of atherosclerotic lesions is that they do not affect the whole vasculature; instead they consistently develop at precise loci. Atherosclerosis develops in the large and mid-size arteries but the venous system as well as the arterioles and capillary network are spared from the disease [63]. Further, lesions do not span the whole arteries but atherosclerosis is focal in nature, accumulating at the crux of bifurcations and highly curved vessels. Figure 1.9 shows the aorta of a transgenic mouse (LDLR-/- ; Low Density Lipoprotein Receptor -/-) stained with oil-red-O to show lipid accumulation. The red staining is mainly seen in the lower curvature of the aorta as well as branching points. From the bottom picture of the artery cut open, it is extremely clear that two regions can be distinguished from the

same vascular bed: atheroprone or atherosusceptible regions where lipids accumulate and atheroprotective or atheroresistant regions free from lesion. These observations extends to other vascular bed, such as the sinus of the carotid bulb and its bifurcation, where lesions develop versus the straight segments away from the bifurcation where there is a low occurrence of the disease.

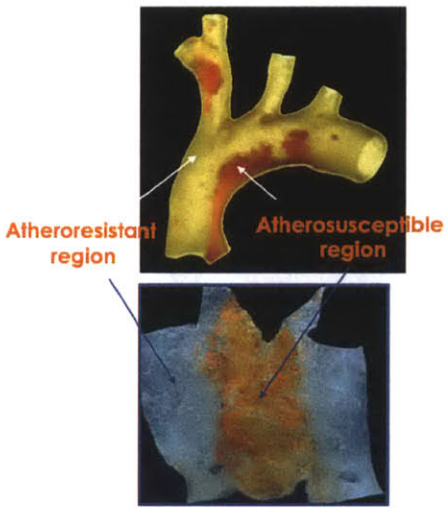

Figure 1.9: Localization of atherogenesis observed through lipid staining of the mouse aorta.

Oil-red-O staining of the aortic arch of an LDLR-/- mouse fed a high fat diet for 8-10 weeks, showing the focal nature of atherosclerosis. The lipids, stained in red, are concentrated in the lower curvature of the aortic arch and its braches but not in the higher curvature [64].

1.3.4 Co-localization of atherosclerotic lesions and regions of disturbed flow

The localization of atherosclerosis remained until the 1960s, one of the most puzzling observations in the study of atherogenesis. Although inflammation had been characterized since Rayer, Hodgson and Virchow, nobody could explain why *irritation* would be confined to certain regions. Moreover, hypercholesterolemia, a systemic factor, was the prevailing hypothesis from the pathogenesis, which conflicted with localization. Pioneers such as Duguid and Robertson [65], Fry [66],

Fox and Hugh [67] and Caro [68] hypothesized that the hemodynamics could cause endothelial injury and explain the localization of fatty streaking.

Now, thanks to the precise analysis of the hemodynamics, we know that atheroprone regions co-localize with the regions of disturbed flow – understood as flow with boundary layer separation, flow reversal, secondary flows, shifting stagnation points and high vorticity – and atheroprotective one correlate with quasi-parabolic velocity distribution of the flow. Figure 1.10 shows that low average shear stress disturbed flow computed from CFD analysis of the aortic arch of the mouse matches with lipid insudation.

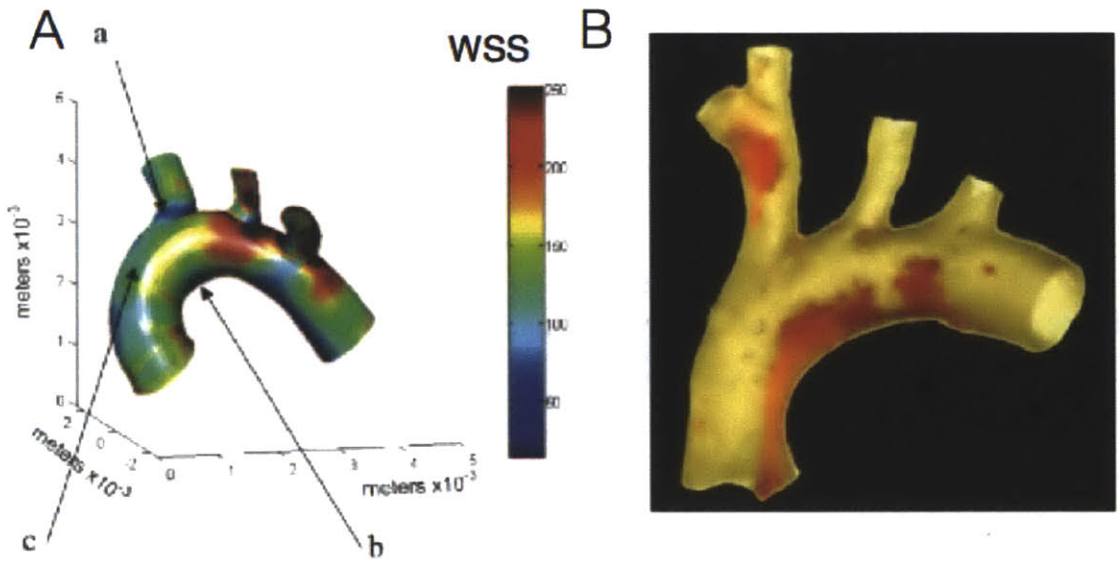

Figure 1.10: Flow disturbance correlate with the localization of atherogenesis.

A. Comparison of the time-average wall shear stress in the mouse aorta (dynes/cm^2) and B. the lipid accumulation. The regions of low wall shear stress, which also correlate with high flow vorticity (not shown), match the regions where the lesions initiate. This suggests that flow is intimately involved in the pathogenesis of atherosclerosis. (Adapted from [7] (left) and [64] (right)).

1.3.5 Atheroprone and atheroprotective flow

The endothelium is a fine mechanosensor that is sensitive to the change in pressure and wall shear stress. Although the pressure does not vary significantly between prone and protective-regions, the WSS, however, does tremendously change between these regions. Dai et al. computed the evolution of WSS during one cardiac cycle in the sinus of carotid bulb with great oscillatory shear index and in a straight portion of the internal carotid artery [8]. Figure 1.11 shows prototypical atheroprone and atheroprotective waveforms. The critical differences between the two waveforms have profound implications on the phenotype of their underlying endothelial cells.

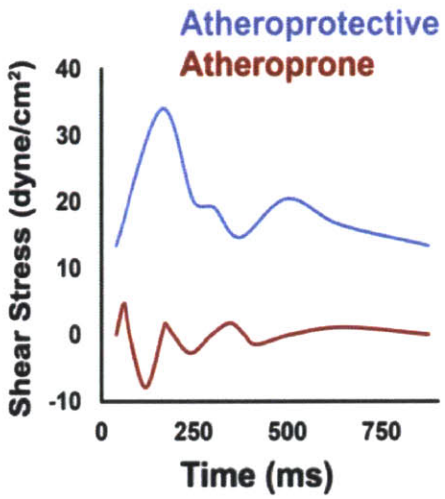

Figure 1.11: Atheroprotective and atheroprone waveforms.

Computed wall shear stress from the carotid of healthy male described in Figure 1.5. The atheroprotective flow is unidirectional, as the sign of the WSS stays constant, whereas the atheroprone flow changes sign, which denotes bidirectional flow. Of notice is the average WSS value over one cardiac cycle. The average WSS of atheroprotective flow averages around 20 dynes/cm^2 but atheroprone WSS is around zero (Courtesy of Dr. Guillermo García-Cardeña).

1.3.6 Pathogenesis of atherosclerosis

Atherosclerosis is a disease of the endothelium and its endothelial cells that begins with endothelial dysfunction and activation of individual cells but rapidly grows into

a broader collective state of injury that results in profound rearrangements of the microstructure of the vessel. Locally, the diseased vessel thickens and hardens due to the accumulation of a collection of molecular and cellular bodies such as lipids, calcium, intima, immune cells and dead cells, organizing thrombosis and excessive fibrogenesis. In vivo and in vitro histological, morphological, biochemical and clinical evidence incriminate endothelial failure and cytoskeletal rearrangement in the disruption of multiple downstream functions exemplified by the loss of regulation of vasomuscular tone [64], which dictates inter- and intra-cellular forces and the chemistry of the extracellular matrix [69], increased permeability that allows for an increase in lipid percolation [70, 71], the modulation of the cell's secretome [33], the expression of adhesion molecules and recruitment of innate and adaptive effectors in the absence of foreign pathogens [72], and the thrombotic cascade. All of these elements contribute to the stability of the heap of highly disorganized material called plaque, which is the major clinical preoccupation.

1.3.6.1 Endothelial dysfunction

Endothelial cells of the atheroprone regions are dysfunctional in many regards: their vasomotor functions are impaired and they are primed for inflammation. Here, we review some of the most important evidence of endothelial dysfunction in atheroprone areas.

As discussed earlier, NO controls the vascular tone and is to a great degree a key regulator of vascular health. eNOS is the enzyme that generates NO. Strikingly, eNOS is expressed in athero-protected but not in the -prone regions. Figure 1.12 presents images of C57BL6 mouse endothelium immunostained for CD31 (endothelial marker) and eNOS and SYTOX (nuclear stain). Spindoidal atheroprotected cells produce eNOS when cuboidal atheroprone cells do not, therefore atheroprotected areas can regulate vascular tone and adapt the diameter of the vessel to the flow, but this function is partially impaired in atheroprone areas.

Another indication that atheroprone endothelium is primed for inflammation during atherogenesis is that the p65 subunit of NF-κB is highly upregulated in those

regions. p65 is involved in NF-κB heterodimer formation, nuclear translocation and activation, hence it is a crucial step towards mounting an inflammatory response. Figure 1.13 shows that p65 accumulates in the cytosol of atheroprone endothelium in C57BL6 transgenic mice but not in atheroprotected regions. Additionally, when Hajra and colleagues added a stimulus, either injection 100 μg of Lipopolysaccharide (LPS) or 2 weeks of 1.25% cholesterol-enriched diet, they observed and measured nuclear translocation of p65 in the atheroprone but not atheroprotective regions. That further suggests the NF-κB pathway is primed in endothelium predisposed to atherosclerosis.

Lastly, toll-like receptors (TLRs) are pattern recognition receptors that recognize pathogens-associated molecular patterns [73]. Their role is broadly to mobilize and activate the innate immune system when potentially infectious material enters the body. The TLR2 is locally expressed in atherosusceptible regions (Figure 1.14).

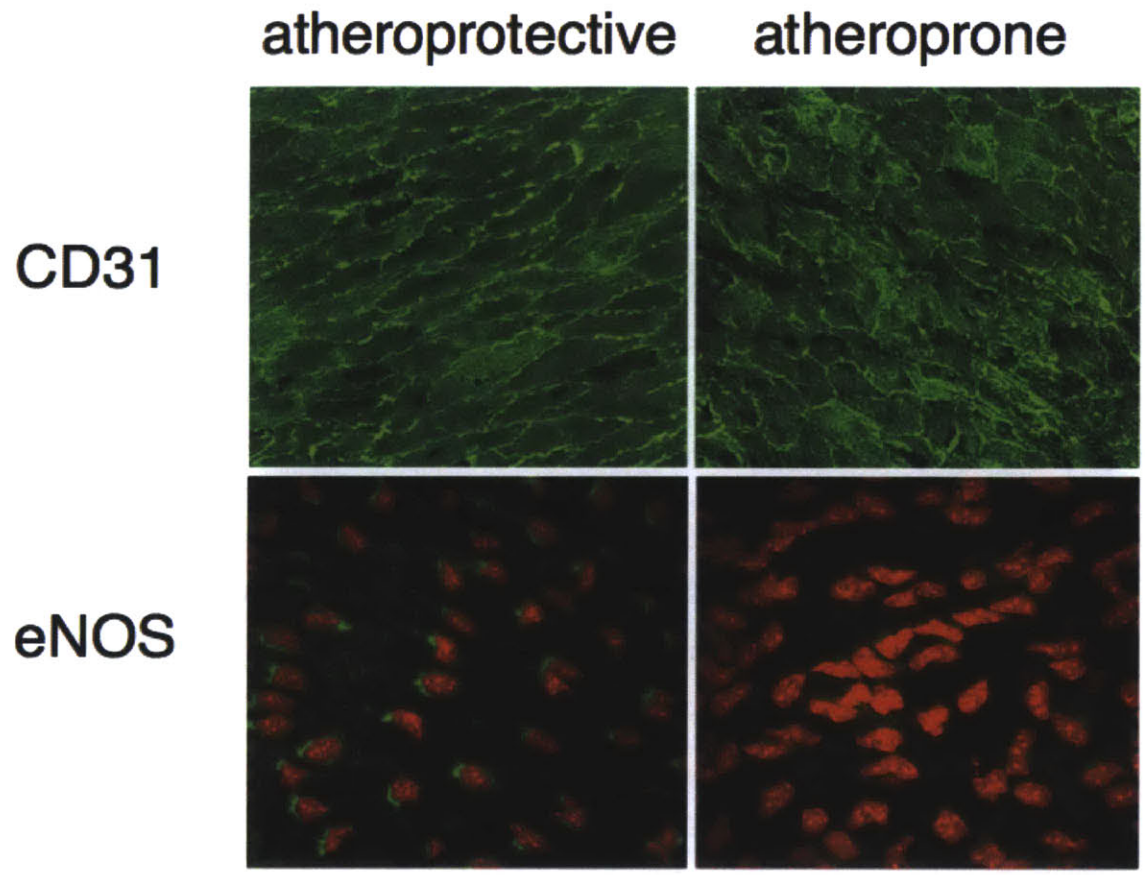

Figure 1.12: Disturbed flow elicits endothelial morphological changes and dysfunction.

En face mounted immunostaining of the lesser curvature (atheroprotective) and descending aorta (atheroprone) of a C57BL6 transgenic mouse on a chow diet. Images in the upper raw were stained with a primary anti-CD31 antibody and FITC secondary antibody. The CD31 staining shows the morphology of the cells: atheroprotective cells are elongated and aligned with the direction of the flow, while atheroprone endothelial cells have no particular orientation (Gimbrone et al. Cardiovascular Pathology 2013). The lower row shows merged images of eNOS staining (FITC, green) superimposed onto SYTOX nuclear staining (red). It is evident, just looking with the naked eye that more cytosolic eNOS protein is present in atheroprone endothelium compared to atheroprotective [64].

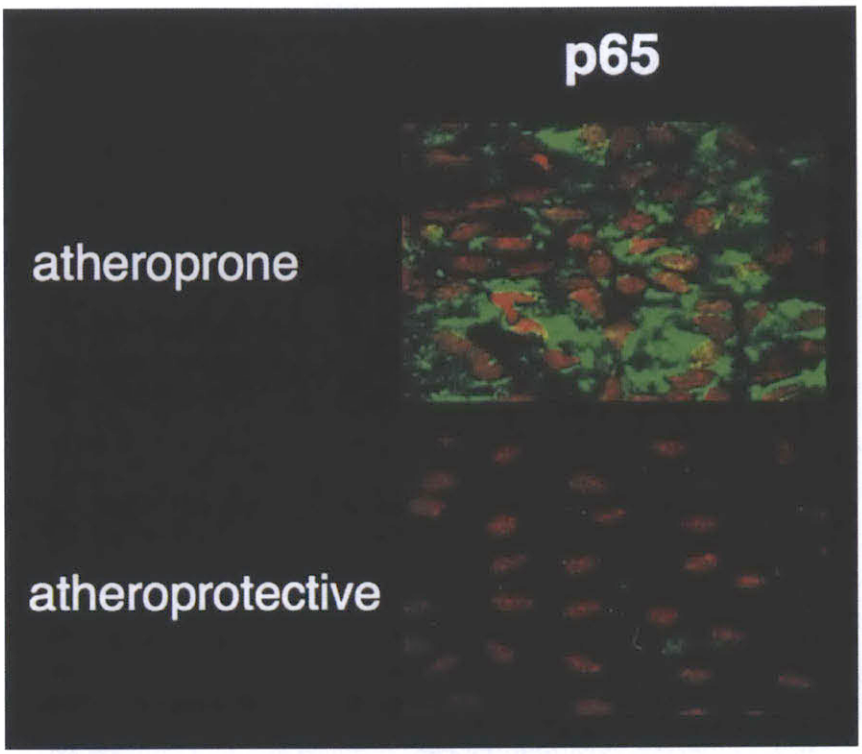

Figure 1.13: Atheroprone regions are predisposed to inflammation.

Immunostaining of the predisposed (atheroprone) and protected (atheroprotective) regions of the ascending aorta of crossed LDLR-/- and C57BL6 transgenic mice on a chow diet (these areas were previously determined by oil-red-O staining). Cytosolic p65 (FITC, green) is abundant in atheroprone endothelium but scarce in atheroprotected endothelium. Nuclei are stained in red with Propidium Iodine (PI). This demonstrates that atheroprone endothelium is primed for NF-κB-mediated inflammation [74].

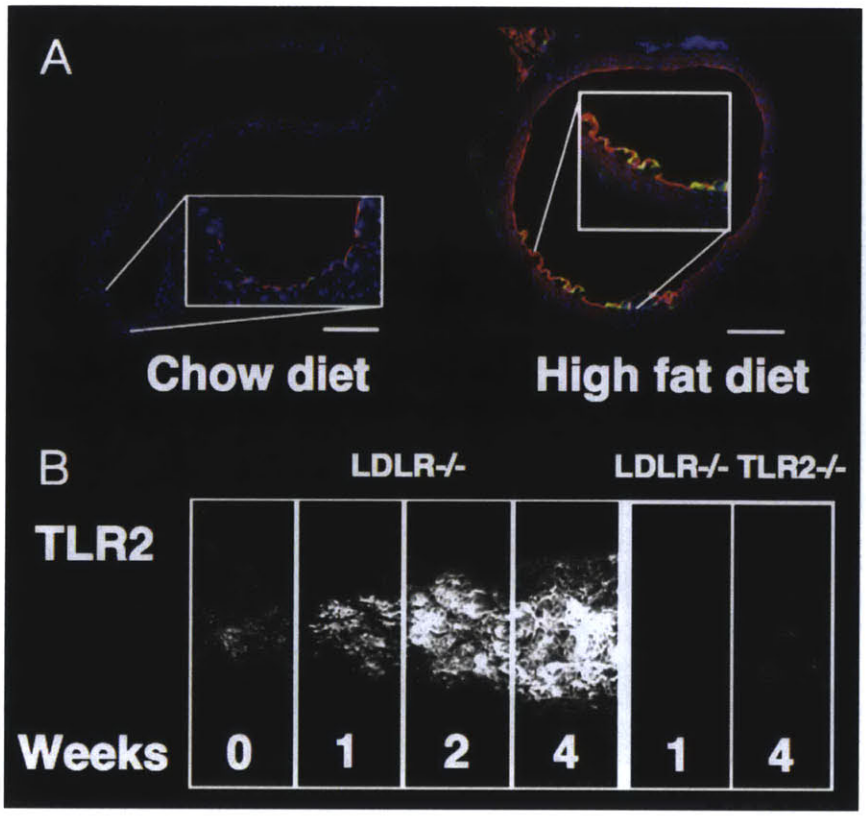

Figure 1.14: Toll-like receptor-2 is expressed in atheroprone regions of the mouse aorta and augmented by high fat diet.

A. Immunostaining of the ascending aorta of crossed LDLR-/- and C57BL6 transgenic mice fed on a chow or high fat diet (1.25% cholesterol and 15.8% fat-enriched diet). Endothelial cells stained with an anti-CD31 antibody (red) of the lower curvature (lower part of the lumen) of the aortic arch, which are exposed to disturbed flow, express TLR2 (green) in both chow and high fat diets, while the upper curvature (upper part of the lumen), exposed to unidirectional flow, is devoid of TLR2 expression. TLR2 expression is highly increased in mouse fed a high fat diet, which confirms that hypercholesterolemia exacerbates endothelial dysfunction. Nuclei are stained with DAPI. B. Hyperlipidemia promotes high expression of TLR2 in the lower curvature of the mouse aorta. Weekly evolution of TLR2 expression in circumferential strips of the aortic arch of LDLR-/- and C57BL6 mice fed a high fat diet for up to 4 weeks. TLR2 expression is confined to regions of the lower curvature, (at the center on the picture strips) and rapidly progresses with time. By the fourth

week TLR2 expression is high compared to LDLR-/- and TLR2-/- mice used at control (week 1 and week 4 shown only) [75].

1.3.6.2 Flow-driven inflammation in atherosclerosis

Unidirectional pulsatile blood flow is critical to maintain vascular health and confers atheroprotective properties to the endothelium [8]. Conversely, disturbed flow is unable to elicit atheroprotection in the monolayer, which develops low-grade inflammation [74].

1.3.6.2.1 Atheroprone promotes a lack of atheroprotection and low-grade inflammation

The morphology of atheroprone endothelium is radically distinct from healthy atheroprone endothelium: cuboidal cells dominate disturbed regions of flow, meaning that cells are square-like and there is no preferential direction of alignment of the monolayer; in contrast, cells under undisturbed unidirectional flow are spindoidal with their main axis oriented parallel to the direction of flow, a vivid evidence that these flow patterns evoke distinct behaviors in endothelial cells (Figure 1.12). In the late 70s, Davies et al. made some of the seminal *in situ* observations of the morphology of endothelial cells of the rabbit aortic arch with scanning electron microscopy that lead to this conclusion [76]. Although crude morphological observations cannot substantiate full phenotypical characterization of prone and protective endothelium, it is the visible consequence of its biological machinery that has crystallized in a body of evidence in recent years.

In vivo, comparative staining of the lower curvature of the aortic arch versus the descending aorta in human and mice have shown elevated levels of reactive oxygen species and the activation of NF-κB, a major pro-inflammatory transcription factor that coordinates the expression of endothelium-leukocytes interactions proteins such as VCAM-1, ICAM-1 or E-Selectin [74, 77]. Moreover, the accumulation of unfolded or misfolded proteins in the endoplasmic reticulum in disturbed flow regions is at the origin of the unfolded protein response detected in atheroprone

endothelium [78, 79]. Its role is to temperate the deleterious consequences of misprocessed proteins and recover homeostasis by up-regulating the chaperones in charge of protein folding, up-regulating the tagging machinery responsible for misfolded proteins degradation by the proteasome and ultimately instructing apoptosis when a healthy state cannot be attained. Multi-sites genomic studies of atherosusceptible and atheroprotected regions of the swine have corroborated the importance of endoplasmic reticulum stress and unfolded protein response in disturbed flow regions.

In vitro studies have successfully confirmed, furthered and explained mechanisms observed *in vivo*. The Edelman and García-Cardeña laboratories were pioneers in the investigation of the role and impact of flow patterns on endothelial cells through the development of an apparatus suited for long-term culture of endothelial cells under specific flow patterns. The Edelman and García-Cardeña laboratories, and others have showed that key protective endothelial programs such as endothelial nitric oxide synthase or COX-2 expression are promoted by atheroprotective flow but lost under atheroprone flow. Prone flow also promotes the expression of leukocyte chemokines like macrophage chemoattractant-1 or interleukin-8 and the rearrangements of the cytoskeleton and the junctional proteins. As it became evident that higher order regulatory elements were orchestrating atheroprotection, the García-Cardeña laboratory implemented a genome-wide microarray screening of cells exposed to protective and susceptible flow that lead to the establishment of complete RNA expression profiles and the identification of Krüppel-like factor 2 (KLF2) as a critical integrator of flow-mediated vasoprotection. HUVEC were exposed to the waveforms described in Figure 1.11 (prone and protective waveforms) and the upregulation of KLF2 by atheroprone flow was confirmed by quantitative Polymerase Chain Reaction (qPCR).

1.3.6.2.2 KLF2 is a master regulator of atheroprotection triggered by flow

KLF2 is a zinc finger transcription factor essential in vascular hemostasis. While we focus here on its endothelial expression, it is worth noting that KLF2 has broader implications than endothelial biology only. KLF2 is a regulator of inflammation in myeloid cells and participates in T lymphocyte quiescence, which unifies its role as a regulator of inflammation. Yet, KLF2 biology is intimately linked to the cell of the intimal compartment. The expression of KLF2 is necessary during development as both KLF2 total and endothelium conditional knockouts are lethal due to vascular instability in mice. Shear activates endothelial KLF2 expression through the MEKK3/MEK5/ERK5/MEF2 pathway and mitigates the execution of the inflammatory cascade in arteries. For instance, endothelial cells expressing KLF2 – induced by flow or viral constructs – are less sensitive to pro-inflammatory challenges like interleukin-1β (IL-1β). More recently, an analysis of all the microRNA (miRNA) in endothelial cells under flow revealed that several sequences are induced by flow and contribute to establishment of a flow-mediated phenotype. For example, miR-92a is constitutively expressed by the endothelium under static and atheroprone conditions and inhibits the translation of KLF2; conversely atheroprone flow inhibits miR-92a and positively regulates KLF2 [80].

1.3.6.2.3 Recent evidence supporting phenotypic differences between athero-prone and -protective endothelium

The regulation of the endothelial state by miRNAs goes beyond its regulation of KLF2. Many miRNA are flow responsive and their expression is either promoted or repressed by athero-protective or -prone flow: miR-17-5p, miR-20a, miR23-b, miR-25, miR-30b and Let-7g are, for example up-regulated by atheroprotective flow; on the contrary, athero-prone flow promotes the expression of miR-21, miR-33, miR-92a, miR-210, miR-217, miR-221, miR-222, 663 and miR-872 [81]. Indeed, the purpose of this review is not to establish an exhaustive list of miRNA linked to flow

or atheroprone EC, but rather to highlight the conceptual novelty of 1) the existence of flow-driven post-transcriptional modulation of EC phenotype and 2) the importance of this phenomenon in polarization of atheroprone endothelium. As expected, most miRNA promoted by protective flow contribute to anti-oxidative and anti-inflammatory pathways, whereas prone flow contributes to the opposite effect [82-84]. Even the number of microparticles produced by the endothelial cells that shuttle miRNA outside of the cytoplasm and can then act as post-translational paracrine regulators of gene expression is differentially regulated by flow [85]. Low levels of wall shear stress (similar to prone flow) compared to high shear stress (similar to protective flow) increase their number; this is particularly relevant to atherogenesis because endothelial miRNA-containing microparticles are able to fuse with the membrane of surrounding cells like smooth muscle cells and alter their function. In a co-culture of KLF2-expressing EC and smooth muscle cells, endothelial exosomes containing miR-143/145 clusters – which promoter is activated by KLF2 – traveled to the smooth muscle cells compartment and elicited a contractile phenotype [86]. Reversely, endothelial cells that did not express KLF2 did not produce miR-143/145, which may contribute to an active mechanism that controls the polarization of smooth muscle cells to a synthetic phenotype.

It is worth noting that the experiments described in this section were performed using a constant laminar flow of ~20 dynes/cm2 as a surrogate of atheroprotective flow and ~2 dynes/cm2 or static conditions to mimic prone flow. It should be clear that there is a difference between the intensity and the evolution of shear stress with time. High shear stress is commonly correlated with protective flow, whereas low shear stress is associated with prone flow because the physiological waveform features flow reversal that makes its average over one cardiac cycle ~ten times lower than protective values. The other major characteristic of shear stress is its waveform. Protective flow is periodic of frequency that of the heart beat, with a pulse corresponding to systole. Prone flow has an average close to zero with periods of positive and negative shear stress. Feaver et al. performed a spectral analysis of both signals; they applied shear stress from single harmonics to EC and showed that

the zeroth (the constant part of the flow: the average) and first (sinusoidal signal of frequency that of the heartbeat) harmonics are the major determinants of gene expression [87].

Flow-mediated endothelial dysfunction is also exemplified by the deregulation of the oxidative state of the cell and the alteration of luminal surface of the endothelium [88]. In this regard, atheroprone flow yet contributes further through the activation of the NLRP3 inflammasome [89] that can notably process premature IL-1β and IL-18, a prerequisite for IL-1β driven inflammation. The activation of the inflammasome occurs via the activation of sterol regulatory element binding protein 2 and the transactivation of NADPH oxidase 2. Synergistically, flow differentially regulates the overall quantity and spatial distribution of the glycocalyx [90]. This organelle, which is largely present in straight atheroprotected segments of the carotid of mice but almost absent at the carotid sinus, acts as negatively charged barrier made of proteoglycans, glycoproteins and glycolipids that prevent the adhesion of immune cells. In an elegant work, Koo et al. showed that atheroprotective flow promotes even and abundant expression of heparan sulfate compared to atheroprone flow.

1.3.6.2.4 Accumulation and transmigration of leukocytes in atheroprone regions

1.3.6.2.4.1 Innate immune system

During development, about 4 weeks following fertilization of the egg, hemangioblasts appear in the dorsal aorta. Some will form structural endothelium while others commit to hematopoietic progenitors that will detach and give rise to the innate immune system that replaces the transient immune system derived from the yolk sac. The common multipotential hematopoietic stem cells, hemocytoblasts, generate myeloid and lymphoid progenitors. The lymphoid lineage engenders, B and T lymphocytes and natural killer cells. The myeloid progenitors generate erythrocytes, mast cells, megakaryocytes (generate platelets) and myeloblasts. The latter is the progenitor to basophils, eosinophils, neutrophils and monocytes.

Neutrophils and monocytes are important in atherogenesis because they are recruited early on in atheroprone regions. They contribute potent inflammatory cytokines and crucial cell:cell interactions to the already low-grade inflammatory milieu. In this work, we concentrate on monocytes because when recruited to the subendothelial compartment they transform to macrophages and subsequently to lipid-engorged dysfunctional macrophages: foam cells.

1.3.6.2.4.2 Monocytes/Macrophages

Monocytes are white blood cells produced in the bone marrow, from hematopoietic stem cells called monoblasts, which are intermediate precursors derived from myeloblasts. More than half of monocytes are stored in the cords of Billroth within the spleen, while the rest are circulating [91]. Contrary to the traditional belief, Swirski *et al.* showed that monocytes have the ability to stay undifferentiated even after tissue invasion, as evidenced by the identification of splenic reservoir monocytes.

Monocytes have a major role in the immune system; they patrol the endothelium and can differentiate into macrophages and dendritic cells to replenish the resident populations under normal conditions as well as being quickly recruited to an injury/infectious site to elicit the immune response. A healthy adult has around 500,000 monocytes per milliliter of peripheral blood. The newly identified splenic monocytes can be mobilized quickly and *en masse* to a site of inflammation during the acute phase to supplement circulating monocytes. Figure 1.15 summarizes the major receptor present at the surface of monocytes.

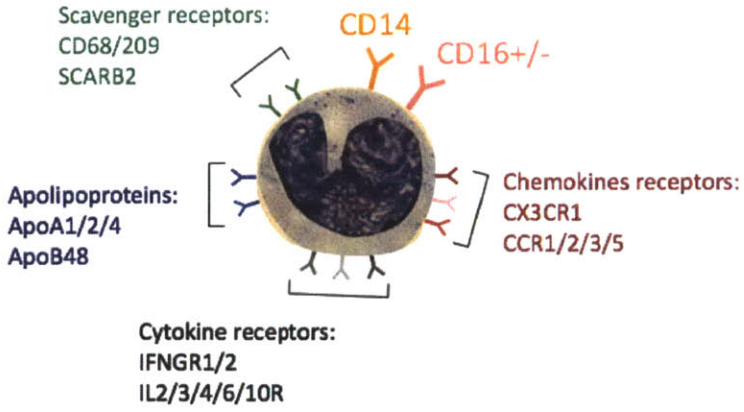

Figure 1.15: Major surface receptors of human monocytes.

Monocytes are best identified by their CD14 receptor but they harbor a variety of other receptors such as CD16; scavenger receptors: CD68, CD209 and SCARB2; apolipoprotein receptors: Apo A1, A2 and A4, and ApoB48; cytokine receptors: IFNGR1 and 2, IL-2, -3, -4, -6 and -10 receptors; and chemokine receptors: CX3CR1, CCR1, 2, 3 and 5.

However, human monocytes are not all born equal and constitute a heterogeneous population with distinct specialized function and markers. Their taxonomy – which is the source of debate – is mainly based on the expression of the CD14 and CD16 surface receptors, morphology, cytochemistry and light-scattering properties, and functional determination. A recent classification approved by the Nomenclature Committee of the International Union of Immunological Societies suggests three sub-categories of monocytes: classical $CD14^{++}CD16^{-}$ monocytes, intermediate $CD14^{++}CD16^{+}$ monocytes and non-classical $CD14^{+}CD16^{++}$ monocytes [92]. They respectively make up for 85%, 5% and approximately 7% of blood monocytes [93] (Figure 1.16). The first category have been labeled "inflammatory" because they respond to cell-surface TLR antagonists (TLR1, TLR2 and TLR4 antagonists) and secrete a wide range of inflammatory cytokines such as interleukins (IL) including IL-1, IL-6, IL-8, CC chemokine ligands (CCL): CCL2 and CCL3, TNF-α, reactive oxygen species (ROS) and NO in response to inflammatory signals e.g. LPS. The third category was labeled "patrolling" as these particular monocytes are able to crawl

along the endothelium for significant distances responding to damage and infection and recruit the "inflammatory" monocytes. Furthermore, it seems that they respond specifically to viruses and immune complexes containing nucleic acids while "inflammatory" monocytes are more likely to intervene during bacterial, fungal or parasitic infections. In the former case, monocytes are the main producers of a small set of pro-inflammatory cytokines: TNF-α, IL-1β, IL-6 and CCL3 via a unique TLR7-8, MyD88 and MEK-dependent pathway. Non-classical monocytes phagocytic potential is lower than "inflammatory" monocytes.

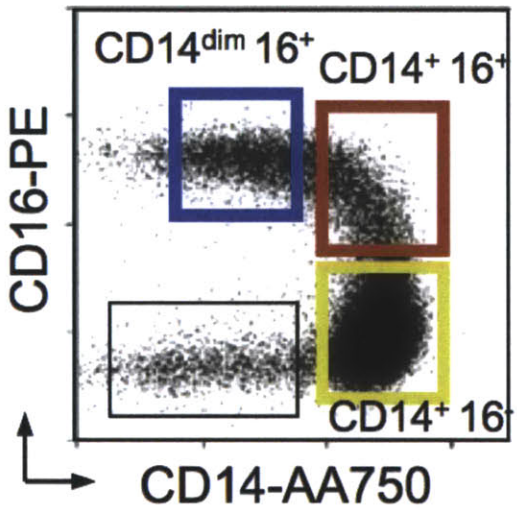

Figure 1.16: Primary blood monocytes constitute an heterogeneous population identified by their CD14 and CD16 expression.

Fluorescence-activated cell sorting (FACS) of primary blood monocytes analyzed by CD14 and CD16 surface expression. Ziegler-Heitbrock groups intermediate monocytes (red square) and non-classical ones (blue square), while Geissmann contests this hypothesis, grouping intermediates (red square) with classicals (yellow square) [93].

Two schools of thoughts debate the inter-relationships between monocytes subsets. Ziegler-Heitbrock hypothesizes that intermediate and non-classical cells should fall in the same super-category, whereas Geissmann pairs classical and intermediate in the "inflammatory" family (Figure 1.16). Despite the controversy all monocytes display a characteristic lobulated nucleus. The size of classical and intermediate

monocytes varies in the range 20-25 μm, whereas non-classical monocytes are smaller and present increased granularity [93].

1.3.6.2.4.3 Monocytes accumulate in atheroprone regions

Transmigration of immune cells in large vessels is the event that seals the dysfunctional and inflammatory fate of the atheroprone endothelium (Figure 1.17). It is the organized consequence of the onset of endothelial dysfunction. *In vivo*, monocytes/macrophages accumulate in the atheroprone regions e.g. in the lower curvature of the aortic arch. Jongstra-Bilen et al. [94] show the contrast between atheroprone regions, where they observed many CD68 positive cells, a marker of macrophages, and the higher curvature of the aortic arch of mice (Figure 1.18).

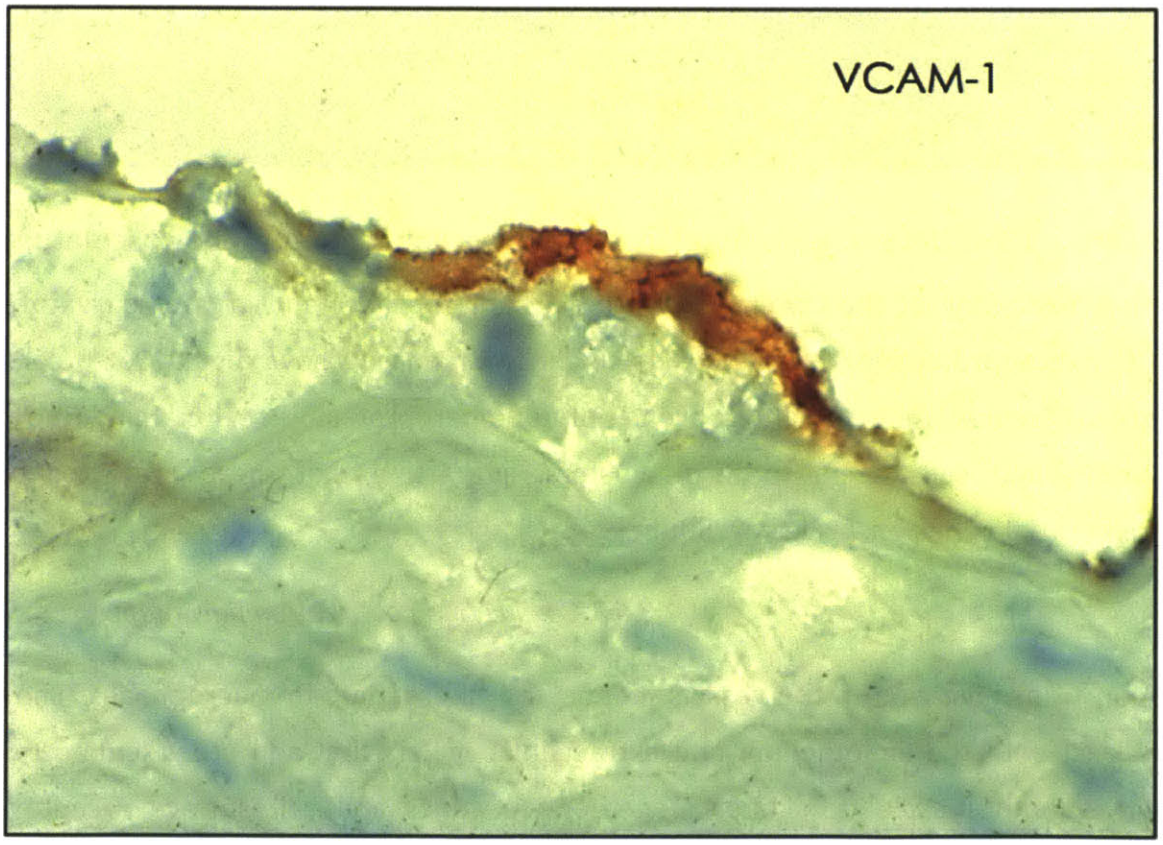

Figure 1.17: Monocyte transmigration is an early event in atherogenesis.

Staining for the adhesion molecule VCAM-1 (orange) in an atherosclerotic lesion. Two monocytes have transmigrated through the activated endothelium and are sitting in the subendothelial space above the basement membrane, seen as a wavy set of fibers. This event constitutes a milestone in the pathogenesis of atherosclerosis and begins the inflammatory cascade [95].

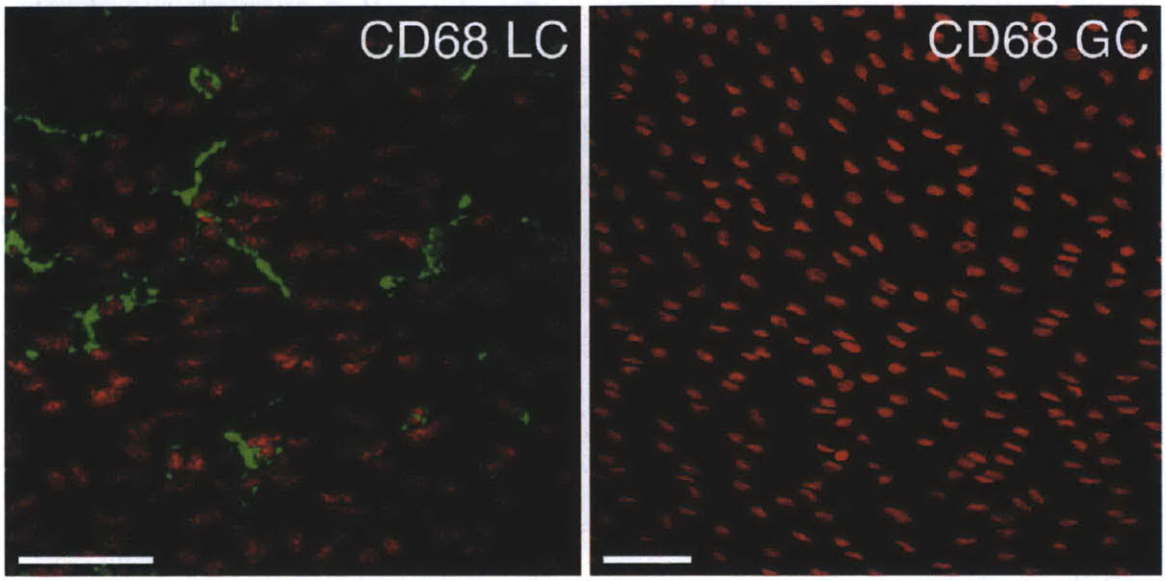

Figure 1.18: CD68+ cells accumulate in atheroprone regions of the vasculature. Immunostaining of the lower curvature (LC; atheroprone) and greater curvature (GC; atheroprotective) of C57BL6 mice fed a standard chow diet. CD68+ cells (green) accumulate in the atheroprone but not atheroprotective region. In addition, the myeloid cells seem to form clusters, suggesting that there are sites of preferential adhesion. Scale bar: 50μm [94].

1.3.6.2.4.4 M1/M2 polarization paradigm

Upon transmigration in the vessels monocytes differentiate to macrophages. They interact with the endothelium and extracellular matrix first and other leukocytes and smooth muscle cells later. Together, cytokines and cell surface receptor-mediated interactions can activate macrophages. M1 or "classical" activation is described as the result of interferon-γ (IFN-γ) or TNF-α priming and is associated with the propagation of inflammation during atherogenesis, while M2 or "anti-

inflammatory" phenotype following IL-4 and IL-13 stimulation is thought to correlate with the resolution of inflammation [96]. At the gene expression level, markers of M1 polarization include TNF and NOS2, and IL10 and ARG1 for the M2 phenotype, while respectively CD284 and CD206 at the protein level. This canonical scheme is obviously a conceptual canvas but other states of polarization have been observed [97]. The activation state of macrophages during atherogenesis is dynamic and should be seen as a distribution spanning the M1/M2 spectrum. In the processes described above, the role and influence of the phenotype of the endothelium is largely unknown.

1.3.7 In vitro models of monocyte transmigration

Many *in vitro* models have been developed to study the interaction of leukocytes and endothelial cells since the seminal paper from Beesley et al. [98] in 1978 that described the co-culture of leukocytes with endothelial cells. *In vitro* models got increasingly elaborate, from adhesion studies in endothelial co-culture with monocytic cells [99] to models build on collagenous gels that showed transmigration of monocytes and homing in the matrix as well as reverse transmigration [100]. Later, tubular vascular constructs exposed to flow have been used to investigate monocyte recruitment [101, 102].

1.4 Interactions between EC and monocytes

Several aspects of the mutual interactions between endothelial cell and monocytes have been described. Monocytes have proliferative [103, 104] and angiogenic [105] potential. Yet, little is known about the interplay between these two types of cells under flow.

1.5 Objective of the project

From the immense legacy of the Italian film director, Sergio Leone, we remember that any great plot has three main characters. In our case, we integrated the canonical constituents of the atherogenesis triad: the regulator (the endothelium), the effector (the monocytes), and the trigger (aberrant flow) to uncover novel

interactions that dictate the progression of atherosclerosis. Ironically, Leone died of a heart attack, the most common and visible clinical manifestation of intimal hyperplasia, which underlines the

Our objective was to build a versatile *in vitro* system to that will encompass both critical cells involved in atherogenesis as well as the key mechanical forces implicated in the pathogenesis.

Atherogenesis is a complex process that involves many cellular participants including endothelial cells, leukocytes, and environmental cues such as lipids and mechanical forces. *In vivo* studies of atherogenesis are extremely insightful because they combine all these aspects and thus give a true image of the disease. They provide an invaluable platform to make critical observations over long periods of time and can effectively probe the impact of specific genes on the progression of a disease. Yet, when it comes to dissecting the molecular pathways underlying the insightful observations, their complexity often overshadows their truthfulness.

In vitro models, on the contrary, are, by construction, partial images of a disease since they lack completeness. The advantage of a simplified system where the number of variables can be greatly reduced, however, is to efficiently delineate the pathways at play. A good model is one that is elaborate enough to capture the phenomenon studied, but simple enough to be able to delineate and elucidate the interactions. I hope we have been able to show earlier in this text that cells and in particular endothelial cells respond to many stimuli. Given the intricacy of cell:cell interactions, we rationalized that increasing the number of cell types in our model would make the problem intractable and suffer the drawbacks from an *in vitro* model while offering a fragmentary view. Hence, we opted for a dual-cell type model. Naturally, we chose endothelial cells since they coordinate the disease from the beginning, and monocyte because their dysfunctional progeny, the lipid-laden foam cells, make up for a substantial fraction of the mature plaque. We also rationalized, as demonstrated by the rich body of experimental data presented above, that the

mechanical forces including fluid forces and the effect of the substrate are essential to the genesis of the disease.

Previous *in vitro* models of endothelial:monocytes co-cultures investigated monocyte adhesion under flow [102, 106] but none looked at how each type of cell modifies the state or phenotype of the other. Although it is well established that cytokines can influence both atheroprone endothelium and transmigrating monocytes, cell:cell communication in the context of flow is unclear. We present in Figure 1.19, the scheme of project i.e. our goal is to build an *in vitro* model that can probe the interactions between endothelial cells and monocytes under atheroprone and atheroprotective flow.

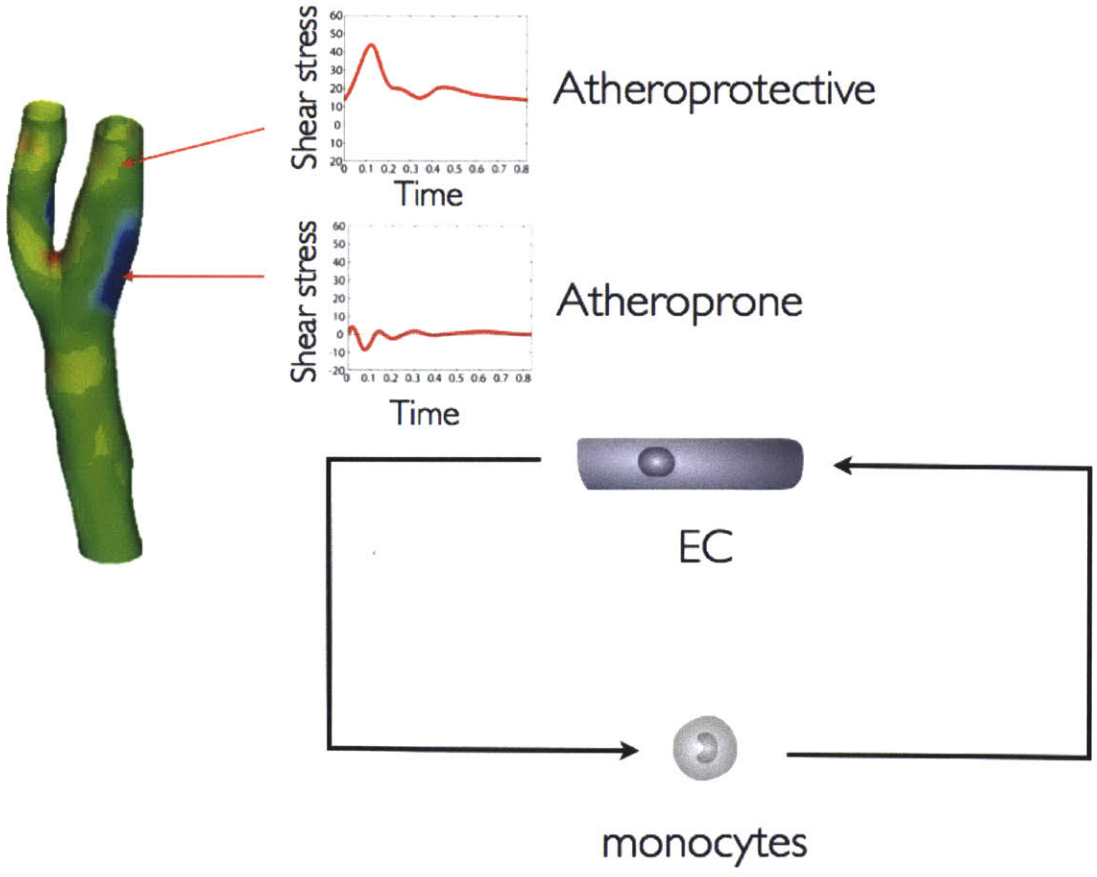

Figure 1.19: Study of the interactions of endothelial cells and monocyte under atheroprone and atheroprotective flow.

The triad endothelial cells, monocytes and flow is omnipresent and essential in atherogenesis. Our goal is to develop an *in vitro* model that can investigate the two-way interactions between endothelium and monocytes under atheroprone and atheroprotective flow.

2 Establishment and characterization of a novel *in vitro* model of transmigration under flow

2.1 Introduction

The variety of atherogenesis models scales with the complexity of the disease. Historically, TNF-α stimulated monolayers of endothelial cells have been used to understand the properties of the inflamed endothelium and the leukocyte adhesion cascade. That was when inflammation emerged again – after having been postulated by the patriarchs Rayer, Hodgson and Virchow – as a central process in the pathogenesis of atherosclerosis. In 1957, Duguid and Roberson [65], followed by McDonald [107] postulated that flow and in particular high shear flow may correlate with atheroprone sites. Fry joined them in showing that there is an upper limit of WSS above which the endothelium suffers irreversible damages that could cause fatty streaking [66]. Caro sought to prove the opposite conjecture: that low shear stress correlates with atheroprone regions [68]. Throughout the 60s and 70s several groups contributed evidence incriminating either low or high shear stress as a stimulus for atherogenesis. Today, we recognize the meticulous observations made by Caro who predicated correctly that low shear stress correlates with the formation of atheroma notably through an increase in the vessel's permeability, which then accumulates and modifies lipids.

Yet, the flow hypothesis lacked crucial *in vitro* evidence that could decorrelate the hemodynamics to the mass transport of molecules. Could flow alone cause endothelial dysfunction? And if so, what type of flow could be incriminated? In 1981, Dewey, Gimbrone and colleagues presented the first *in vitro* model able to apply flow on endothelial cells [108] and lead the way to studying the effects of flow on the endothelium. Their early model has improved and is now able to apply more realistic shear stress waveforms present in the human circulation on endothelial cells. Others have used matrices to study transmigration, differentiation and lipid uptake of monocyte/macrophages [100, 102, 109-111].

Here, we combine the unique flow apparatus pioneered by Dewey and Gimbrone, modernized by García-Cardeña and colleagues, with advanced transmigration models of monocytes to create a novel *in vitro* model. In essence, we associate the power of culturing endothelial cells under realistic human waveforms in the presence of monocytes and a subendothelial space to investigate a timely problem with high translational potential.

2.2 Materials and methods

Cell cultures

Endothelial cell cultures Primary Human Umbilical Vein Endothelial Cells (HUVECs) were isolated and cultured in our Core Facility as previously described [112]. All HUVEC are used between passages 2-4. HUVECs were cultured in EGM2 (Lonza) with an additional 5% Fetal Calf Serum (FCS) on gelatin-coated tissue culture plates or fibronectin-coated collagen gel. Cells were passaged by detachment with trypsin and split 1 to 4. Cells and debris were removed by centrifugation (5 minutes, 500g). Cells were cultured under standard conditions (37°C, 5% CO2, Heracell).

For al flow experiments, HUVEC were plated at a density of 60,000 cells/cm2 on gelatin-coated plasma-treated custom plastic plates or fibronectin-coated collagen gels for 24h in static conditions then subjected to flow.

Monocytes cultures Human THP-1 monocytes were from ATCC (TIB-202). They were cultured in RPMI-1640 (ATCC or Lonza) containing 2 mM L-glutamine, and 10 mM HEPES and 1 mM sodium pyruvate, supplemented with 10% FCS. Cells were expanded according to the manufacturer's recommendations, aliquoted and kept in a 5% DMSO solution, in liquid nitrogen at -196°C.

All FCS used for cell culture was heat inactivated, aliquoted and kept at -20°C.

Chemicals and reagents

Cell membrane fluorescent dyes In appropriate cases, cells were stained with CellTracker Green or Orange (Invitrogen) at 5 μM in culture medium for 30 min in the incubator. The cells were then rinsed, spun (5 minutes, 500g) and resuspended in dye-free culture medium.

Molecules and cytokines Phorbol 12-myristate 13-acetate (PMA) and LPS were from Sigma-Aldrich (P8139); IFN-γ was from R&D Systems (285-IF-100); IL-4 was from BD Bioscience (554605) and IL-13 was from Life Technologies (PHC0134). In some gels, we added some Acetylated-Low Density Lipoproteins (Ac-LDL; Biomedical Technologies) at a concentration of 100 μg/mL of gel.

Matrix

Collagen gels were made from 57.1% v/v bovine collagen type I (3 mg/mL, PureCol; Advanced BioMatrix) mixed with 35.7% v/v 0.05 N NaOH buffered in HEPES (2.2 grams of NaHCO3, 2.77 grams HEPES, 0.1 N NaOH 50 ml add LPS-free water to a final volume of 100ml and filter solution) and supplemented with 7.1% v/v 10x M199 (Sigma-Aldrich).

The gels were gently mixed on ice to avoid bubbles and spread on plasma-treated polystyrene plates. The gels were allowed to polymerize at 37°C in the incubator for 1h and 30min. Then they were submerged with full EGM-2 culture medium and used within a week. Prior to seeding with endothelial cells, the gels were fibronectin-coated for 30 min (Sigma-Aldrich, 50μg/mL).

Cells cultured on gels were either analyzed *in situ* for immunofluorescence experiments, lysed directly for gene expression experiments or detached by digesting the matrix with warm collagenase D (2mg/mL; Roche) in M199 medium for 40 minutes at 37°C. Cells were then filtered through a nylon mesh (50 μm pores; Becton Dickinson).

Atomic Force Microscopy

The stiffness of the collagen gels was measured with atomic force microscopy (AFM; MFP-3D Asylum Research) using cantilevers with 20 or 45μm polystyrene spheres at the end. The cantilevers spring constant varied between 0.2 and 35 N/m. Results were analyzed with Asylum Research software. The curves were fitted to Hertzian contact models to deduce Young's modulus. A grid of 4 by 4 points through a square of 10μm was probed to account for local variability.

Fluorescence-Activated Cell Sorting

Cells were detached, treated with an Fc receptor blocking solution and stained using antibodies as recommended by the manufacturer. Isotype controls were also used as recommended by the manufacturer. Samples were incubated with nuclear stains such as PI (1μg per 1 million cells; BD Bioscience) and analyzed on a FACSCalibur flow cytometer (Becton Dickinson) and the results were processed with FlowJo (Tree Star, Inc.). Cell debris were excluded according to the forward (FSC) and side scatter (SSC) signal levels, doublets were excluded by plotting the height of the FSC signal versus the area of the same signal and keeping the cells on the diagonal. Finally, dead cells were excluded through the level of fluorescence in the PI channel before appropriate analysis of the signal in other channels.

The following antibodies were used (unless stated otherwise, antibodies were used according to the manufacturer's recommendation): primary mouse anti-human VCAM-1, ICAM-1 and E-selectin antibodies were made in-house and used with goat anti-mouse Alexa 488 IgG secondary antibody (1:400; Life Technologies).

Cellular and molecular assays

ELISA assay We measured the concentration of cytokines in supernatants using an IL-1B ELISA sandwich assay kit (BioLegend) following the manufacturer's recommendations and quantified absorbance with an ELISA plate reader (Molecular Devices). Results were analyzed with Excel (Microsoft).

Phagocytosis assay We seeded $7.5.10^6$ red fluorescent 2μm in diameter latex beads (Sigma-Aldrich) into the gel mixture to assess phagocytosis in

transmigrated THP-1. Endothelial and THP-1 cells were prepared as described previously.

Macrophage polarization assay and activation of endothelial cells We used PMA at a concentration of 320 nM for 18h in complete THP-1 culture medium to differentiate THP-1 monocytes into adhering macrophages. M1 and M2 polarization of THP-1 was achieved by respectively using a cocktail of LPS (100 ng/mL) and IFN-γ (20 ng/mL) or IL-4 (20 ng/mL) and IL-13 (20 ng/mL) for 24h. After PMA treatment, "plain" macrophages (MΦ) were kept in RPMI-1640 medium with 10% FCS. We collected the supernatant of M1, M2 and MΦ and transferred it onto three different confluent cultures of endothelial cells for 24h. Supernatant was collected and stored at -80°C before measurement of IL-1 concentrations by ELISA sandwich assay. Then, we rinsed thoroughly the endothelial cells and added complete EGM-2 culture medium to all for 24h. After this period, supernatant was collected again and stored at -80°C before measurement of IL-1 concentrations by ELISA sandwich assay. In the meantime all three cultures of endothelial cells were detached with trypsin and stained with a VCAM-1 antibody for FACS analysis.

Hemodynamic Shear Stress in vitro System

Figure 2.1 is a 3D model of the flow apparatus used for the flow experiments. The experiments implementing the atheroprotective and atheroprone shear stress waveforms were conducted in a modified dynamic flow system as previously described [8]. Briefly, shear plates compatible with our flow apparatus were made from sterile components. Polystyrene disks (yellow) were sandwiched between two metallic frames. Gels were made on the polystyrene surface and cells were seeded on top of the gels. The shear plates were assembled in the flow apparatus comprising a base and top part. The top part features a rotating cone (orange) immerged in the shear medium. The polystyrene cone, which has an angle of 0.5 degree, is linked to a step motor via a belt (black). The motor is connected to a computer and controlled by dedicated software. The whole apparatus sits on a Nikon TE-2000 Eclipse microscope that can produce live imaging of the cells.

For these experiments, the culture medium was supplemented with 1.7 % dextran (MW 1.5-2.8 million, Sigma-Aldrich) to increase media viscosity to 2.1 cP. The flow system was enclosed in clear plastic case (not shown) and maintained at 37°C with 5% CO2 in a humidified environment.

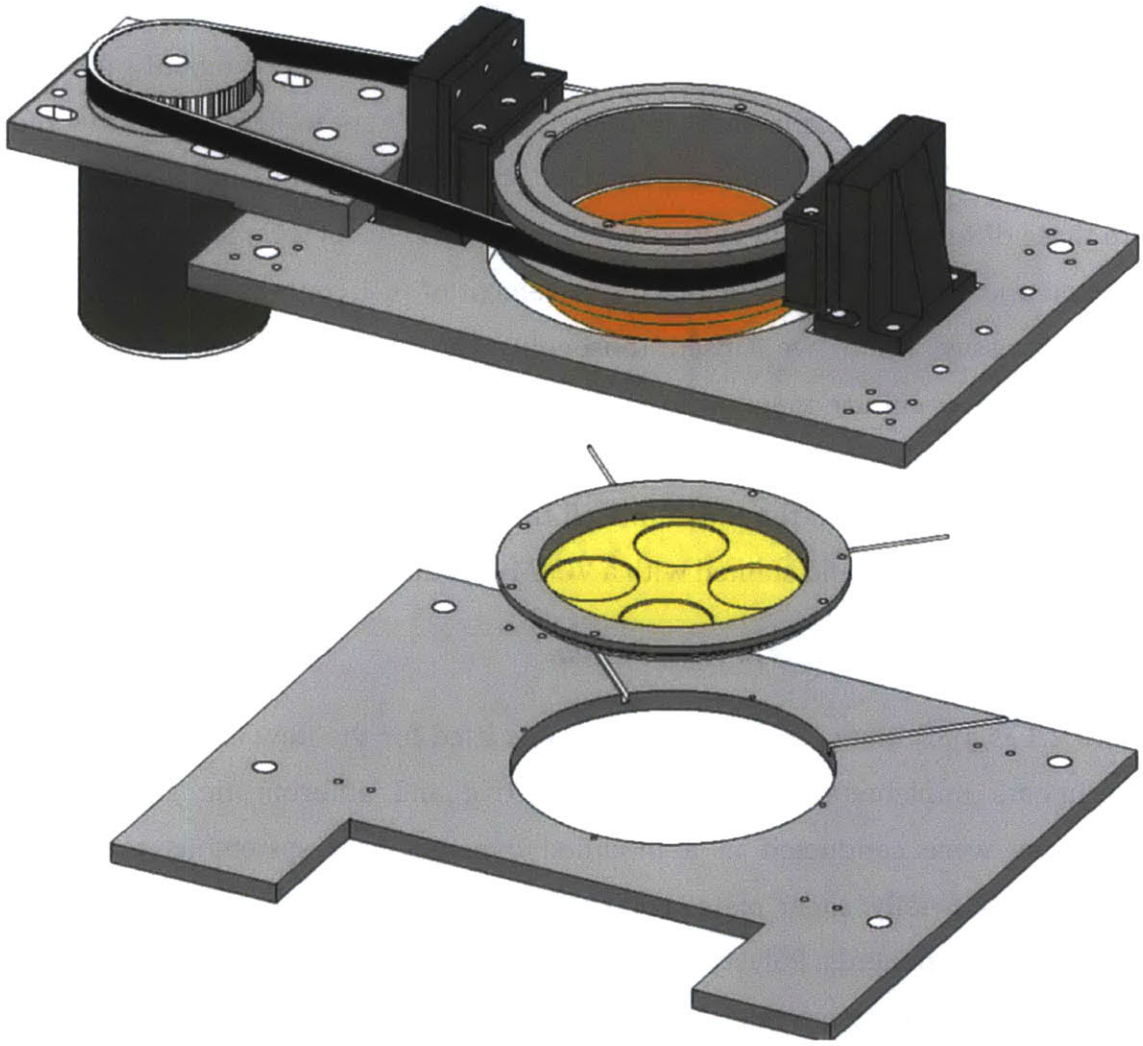

Figure 2.1: Flow apparatus.

3D model of the flow apparatus. It comprises three functional assemblies. At the bottom, a base is securely fixed on a microscope stage. In the middle, the shear plate is composed of a polystyrene disk (yellow) mounted in between a circular metallic frame and supporting metallic base. The shear plate features an inlet and outlet port

for medium renewal. The top part is contains the rotating cone (orange) that produces the controlled WSS on the cells. The cone is attached the rotating metallic cylinder connected to a motor via a belt (black). The cone is precisely positioned with respect to the cells thanks to two micrometric screws on the z-axis. Dedicated software controls the motion of the cone. (Courtesy of Dr. Guillermo García-Cardeña).

Phase contrast microscopy

Cells were routinely imaged with a phase-contrast microscope (Nikon Eclipse 2000-E or 2000-S) equipped with 4X, 10X and 20X objectives and an Insight 2 camera (SPOT). Sequential images of flow experiments were acquired at 10 min to 1h intervals. Images were analyzed using ImageJ or SPOT software.

Immunofluorescence staining and epifluorescence microscopy

Cells on polystyrene dishes were washed, fixed (10 minutes, 4% paraformaldehyde, 37°C), aldehydes quenched with a 0.1% Glycine solution, permeabilized with 0.25% Triton X-100, and incubated with primary antibodies overnight at 4°C. Fluorescently-labeled secondary antibodies were added for two hours at room temperature in the dark. Cells were then washed, coverslipped (ProLong Gold antifade medium, Invitrogen), and imaged using an epifluorescence microscope (Nikon TE-2000-E Eclipse) equipped with an Insight 2 camera (SPOT). Images were analyzed using ImageJ.

Laser scanning confocal microscopy

Cells on polystyrene dishes were washed, fixed (10 minutes, 4% paraformaldehyde, 37°C), aldehydes quenched with a 0.1% Glycine solution, permeabilized with 0.25% Triton X-100, and incubated with primary antibodies overnight at 4°C. Fluorescently-labeled secondary antibodies were added for two hours at room temperature in the dark. Cells were then washed, coverslipped (ProLong Gold

antifade medium, Life Technologies), and imaged using a Zeiss LSM710 Laser scanning confocal microscope. Images were analyzed with Zeiss software or ImageJ.

Scanning electron microscopy

Cells were fixed with a mixture of 2% formaldehyde and 2.5 % glutaraldehyde in 0.1 M Sodium Cacodylate buffer, pH 7.4, embedded in epoxy resin, cut in thin sections, metal-coated (Edwards Auto 306 Vacuum Evaporator) and imaged with a conventional transmission electron microscope (JEOL 1200EX) equipped with an AMT 2k CCD camera.

Statistics

All experiments were performed at least three times independently (HUVECs from a different culture each time). Results are expressed as mean ± standard deviation. Comparison of two groups was performed using a student's t-test. $p < 0.05$ was taken as statistically significant.

2.3 Results

We have extensively characterized our novel model of transmigration under flow: we have measured the mechanical properties of the matrix, we have described the state of both the endothelium and the THP-1 monocytes and we have imaged transmigrating cells under static conditions and flow. Here we summarize all the experiments that demonstrate functionality of the model.

2.3.1 Description of the model

Our novel model of transmigration combines the flow capabilities our unique flow apparatus to specialized matrices that permit the growth of endothelial monolayers and support monocyte transmigration. Figure 26 presents the architecture of the system. Endothelial cells are cultured to confluence on a fibronectin-coated collagenous matrix, then co-cultured with THP-1 cells in a flow chamber. The flow

chamber comprises a rotating cone (Figure 2.2) that imprints a specific waveform of WSS.

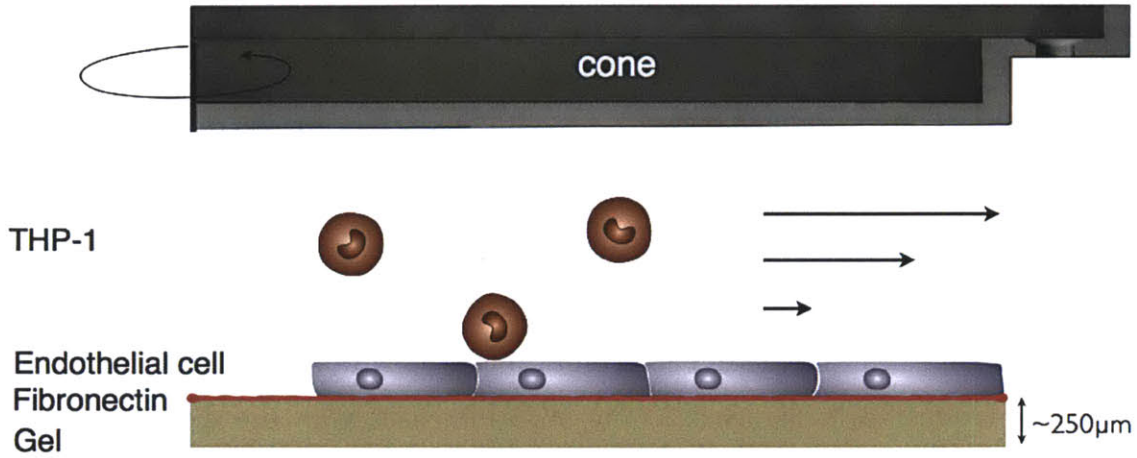

Figure 2.2: Description of the model.

Global architecture of our *in vitro* transmigration model (we only show half of the system since it is axisymmetric; the axis of symmetry is vertical and goes through the left side of the illustration). Endothelial cells are cultured on a 250µm thick collagen type I matrix coated with fibronectin. THP-1 monocytes are introduced as freely floating cells in the supernatant. The rotation of the immerged cone produces the desired WSS. The matrix was engineered to allow the growth of an endothelial monolayer, and transmigration and differentiation of monocytes. A bottle containing fresh culture medium is connected to the inlet of the system so that it is constantly perfused; at the same time medium is drawn from the chamber to ensure the turnaround of growth factors and serum and prevent the accumulation of waste. The system is perfused at a rate of ~50mL per 24h.

The cone is immerged in the culture medium. When in motion, the cone drags the culture medium thanks to its viscosity. Theoretical calculations predict that an infinite cone with a low slope or high aperture (close to 180 degrees), rotating over an infinite plate in a Newtonian fluid will produce a linear velocity profile normal to the plate. Indeed, the velocity of the fluid is null at the surface of the plate and equal to the cone's velocity at the cone. Thus using the mathematical definition of WSS

from Figure 1.2 (c.f. paragraph Characteristics of flow) is simply the product of the viscosity of the medium by the slope of the velocity distribution normal to the plate. The formula that describes the radial evolution of WSS on the plate is:

$$WSS = \mu\omega \frac{r}{h + r\alpha}$$

where, μ is the dynamic viscosity of the medium in Pa.s, ω is the angular velocity in rad.s^{-1}, α is the complementary of the half angle of the cone (here 0.5 degree) and r the radius from the axis of the cone. Additional complications arise from the fact that the cone is not touching the plate but there is the finite distance h, between the vertex of the cone and the plate. The evolution of WSS with radius from the axis of the system is plotted in Figure 2.3. The WSS increases with the distance to the center of the plate for a given angular speed. To avoid phenotypic variability between cells at the center and at the periphery, we excluded a central disk by using a central Teflon insert during the making of the gels and endothelial cell seeding. This results in shear stress values that vary within 10% of the median value between the inner and outer diameter of culture.

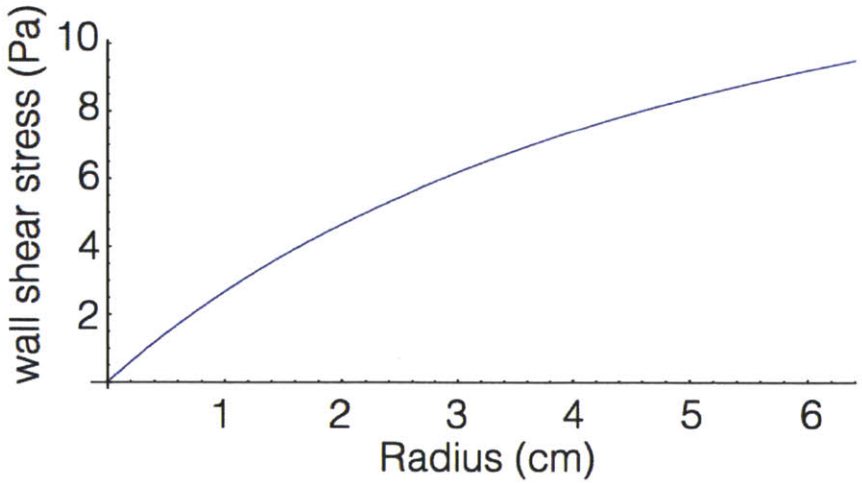

Figure 2.3: Wall-shear stress is quasi-homogenous across our flow chamber.

Intrinsically cone-and-plate flow chambers produce increasing WSS away from the center. The plot shows how the WSS evolves with distance from the center of the system for a given angular speed of the cone. The radially variable WSS is

problematic, but we go around this variability by excluding the center of the plate that does get gel or cells.

2.3.2 Fibronectin-coated gels

2.3.2.1 Composition

The matrix used in our system is a type I collagenous gel extracted from bovine hide. It is made from 57.1% collagen mixed with 35.7% of an NaOH solution buffered in HEPES supplemented with 7.1% concentrated M199. We adjusted the volume of the solution of each plate with respect to the surface area to obtain a thickness ~250μm (Figure 2.4).

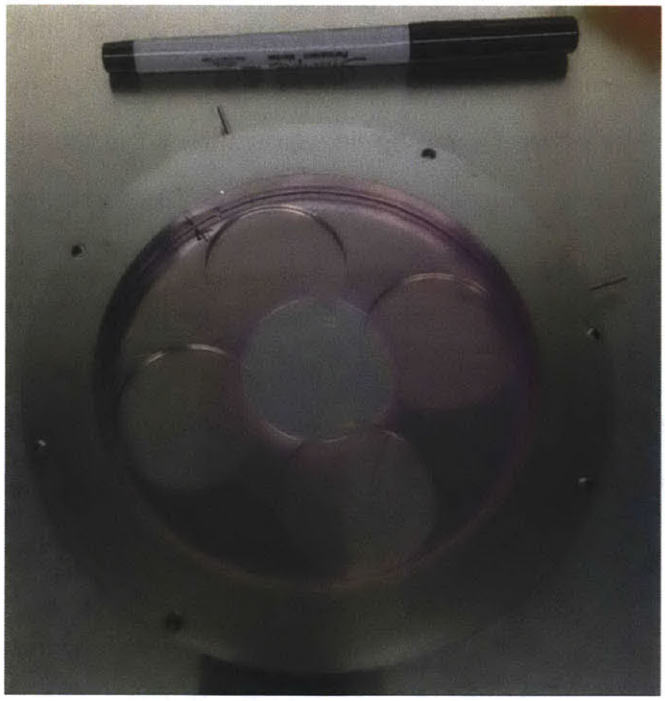

Figure 2.4: Picture of a shear plate coated with the polymerized gel.

The pink color comes from the addition of concentrated M199. At the center, the Teflon insert excludes the central regions from receiving gel and cells.

2.3.2.2 Mechanical properties of the gel

We used AFM to characterize the stiffness of our gels. AFM is a sensitive tool that can measure the topology of surfaces and their stiffness when used in indentation

mode. A cantilever with a tip (cone, pyramid, sphere, cylinder etc.) is lowered on the sample that produces a deflection. The deflection is a function of the cantilever and sample's stiffness. The deflection is quantified by the change in position of a reflected laser beam pointed at the cantilever's tip (Figure 2.5). The machine's raw output is the voltage measured by photodetector (proportional to the deflection) that needs to be converted to a force following Hooke's law:

$F = k\delta$

where F is the force in Newton, k is the spring constant of the cantilever in N/m and δ is the deflection of the cantilever in m. Experimentally this is achieved by first measuring the deflection sensitivity of the cantilever (in nm/V). It is the voltage generated by a given deflection. This was measured on a hard surface (glass slide) to avoid any indentation of the surface. The second step is to measure the spring constant of the cantilever, which can be precisely measured using a thermal method. The cantilever is extremely thin, thus the collision of air molecules on its surface due to thermal energy creates Brownian motion of the cantilever. The system has basically only one degree of freedom, thus it oscillates around a position of equilibrium, which can be accurately described as a harmonic oscillator. In this framework the frequency of the oscillations is only a function of the cantilever's mass and spring constant. Ultimately, the oscillation frequency is linked to the thermal energy of the system using the equipartition theorem (from thermodynamics) that states that the kinetic energy is half of the thermal energy stored in the system. This method is much more precise than deriving the spring constant from the cantilever's dimension since the thickness is extremely small and variable through the length of the beam. Experimentally, we recorded the voltage change of the free-floating cantilever in air and culture medium in the frequency domain (Figure 2.6). The resonance peak being a function of the spring constant, we were able to calculate the spring constant of the cantilever. We tried three sets of probes with respective values around 0.2 N/m, 18 N/m and 35 N/m.

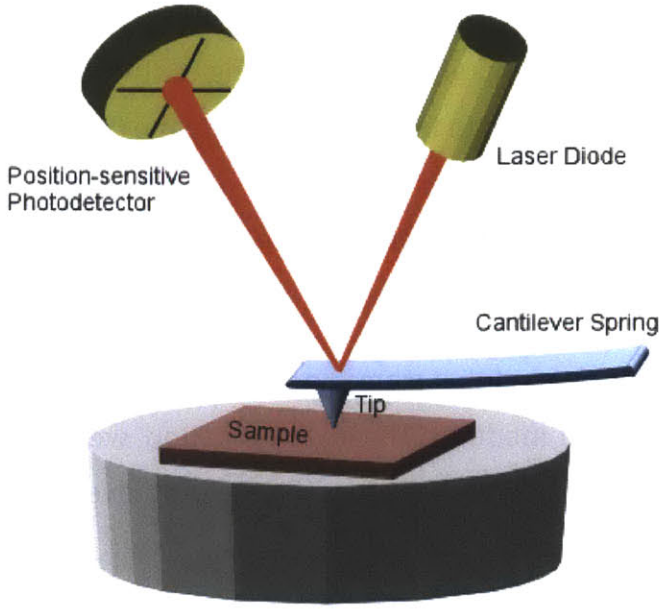

Figure 2.5: Method of action of an AFM apparatus.

A laser spot is reflected on the tip of a cantilever and its position is monitored by an array of photodiodes. When the cantilever contacts the sample, it is deflected and the reflected spot changes position, which produces a voltage in the photodetector. Piezoelectric actuators monitor the lowering of the base of the cantilever. (Source: http://www3.physik.uni-greifswald.de/method/afm/AFM_laser.gif).

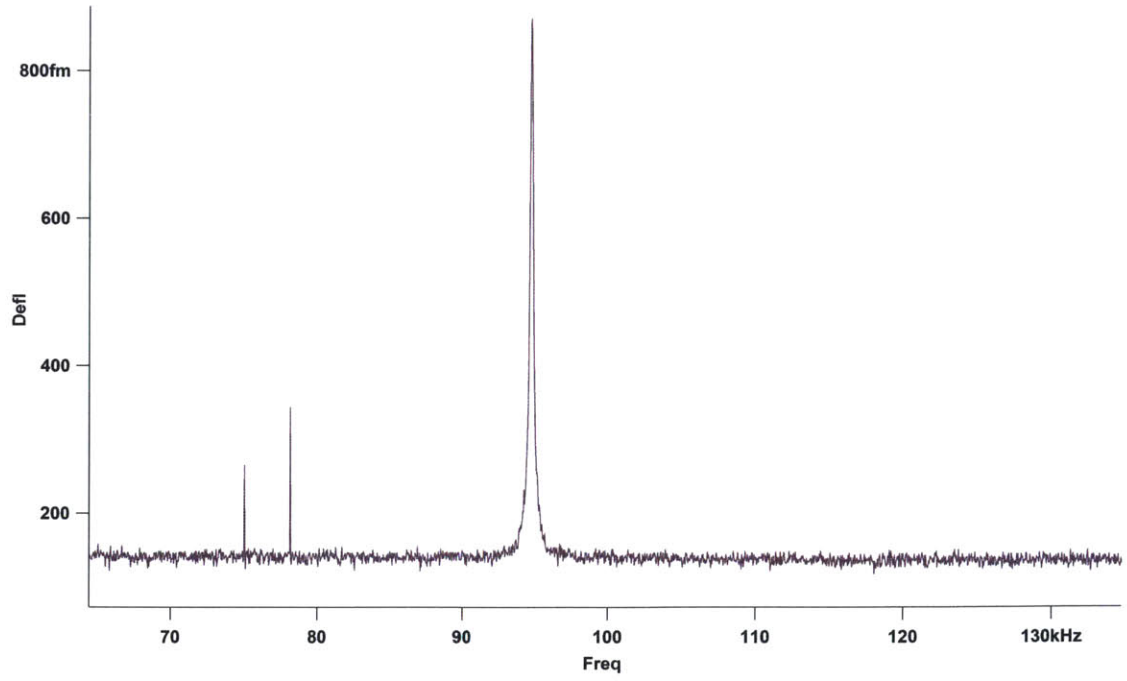

Figure 2.6: Determination of the stiffness of the cantilever probe.

Measurements of the motion of the free-floating cantilever. The voltage fluctuations are converted to a deflection in femtometer – note the units and sensitivity – and are plotted in the frequency domain. The peak of resonance at ~95 kHz is used to determine the spring constant of the cantilever. The two peaks at 75 kHz and 78 kHz are noise.

We calculated Young's modulus from the Hertzian theory of contact, which couples force, deformation and modulus. During indentation, we calculated and plotted the force versus the motion of the base holding the cantilever in the z-axis (Figure 2.7). We fitted the best equation model to the curve and deduced Young's modulus. Figure 2.8 presents a 4 by 4 map of Young's modulus on a square of 10 by 10μm to assess the spatial variability of the gel. From the analysis of the stiffness maps, we conclude that our gels are a monolithic solid of average Young's modulus equal to **9.3 ± 0.8 kPa**.

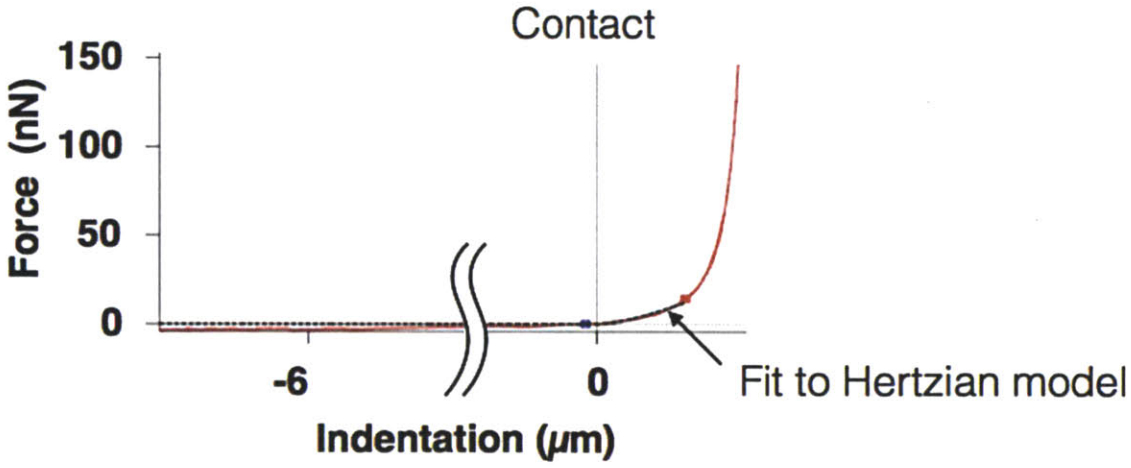

Figure 2.7: Determination of the Young's modulus of our gels.

Experimental curve of the evolution of force versus indentation (red). As soon as the sphere at the end of the cantilever contacts the gel, the force calculated from the deflection of the cantilever increases. The Hertzian model (dotted line) describes

well the experimental curve at low values of indentation. At higher indentation values, the effects of the substrate under the gel modify the Hertzian behavior.

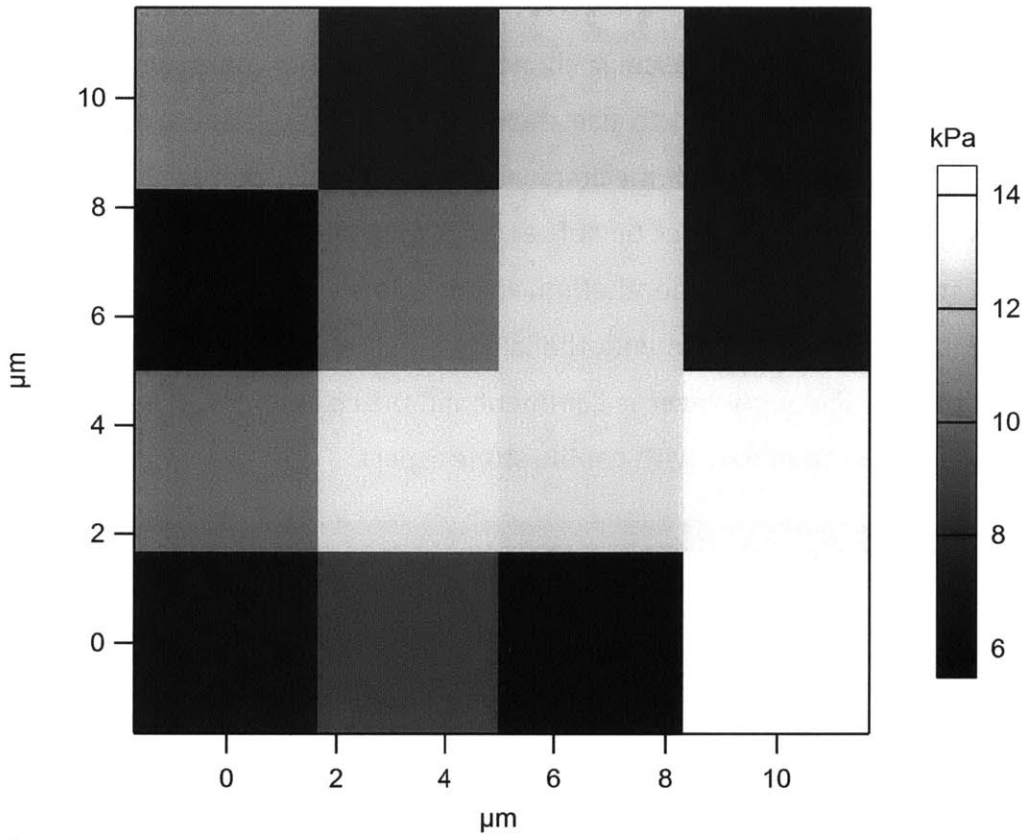

Figure 2.8: Map of stiffness in our collagenous gel.

The values range from 6 to 14 kPa, which is an acceptable variability for a biological system.

2.3.3 Human Umbilical Vein Endothelial Cells

Endothelial cells are central to atherogenesis as they sense the luminal elements and the microenvironment in the extracellular matrix and feel the fluid forces from above and strain from bellow, and respond to this stimuli by modifying their secretome and proteome. Therefore, they occupy a privileged role in our model.

We have characterized their state on the gel and under flow, and compared cells cultured on plastic under static conditions or flow because we and others, have

extensively studied these cells states. Here we report the morphology of the endothelial cells on the gel and basal levels of cell adhesion molecules.

2.3.3.1 Integrity of the monolayer

Collagen gels are used in vascular biology for various purposes, including angiogenesis assays; we wanted to use them as a matrix to home transmigrating monocytes. Thus, we tailored the mechanical properties such that cells would form monolayers – and not tubes – yet be soft enough that the monocytes could invade the gel and interact with the endothelium in the subendothelial space. Figure 2.9 shows a photomicrograph of the endothelial cells 24h after they were seeded and cultured on the gel. The monolayer is confluent and the cell morphology is similar to the one encountered on plastic with cobble stone aspect.

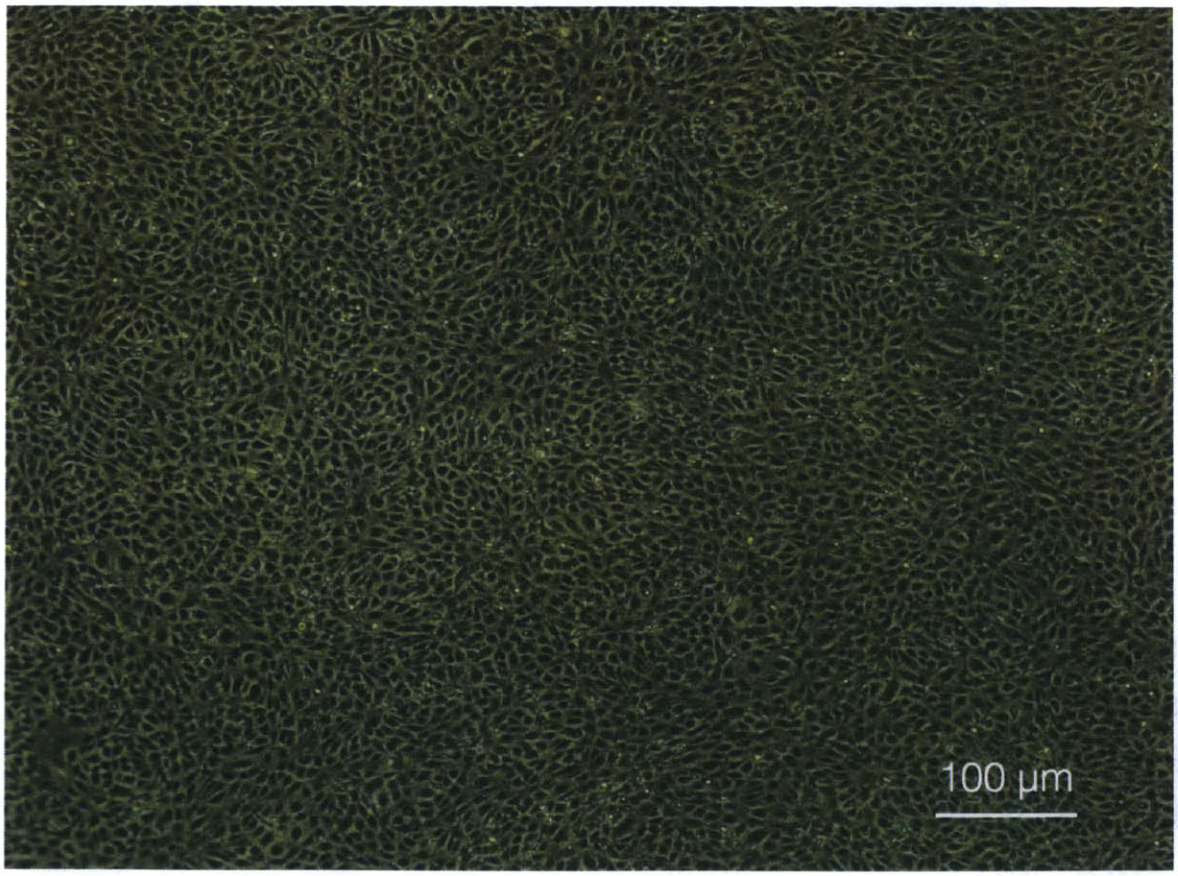

Figure 2.9: Morphology of endothelial cells after 24h of culture in static conditions on a fibronectin-coated collagen gel.

The cells are confluent and look healthy. The picture was taken on a phase contrast microscope with a 4X objective.

2.3.3.2 Cell Adhesion Molecules

Cell adhesion molecules participate in the recruitment of immune cells. They create bonds with adhesion molecules present on the leukocytes to stop their motion and escort their entry in the tissues. Among the many cell adhesion molecules, VCAM-1, ICAM-1 and E-selectin are some of the most important and potent molecules. We have measured their surface expression in static cultures to assess our starting material (Figure 2.10).

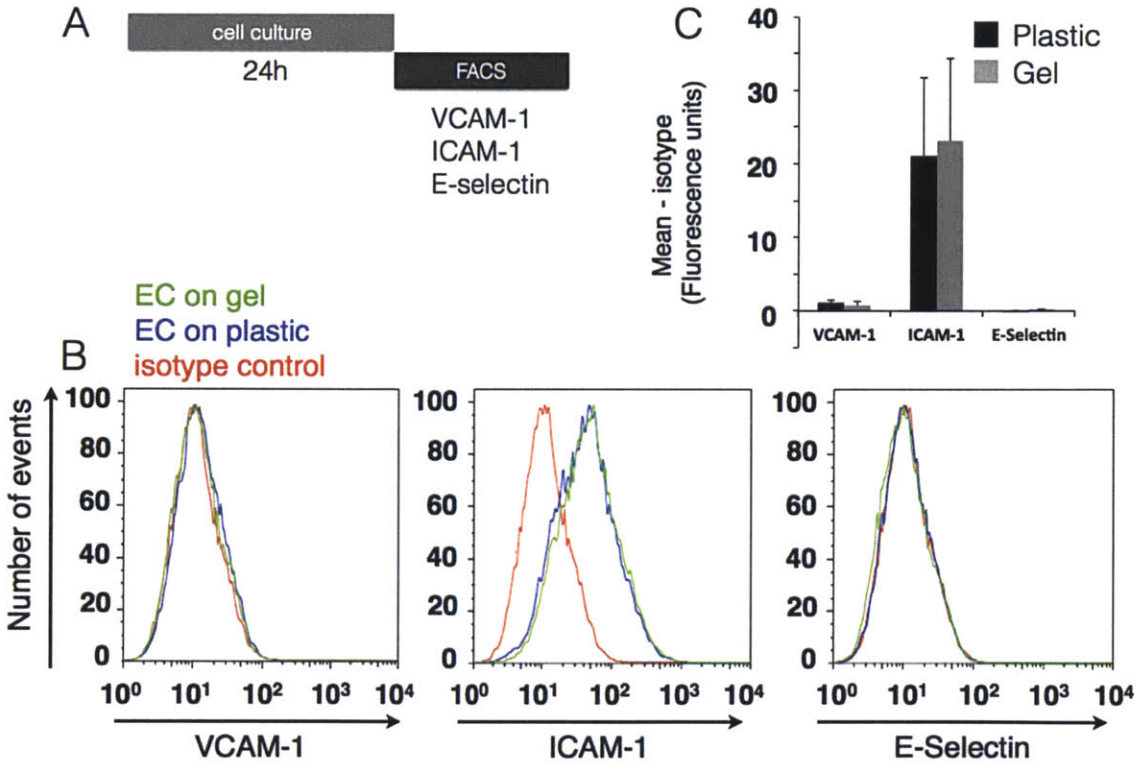

Figure 2.10: Expression of cell adhesion molecules in endothelium cultured on gel and plastic.

A. Timeline of the experiment; after 24h of culture on gel or plastic cells are detached and analyzed by FACS. B. Surface expression of VCAM-1, ICAM-1 and E-selectin on endothelial cells cultured on collagen gel (green) or plastic (blue).

Isotype control is the red trace. C. Quantification of relative average fluorescent intensity of cells stained with antibodies minus isotype control. Endothelial cells on gel express under static conditions basal levels of ICAM-1 but no VCAM-1 or E-Selectin that is comparable to cells grown on plastic.

2.3.4 THP-1

Monocyte are free-floating cells in the blood at a count of 200,000 to 900,000 per mL of blood in healthy adults [113]. They do not proliferate under normal circumstances and are easily activated by various stimuli such as cytokines, LPS or shear [114-116]. Their extraction is delicate and requires high quantities of blood from donors because the yield is only around 200,000 per mL of blood. The major isolation technique for monocytes is to extract the mononuclear cells by density gradient with Ficoll-Paque. This procedure alone causes much of the losses. Then monocytes can be tagged with antibodies and functionalized metallic microbeads to separate them from the other mononuclear cells. While building our *in vitro* model, we estimated that we would need 20+ million monocytes per experiments, which translates to 100mL of blood for each experiment. We realized that this quantity was too high for the development of a model so we engaged into searching for a model of monocyte. After a thorough review of the literature, we identified THP-1 cells as the best choice for our study. THP-1 cells are human monocytic cell line isolated from peripheral blood of infants with acute monocytic leukemia [117, 118]. THP-1 cells proliferate at a rate of approximately one division per 24h in the exponential phase, which made it convenient for use to expand large quantities of monocytes.

We have assessed the surface expression of CD14 and CD16 in THP-1 cells and their ability to differentiate and get polarized. Below, we summarize the experiments to characterize THP-1 cells.

2.3.4.1 CD14/CD16

CD14 and to a lesser extent CD16 are the two best-established markers of monocytes. As discussed in Chapter 1, there are at least three subsets of monocytes

thus it was important to us to characterize the populations present in our cultures. Figure 2.11 presents FACS data on the expression of CD14 and CD16 in THP-1 cells compared to their associated isotype controls. We observed that the CD14++CD16- population almost exclusively dominates our THP-1 cultures, with over 92% THP-1 being positive for CD14 while only under 3% express CD16. This observation is interesting because it means that we are work with a homogenous population and thus expect less variability than if several subpopulations were present.

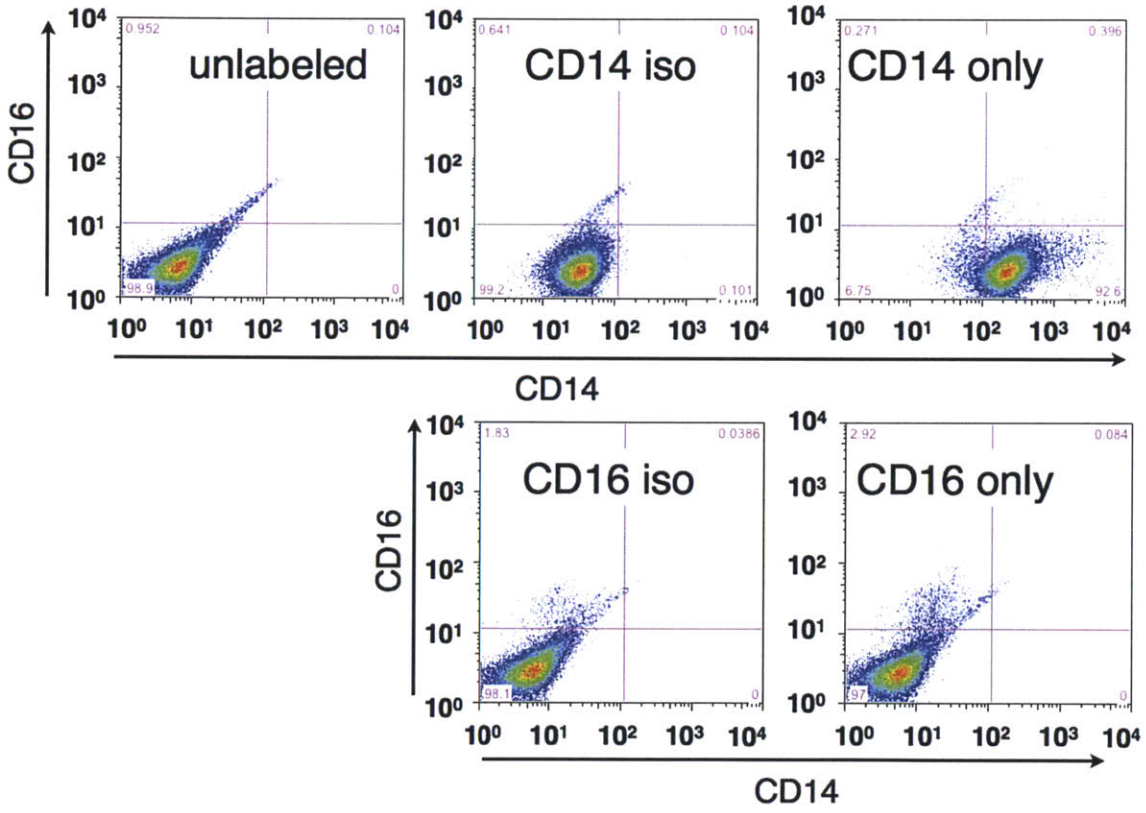

Figure 2.11: Expression levels of CD14 and CD16 in THP-1 cells compared to isotype controls.

The gates are set by the isotype controls.

2.3.4.2 M1/M2 polarization

THP-1 monocyte can be differentiated into macrophages and polarized into M1 and M2 macrophages. We showed that M1 inflammatory macrophages secrete high

levels of IL-1 but not M2 or MΦ. We also show that the supernatant from M1 macrophages but not M2 or MΦ macrophages can activate endothelial cells, as evidenced by surface expression of VCAM-1 (Figure 2.12).

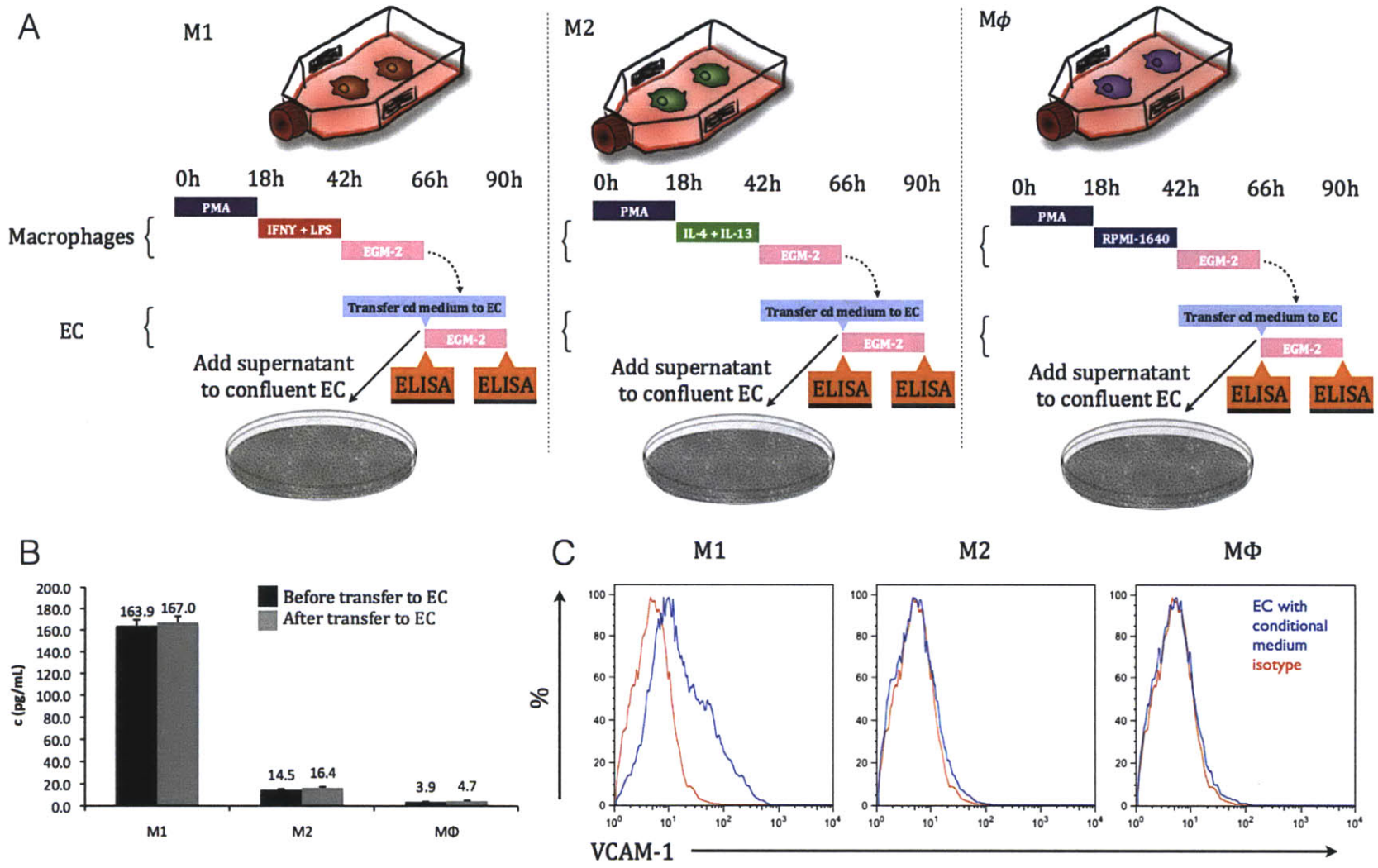
A
M1
M2
Mφ
0h
18h
42h
66h
90h
Macrophages
EC
PMA
IFNγ + LPS
IL-4 + IL-13
RPMI-1640
EGM-2
Transfer cd medium to EC
Add supernatant to confluent EC
ELISA
B
Before transfer to EC
After transfer to EC
c (pg/mL)
163.9
167.0
14.5
16.4
3.9
4.7
M1
M2
MΦ
C
M1
M2
MΦ
%
VCAM-1
EC with conditional medium
isotype

Figure 2.12: M1-macrophage secretions can activate endothelial cells through IL-1 production.

A. Flow diagram of the experimental design. Briefly, THP-1 cells are differentiated into macrophages with PMA (320 nM for 18h) then polarized to M1 or M2, using LPS (100 ng/mL) and IFN-γ (20 ng/mL) or IL-4 (20 ng/mL) and IL-13 (20 ng/mL) respectively for 24h. After PMA treatment, "plain" macrophages (MΦ) were kept in RPMI-1640 medium. B. IL-1β secretions by M1, M2 and unpolarized macrophages assessed by ELISA before and after transfer of the conditional medium onto confluent EC. C. Surface expression of VCAM-1 on EC cultured for 24h with M1, M2 and MΦ conditional medium. M1 conditional medium only can activate EC as shown by significant VCAM-1 expression **(only 2 replicates)**.

2.3.5 Transmigration

Transmigration of leukocytes in atheroprone regions is the crucial event that marks the beginning of atherogenesis. It is the first episode that profoundly modifies the ultrastructure of the vessel. We have showed that our system supports transmigration of THP-1 cells in static conditions and in the context of atheroprone and atheroprotective flow **in the absence of external pro-inflammatory stimuli such as cytokines.** We show the cell adhesion profiles of cells under flow to explain the meditators of transmigration.

2.3.5.1 Transmigration under static conditions

We first optimized the parameters of the system in static conditions. Here we report data transmigration gathered through imaging of the system. We clearly show diapedesis of THP-1 monocytes through confocal and scanning electronic microscopy.

2.3.5.1.1.1 Confocal microscopy of transmigration monocytes

We imaged the system with confocal microscopy and observed adhesion and transmigration of monocytes through a confluent monolayer of endothelial cells

(Figure 2.13). We also seeded fluorescent beads inside the gel to measure the phagocytic potential of transmigrated monocytes. As shown in Figure 2.14, transmigrated cells are able to phagocytose beads.

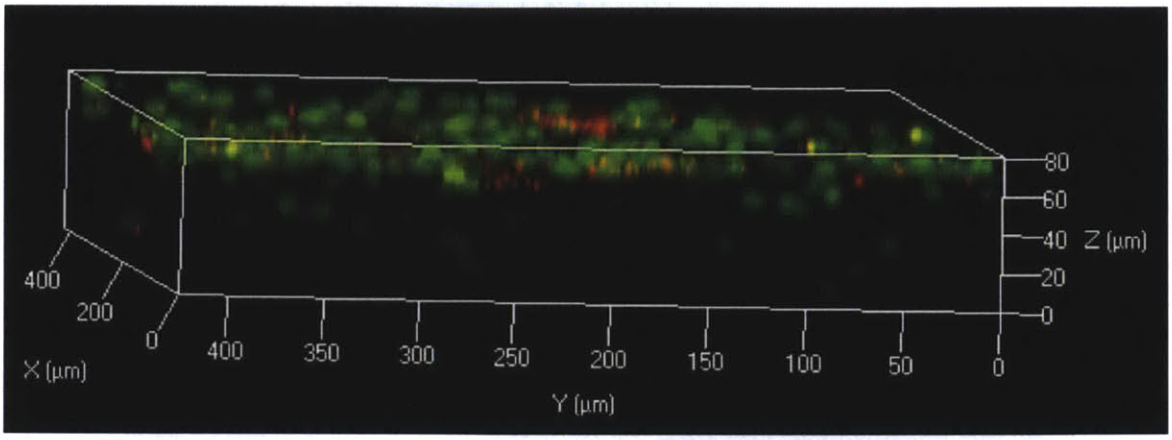

Figure 2.13: Adhesion and transmigration of THP-1 monocyte through endothelium cultured in static conditions.

The reconstruction of z-stack images acquired with confocal microscopy show adherent and transmigrated monocytes (green) through an endothelial monolayer (red) after 72h.

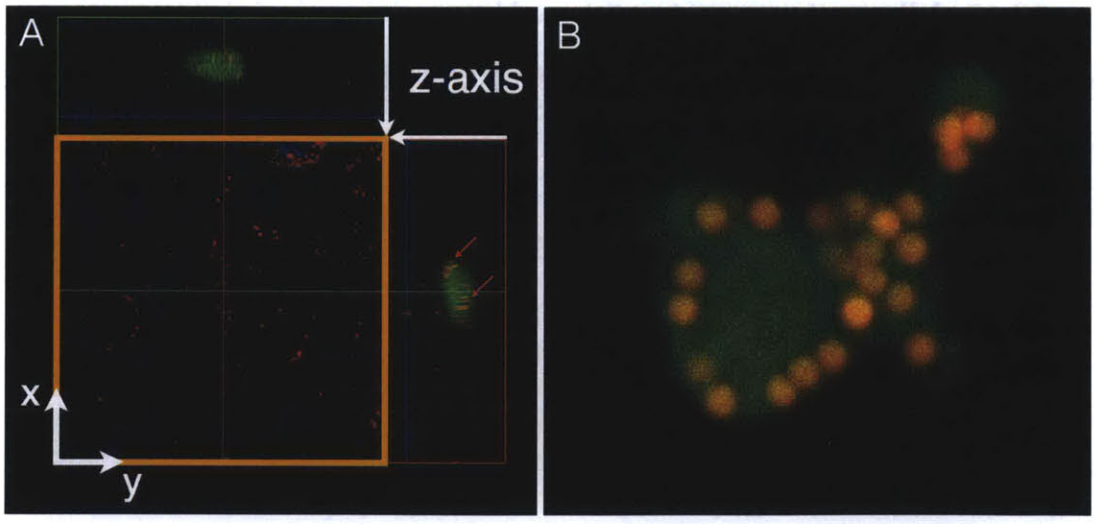

Figure 2.14: Transmigrated monocytes can phagocytose latex beads.

Phagocytosis assay. A. Fluorescent beads (red) were seeded inside the gel and green-labeled THP-1 were co-cultured over a confluent monolayer of endothelial

cells as seen on the VE-Cadherin staining (blue) in the orange-lined panel. The side views are assembled z-stacks images showing red beads inside a transmigrated THP-1. B. Close-up on a transmigrated THP-1 loaded with beads.

2.3.5.1.1.2 Scanning electron microscopy of transmigrated monocytes

Monocytes co-cultured with endothelial cells adhere to the endothelium in our system under static conditions and transmigrate. Figure 2.15 and Figure 2.16 show evidence of these processes with electron micrography.

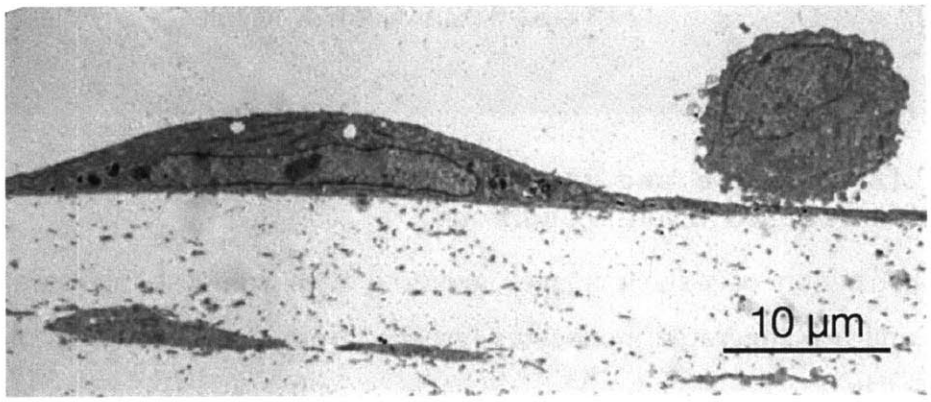

Figure 2.15: Adherent monocyte captured by scanning electron microscopy.

The endothelial cell is sitting on the collagen gel. A THP-1 monocyte tethered by the endothelial cell.

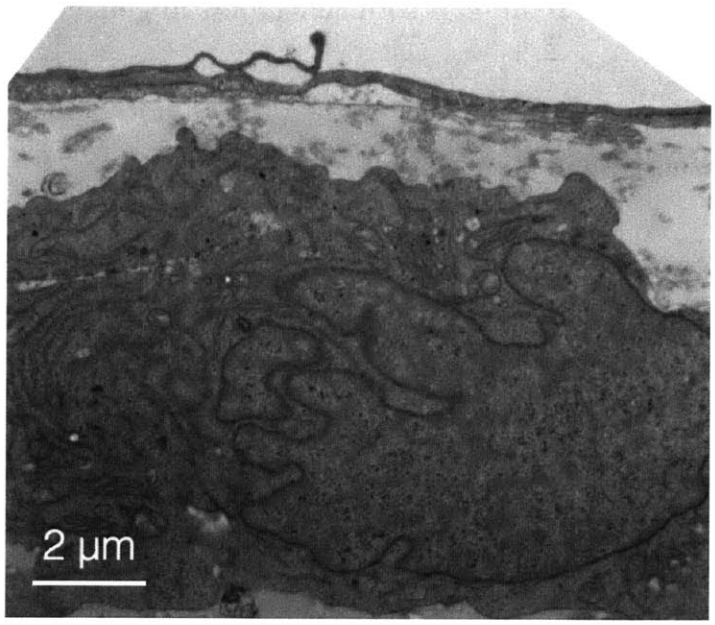

Figure 2.16: Electron micrograph showing a transmigrated monocyte.

Given its size and morphology, the transmigrated cell has the characteristics of a differentiated cell, a macrophage (72h of co-culture). At the top of the picture, the junctions between two endothelial cells can be seen.

Our novel *in vitro* model is a versatile platform that can be used with many types of matrices or additives seeded in the gel. We leveraged this advantage to further the definition of the system. We made gels that incorporated Ac-LDL, seeded endothelial cells and co-cultured them with THP-1 monocytes. After 72h of co-culture, we observed morphological evidence of differentiation and lipid engulfment and accumulation (Figure 2.17).

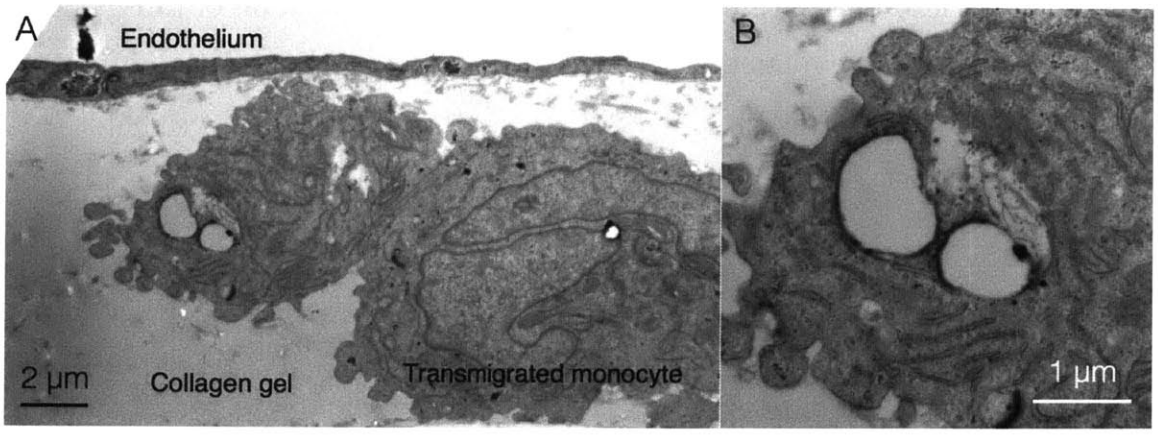

Figure 2.17: Evidence of foam cell differentiation in gels containing modified lipids.

A and B. Two transmigrated THP-1 featuring morphological evidence of macrophage differentiation.

2.3.5.2 Characterization of the system under flow

Flow-mediated atheroprotection, or the lack thereof, influences the phenotype of the endothelium and results in localized regions of inflamed highly permeable endothelium traversed by monocytes. KLF2 acts as a critical integrator of flow-mediated endothelial vasoprotection, which expression controls many mediators of inflammation including endothelial:monocyte interactions. In this section, we report data on the expression of endothelial KLF2 (relative mRNA expression), cell adhesion molecules expressed by the endothelium under atheroprone and atheroprotective flow and we present microscopic evidence of transmigration under flow.

2.3.5.2.1 Krüppel-like factor 2 expression

We have first assessed the responsiveness of endothelial cells in our system to atheroprone and atheroprotective flow through KLF2 expression. KLF2 is a mechanoresponsive gene; both our laboratories have extensively documented its central role in vasoprotection and its upregulation in protected regions of the vasculature. Figure 2.18 shows that KLF2 is upregulated ~7 times after 24h of atheroprotective flow (compared to atheroprone flow) in our system. As a comparison, atheroprotective flow induces a ~8-fold upregulation of KLF2 in cells grown on plastic. These numbers are similar and denote a neutrality of the matrix towards KLF2 expression.

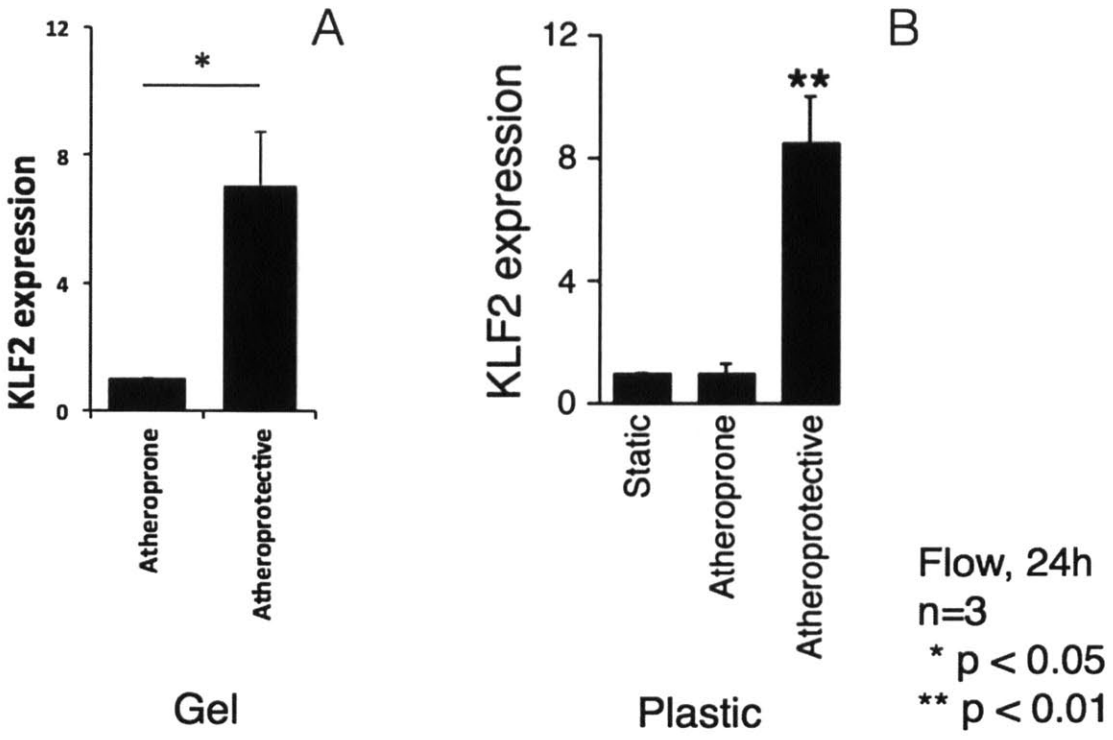

Figure 2.18: KLF2 expression on gel and on plastic.

Atheroprotective flow elicits respectively a ~7 and ~8 times upregulation of KLF2 in endothelial cells cultured on gel or on plastic.

2.3.5.2.2 Cell adhesion molecule landscape

After 24h of flow, endothelial cells exposed to both atheroprone and atheroprotective flow express ICAM-1 but not VCAM-1 or E-Selectin. There are no significant changes between the response to atheroprone and atheroprone flow (Figure 2.19).

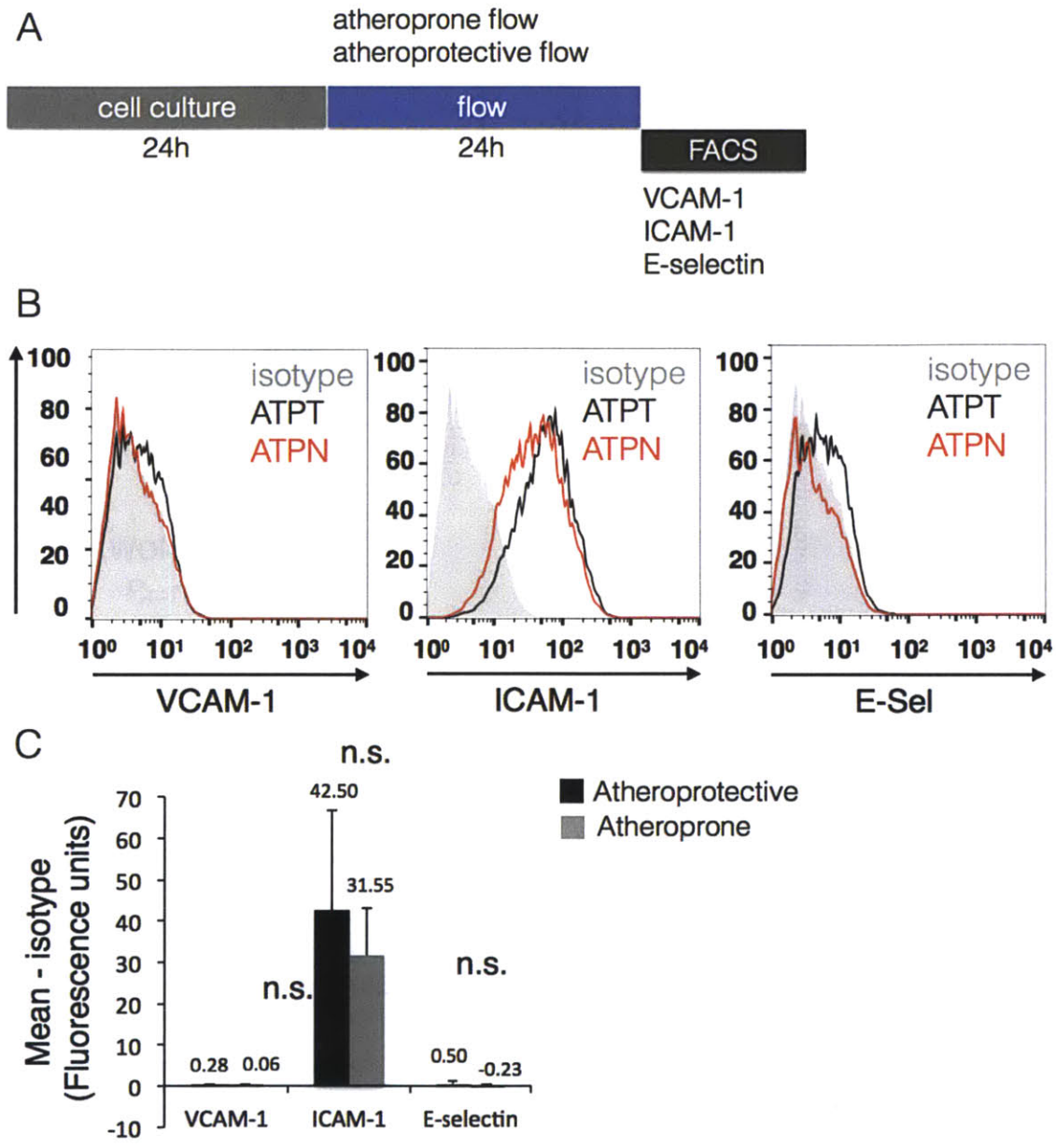

Figure 2.19: Expression of CAM of endothelial cells under atheroprotective and atheroprone flow.

A. Timeline of the experiment. Endothelial cells were cultured for 24h and exposed to flow for another 24h then analyzed by FACS. B. FACS plots of VCAM-1, ICAM-1 and E-Selectin expression in cells exposed to atheroprotective (black) and atheroprone flow (red) compared to isotype control (solid gray). C. Aggregated bar

graphs of the expression of cell adhesion molecules exposed to flow. The pattern of surface expression at 24h is similar between the two types of flow.

2.3.5.2.3 Imaging of transmigration following flow

Our model supports transmigration of THP-1 cells under flow. We have observed fluorescently labeled THP-1 under intact monolayers of endothelial cells exposed to atheroprone or atheroprotective flow (Figure 2.20). This was a major achievement in the development of our model because it means that we can study the interaction of these two types of cells under controlled fluid shear stress relevant to atherogenesis.

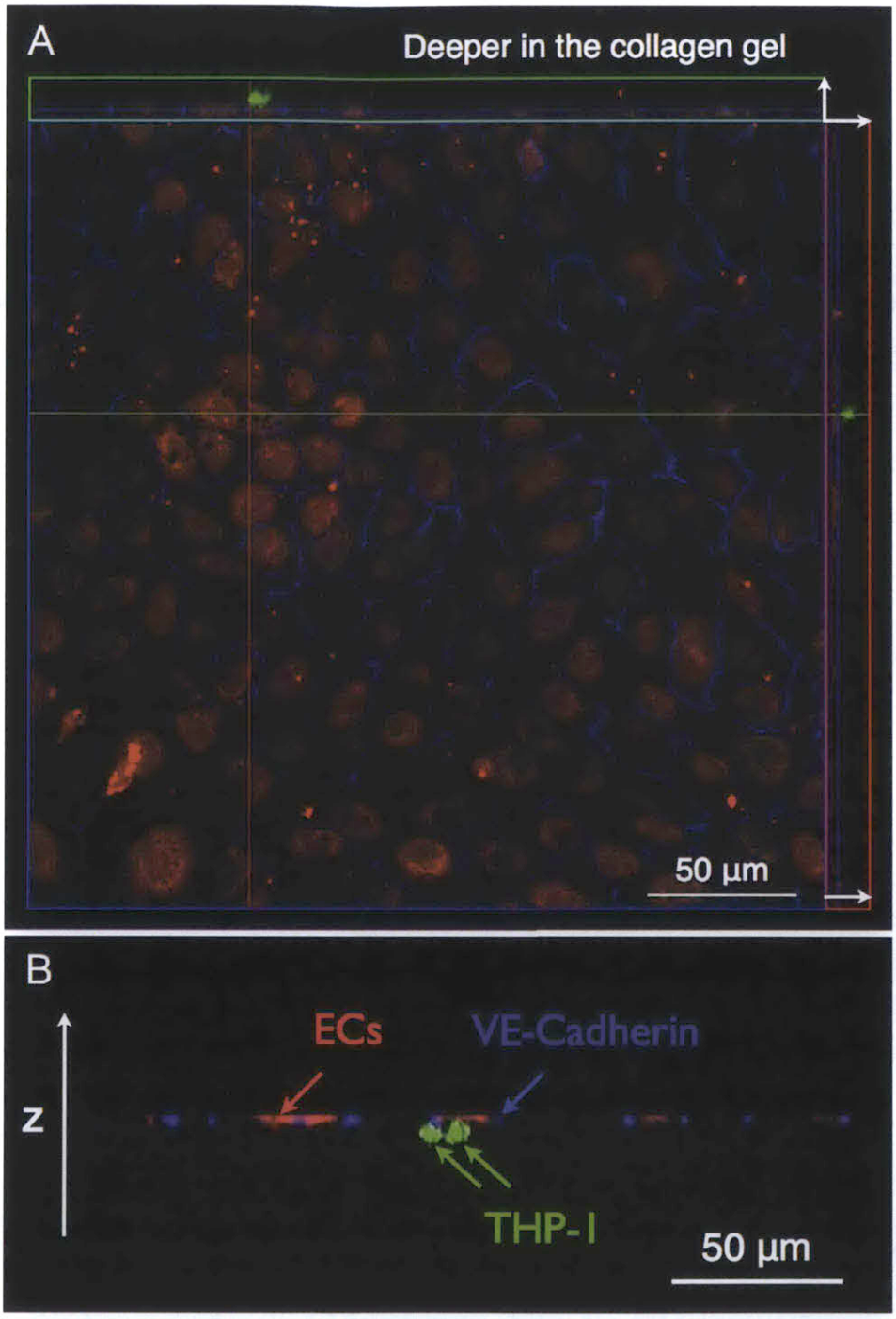

Figure 2.20: THP-1 cells transmigration through endothelium exposed to flow in our *in vitro* system.

A. Transmigration of THP-1 cells (green) through a confluent monolayer of endothelial cells (red) exposed to atheroprone flow observed by confocal microscopy. The integrity of the monolayer is demonstrated by the continuity of the

VE-Cadherin staining (blue) that delineates cell borders. The two side panels (green lining at the top, red lining on the right) are aggregated z-stacks of confocal images. The white arrows indicate decreasing z values. We can clearly observed green signal under the surface of the endothelium. B. This region was mapped with more precision. Assembled z-stack images show two transmigrated THP-1 cells (green).

2.4 Partial conclusion 1

The objective of this section was to develop an *in vitro* model that incorporates three interacting elements: endothelial cells, monocytes and flow, through a platform that can be integrated with the unique flow system available in our laboratory. We wanted to observe transmigration of monocytes in the context of atheroprone and atheroprotective flow in order to study this fundamental step of atherogenesis. In addition, we wanted to characterize the behavior of each cell type in our system under mechanical stimulation. In this regard, we have successfully met the objective and we summarize here our major findings.

We successfully engineered and integrated collagen matrices to our existing flow device. Based on our knowledge of polymers and the literature, we tailored and then measured with AFM, the mechanical properties of the matrix to obtain gels stiff enough to support the growth of a confluent monolayer of endothelial cells (but not tube formation like in angiogenesis assays), yet soft enough to permit THP-1 cell invasion and homing. The Young's moduli of our collagen gels range from 6-14kPa, which is sufficient for the growth of endothelial monolayers as demonstrated by phase contrast imaging.

The central finding of this section is that our co-culture model supports adhesion and transmigration of THP-1 monocytes in both static, atheroprone and atheroprotective conditions. We showed that monocyte diapedesis occurs with confocal and scanning electron microscopy and interrogated the endothelial cells before the co-culture to clarify the potential underlying mechanisms of transmigration. We found that in all static, atheroprone and atheroprotective flow,

ICAM-1 is expressed at basal levels in the absence of external stimuli such as pro-inflammatory cytokine. Given the rich literature on monocyte transmigration and on cell adhesion molecules, we propose ICAM-1 as potential mediator of transmigration in our system.

We also characterized the rest of the system, namely, THP-1 cells, their ability to polarize into M1 and M2 macrophages and influence endothelial activation, and the response of the system to flow through the lens of the mechanosensitive gene KLF2. We found that THP-1 cells are a homogenous population of $CD14^{++}CD16^{-}$ cells and that they can be polarized with cytokines stimulation. Further the secretions of the polarized THP-1 cells can trigger surface expression of VCAM-1 in the endothelium.

The model that we have developed and characterized is a research instrument and has *in fine* only on purpose: uncovering interactions between endothelial cells and monocytes under flow and dissecting molecular pathways involved in atherogenesis. Thus even if meticulous characterization was required, the biological insight brought by the model is the only currency that matters. In the next section, we used our model to try to recapitulate key processes of atherogenesis and test two hypotheses about the how flow shapes the interplay between endothelium and monocytes. Other *in vitro* models [102, 106] have established useful results concerning the adhesion of monocytes on endothelial cells exposed to flow from atheroprone regions. Yet, the extent of biological insight brought by these models has been greatly limited by the available number of cells of interest. Indeed, replica of arteries prone to atherosclerosis – such as the bifurcation of the common carotid artery into the external and internal carotids – only provides with limited area of dysfunctional endothelium – i.e. the region of the bulb or crux of the bifurcation for the carotid. The architecture of our model (where millions of endothelial cells are subjected to the same type of flow) overcomes these constraints and is the only one that can practically study the biological interactions between endothelium and monocytes beyond adhesion.

Lastly, we want to highlight the versatility of the platform. Indeed, the matrix that we used can be supplemented with additives such as lipids or modified lipids, known to accumulate in the subendothelial space in atheroprone areas in response to increase endothelial permeability and influence the biology of macrophages and endothelial cells. Cholesterol crystals are also present in the nascent atheroma; they contribute to the polarization of the macrophages because their phagocytosis triggers the activation of the NLRP3 inflammasome – a necessary step to convert pro-IL-1β into mature IL-1β [119]. Our gels can easily accommodate the presence of crystals. Further, the architecture of the model is also flexible to changes or addition of cell types. For example, we could substitute monocytes for neutrophils, which are early responders to inflammation, or a mixture of monocytes and lymphocytes, since lymphocyte may contribute to macrophage differentiation and polarization. Finally, our model is a great avenue for drug discovery, both in terms of the proteomics and identification of new therapeutic targets, and testing of small molecules to mitigate deleterious endothelial:monocyte interactions under flow.

3 Biological insight drawn from the model

3.1 Introduction

We have developed a new tool for research in atherosclerosis, which we have used to investigate critical interactions between endothelial cells under atheroprone and atheroprotective flow. It is an important tool since, to the best of our knowledge, our model of transmigration that incorporates atheroprone and atheroprotective flow is unique and we already know that flow plays a central role in atherogenesis. We have carefully characterized the model but, indeed, its purpose is to further insight of a biological process. Hence, in this Chapter we present hypotheses and data on the interactions of endothelial cells and monocyte under flow that we have collected thanks to our novel model.

The spatial proximity of monocytes and endothelial cells after diapedesis in vascular regions susceptible to atherosclerosis underlines the importance of the cross talk between these two types of cells. In this section, we first confirmed that our model recapitulates key events of atherosclerosis such as the localized recruitment of monocytes to atheroprone regions. Second, we have successively investigated the effect of endothelium exposed to atheroprone and atheroprotective flow on monocyte fate and the consequences of the presence of monocytes in atheroprone regions.

Many before us [33, 101, 120-125] have shown that endothelial cells and monocytes signal to each other and that monocytes secrete pro-inflammatory mediators during atherogenesis. We add to this body of knowledge by postulating a coupling between the flow-mediated states of the endothelium and the monocytes fate. More generally, we believe that any dysfunctional state of the endothelium gets communicated to infiltrating cells and ultimately leads to their polarization. Specifically, we hypothesized that monocytes transmigrating cells through dysfunctional endothelium exposed to atheroprone flow will become "pro-inflammatory" M1 macrophages.

As shown in Chapter 1, the endothelium exposed to atheroprone flow is dysfunctional in many regards; morphological rearrangements leading to increased permeability, changes in extracellular matrix production, impaired NO production, increased susceptibility to inflammation to low-grade inflammation. We also examined in this section the effect of monocyte on already beset atheroprone endothelium. We posit that monocytes in the context of atheroprone endothelium and atheroprone flow exacerbate this dysfunctional phenotype.

3.2 Materials and Methods

Cell cultures

Cf. Chapter 2.

Chemicals and reagents

Cell membrane fluorescent dyes In appropriate cases, cells were stained with CellTracker Green (Life Technologies; C7025) or with CellTracker Orange (C34551) at 5 μM in culture medium for 30 min in the incubator. The cells were then rinsed, spun (5 minutes, 500g) and resuspended in dye-free culture medium.

Matrix

Cf. Chapter 2.

Hemodynamic Shear Stress in vitro System

Cf. Chapter 2.

Recruitment of THP-1 cells under flow

We used our *in vitro* system to measure the fraction of THP-1 recruited to endothelium exposed to atheroprone and atheroprotective flow. We exposed red fluorescent endothelial cells cultured on fibronectin-coated gels alone to flow for 48h. Then, we co-cultured THP-1 and endothelial cells under flow for another 48h. Before the addition of the THP-1 cells, the endothelium was washed with PBS twice.

Later, we introduced 12 millions fluorescent THP-1 cells in the flow chamber through the supernatant as a cell solution to achieve a 2:1 monocyte to endothelium ratio. The THP-1 cells were pre-treated with a green cell dye. At the end of the experiment, the cell cultures were washed twice to remove non-adherent cells and the gels were degraded using a solution of collagenase D (2mg/mL, Roche). The cells in the degraded collagen solution were washed and filtered through a nylon mesh (50μm pores, BD Bioscience).

Analysis of the different fractions of THP-1 co-cultured with endothelial cells under atheroprone flow

We exposed endothelial cells cultured on fibronectin-coated gels alone to atheroprone flow for 24h, then we co-cultured THP-1 and endothelial cells for another 24h. Before the addition of the THP-1 cells, the endothelium was washed with PBS twice. Later, we introduced 12 millions fluorescent THP-1 cells in the flow chamber through the supernatant as a cell solution. The THP-1 cells were pre-treated with a green cell dye. At the end of the experiment, three fractions of cells were collected: cells of the supernatant, adherent cells and cells in the gel. After the collection of the supernatant, the cultures were washed with PBS (containing Ca^{2+} and Mg^{2+}) twice to remove potential non-adherent cells. Adherent cells were collected with an EDTA solution (10 mM, Life Technologies). Cell cultures were washed twice again with PBS (Ca^{2+} and Mg^{2+} free) and the gels were degraded using a solution of collagenase D (2mg/mL, Roche). The cell solutions were washed and filtered through a nylon mesh (50μm pores, BD Bioscience) before sorting with FACS.

Analysis of the endothelium exposed to atheroprone flow in the presence or absence of THP-1 cells

We exposed endothelial cells cultured on fibronectin-coated gels alone to atheroprone flow for 24h, then we co-cultured 12 millions THP-1 and endothelial cells for another 24h. At the end of the experiment, the cultures were washed with PBS (Ca^{2+} and Mg^{2+}) twice to remove non-adherent cells and the gels were degraded

using a solution of collagenase D (2mg/mL, Roche). The cell solutions were washed and filtered through a nylon mesh (50μm pores, BD Bioscience). Cells were stained with an anti-CD144 (VE-Cadherin) antibody and distributed in several FACS tubes for further staining of VCAM-1, ICAM-1, E-Selectin and isotype control. Cells were finally analyzed and sorted with FACS for gene expression analysis.

Analysis of THP-1 monocyte recruitment by endothelial cells transfected with a KLF2 adenovirus or GFP control

We seeded HUVEC to confluence on fibronectin-coated collagen gels in 6-well plates (3516, Corning) and kept them in culture for 24h. HUVEC were then either transfected with an adenovirus encoding KLF2 or an empty vector (as control) for 24h with an MOI=50. Both viruses contained a GFP reporter gene. Transfection was visually assessed by fluorescence microscopy. Each well received 1 million of orange-labeled THP-1 cells for 24h in 2mL of EGM-2 culture medium. The supernatant was removed and the cell were washed twice with PBS; then another 1 million of orange-labeled THP-1 cells were co-cultured with the endothelial cells for 24h. At the end of the experiment, the supernatant was aspirated and the cells were gently was twice with PBS. Collagenase D was used to digest the gels for 40 min at 37°C. The cells suspension was spun down by centrifugation (500g, 5min). The supernatant was removed and the cell pellet was lysed with 350μL of 0.1% SDS solution. The lysate was homogenized by passing it through a 27G needle at least 10 times. Fluorescence in the orange spectrum (Excitation: 548nm; Emission: 576nm) of the lysate was measured with a spectrophotometer (SpectraMax M3, Molecular Device) as a surrogate for the number of recruited orange THP-1 cells.

Gene expression analysis

Total RNA was purified (RNA Purification trays and 6100 Nucleic acid Preparation Station; Applied Biosystems), the concentration of the RNA isolates was measured (Nanodrop 2000; Thermo Scientific) and cDNA was synthesized (TaqMan reverse transcription reagents and Veriti 96 well Thermal Cycler PCR machine; Applied Biosystems) with the same amount of RNA with each experiment. Real-time PCR

analysis was performed with a qPCR 7900HT Fast Real Time PCR System (Applied Biosystems) using TaqMan Universal PCR Master Mix (Applied Biosystems) and appropriate primers. Gene expression was quantified using the ΔCt or ΔΔCt method, with GAPDH as a housekeeping gene. Primer sequences are listed below. Results were analyzed with Excel (Microsoft).

Gene	Reference
GAPDH	Hs_99999905_m1
CDH5	Hs_00901463_m1
CD14	Hs_02621496_s1
ANGPT2	Hs_00169867_m1
ARG1	Hs_00968978_m1
E-Sel	Hs_00360439_m1
KLF2	Hs_00164932_g1
ICAM-1	Hs_00164932_m1
ββββ	Hs_00174097_m1
IL6	Hs_00985639_m1
IL8	Hs_00174603_m1
NOS2	Hs_010755529_m1
NOS3	Hs_01574659_m1
TAGLN	Hs_00162558_m1
VCAM-1	Hs_00174239_m1
SIRT1	Hs_01009006_m1
VIM	Hs_00185584_m1
STAT1	Hs_01013996_m1
STAT6	Hs_00598625_m1
SNAI1	Hs_00195591_m1
TNF	Hs_01113624_g1
TIE2	Hs_00945146_m1

Fluorescence-Activated Cell Sorting

Cells were detached, treated with an Fc receptor blocking solution and stained using antibodies as recommended by the manufacturer. Isotype controls were also used as recommended by the manufacturer. Samples were incubated with nuclear stains such as PI or DAPI and analyzed on a FACSCalibur flow cytometer (Becton Dickinson) or sorted on a FACS Aria III SORP (Becton Dickinson) and the results were processed with FlowJo (Tree Star, Inc.). Cell debris were excluded according to the forward (FSC) and side scatter (SSC) signal levels, doublets were excluded by plotting the height of the FSC signal versus the area of the same signal and keeping the cells on the diagonal. Finally, dead cells were excluded through the level of fluorescence in the PI or DAPI channel before appropriate analysis of the signal in other channels.

The following antibodies were used (unless stated otherwise, antibodies were used according to the manufacturer's recommendation): Alexa 647-conjugated mouse anti-human CD144 (VE-Cadherin; BD Bioscience) and recommended Alexa 647-conjugated isotype control (BD Bioscience); primary mouse anti-human VCAM-1, ICAM-1 and E-selectin antibodies were made in house and used with goat anti-mouse Alexa 488 IgG secondary antibody (1:400; Life Technologies).

Phase contrast microscopy

Cells were routinely imaged with a phase-contrast microscope (Nikon Eclipse 2000-E or 2000-S) equipped with 4X, 10X and 20X objectives and an Insight 2 camera (SPOT). Sequential images of flow experiments were acquired at 10 min to 1h intervals. Images were analyzed using ImageJ or SPOT software.

Statistics

All experiments were performed at least three times independently (HUVECs from a different culture each time). Results are expressed as mean ± standard deviation. Comparison of two groups was performed using a student's t-test. $p < 0.05$ was taken as statistically significant.

3.3 Hypothesis 1

We posit that the dysfunctional endothelium from the atheroprone regions communicate inflammatory signals to transmigrating monocytes in order to influence their fate to an M1 "pro-inflammatory" polarization. Conversely, healthy atheroprotective endothelium will promote an M2 "anti-inflammatory" phenotype to the transmigrating cells. We consider flow as the determinant of endothelial dysfunction for this work, but we generally believe that our hypothesis can be generalized to any endothelial dysfunctional state. Figure 3.1 is a graphical illustration of our hypothesis.

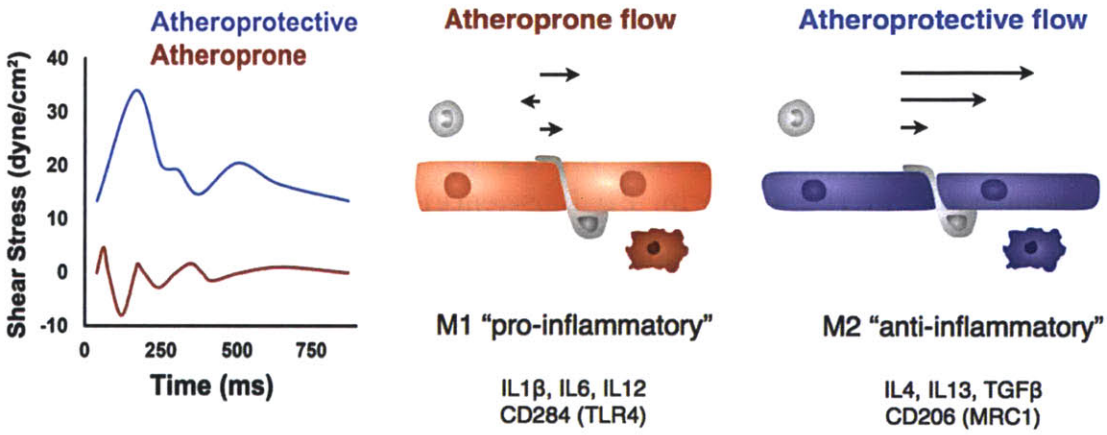

Figure 3.1: Graphical hypothesis: phenotypic modulation of transmigrating monocytes.

We surmise that there is a coupling of the flow-mediated state of the endothelium and the polarization of transmigrating monocytes. We thus hypothesize that atheroprone endothelium promotes an M1 phenotype of transmigrated monocytes/macrophages characterized by the expression of IL1β, IL6, IL12 and CD284, while atheroprotective endothelium promotes an M2 phenotype characterized by the expression of IL4, IL13, TGFβ and CD206. TLR4: Toll-like receptor 4; MRC1: Mannose receptor, C type 1.

3.4 Monocyte recruitment: atheroprotective versus atheroprone flow

Localized recruitment of leukocytes in atheroprone regions is a fundamental characteristic of atherogenesis; therefore, we examined the recruitment of THP-1 cells in our model and compared the results for athero-prone and -protective flow. We opted for a priming of the endothelium for 48h to maximize endothelial dysfunction, followed by 48h of co-culture. Figure 3.2 and Figure 3.3 show that atheroprone but not atheroprotective flow recruits monocytes. Immunostaining of the co-culture show a preferential recruitment in the case of atheroprone flow. In addition, we observed that THP-1 cells tend to cluster in islands of adherent monocytes. The ratio of endothelial cells (green events) to the total number of events is ~8 times higher for atheroprone flow compared to atheroprotective flow. Notice that we chose a green dye for the monocytes and an orange/red dye for the endothelium to avoid bleeding of the endothelial dye into the monocyte channel. In fact, on a frequency plot, the emission spectrum of the red dye begins after the upper bound of the green filter used to detect monocytes of the FACS machine.

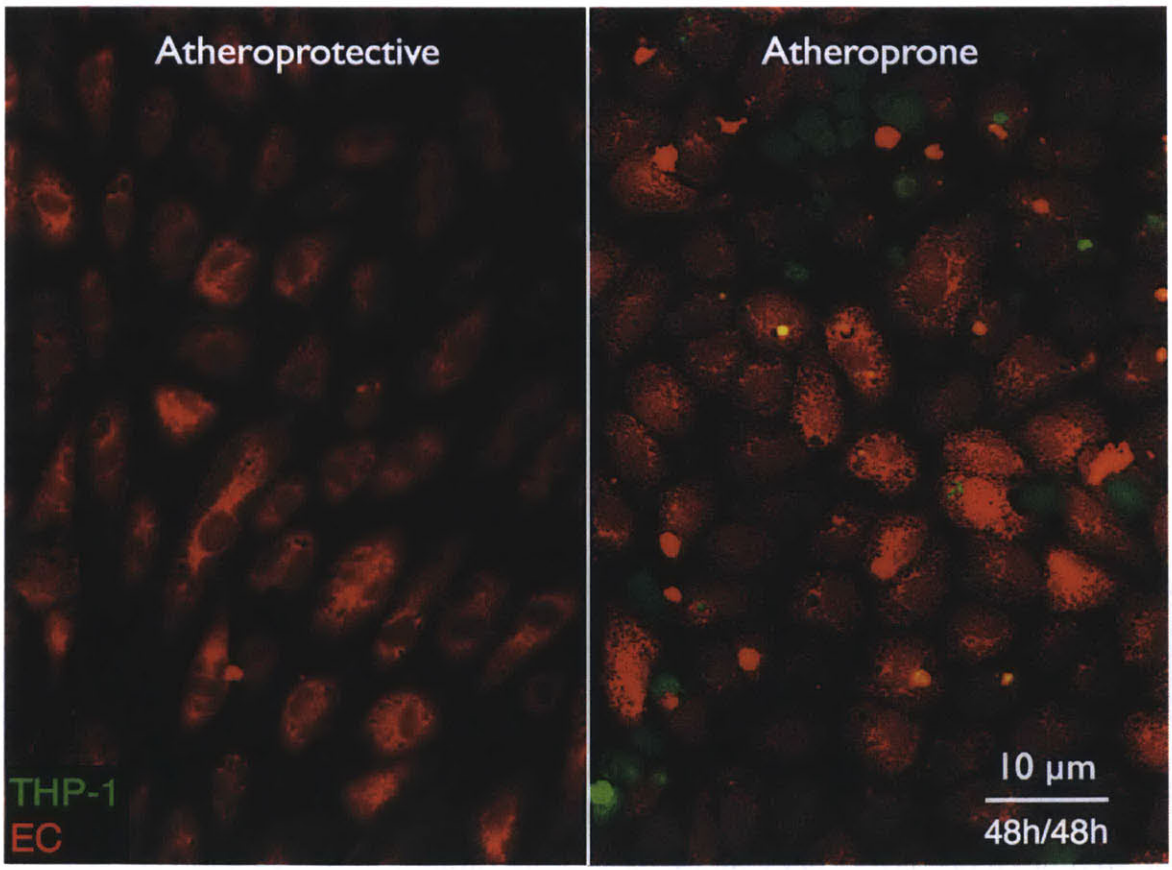

Figure 3.2: Differential recruitment of THP-1 monocytes under protective and prone flow.

Immunostaining of endothelium:monocytes co-cultures under atheroprone and atheroprotective flow. Atheroprotective flow promotes spindoidal morphology of the endothelial cells and no monocyte can be seen in this picture. On the contrary, atheroprone flow promotes a cuboidal morphology, typical to endothelial dysfunction and many clusters of adherent THP-1 monocytes can be observed.

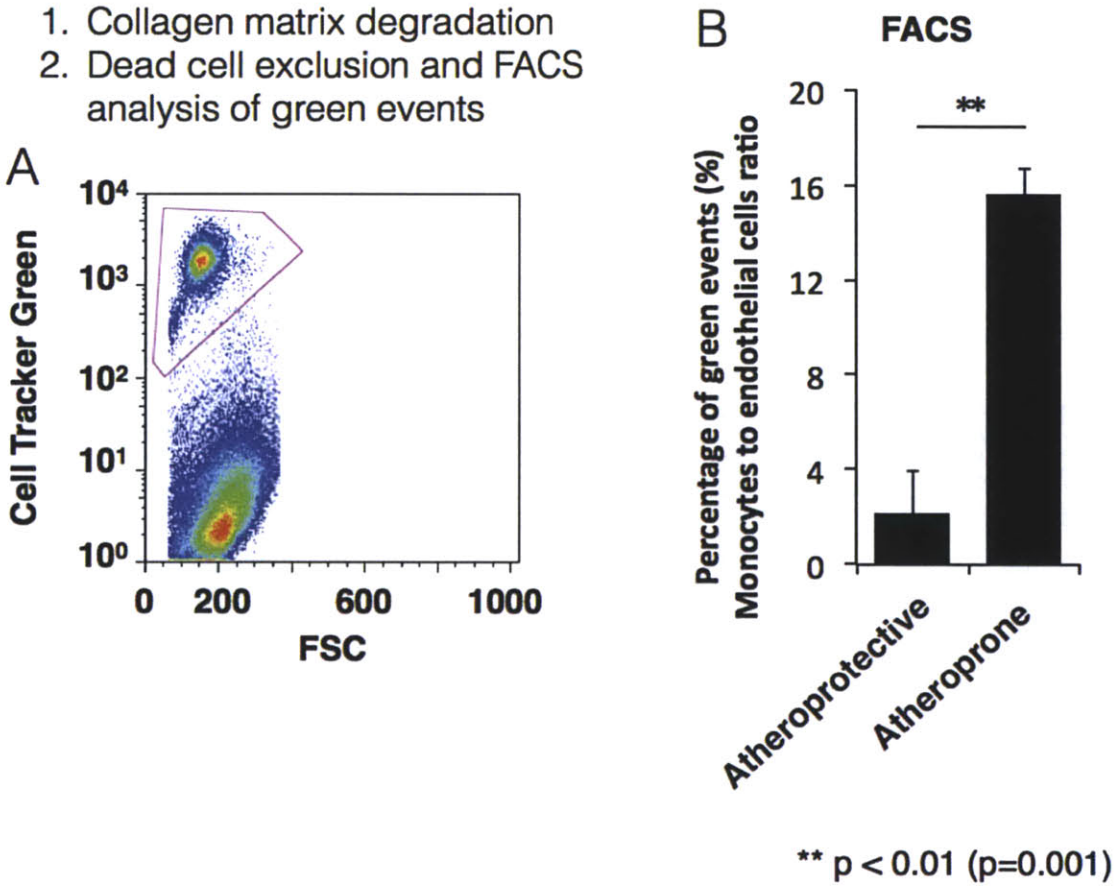

Figure 3.3: Quantification of recruited monocytes.

A. FACS plot used for the analysis of the ratio of adherent/ transmigrated THP-1 cells to total number of cells. THP-1 cells were detected by their green label (unlabeled EC). B. Quantification of the relative recruitment of THP-1 cells for atheroprone and atheroprotective flow. Atheroprone flow promotes the recruitment of ~8 times more THP-1 per endothelial cell than atheroprotective flow.

3.5 KLF2 suppresses monocyte recruitment to endothelial cells.

We measured the recruitment of THP-1 cells by endothelial cells overexpressing KLF2 with a control to examine the importance of this gene in the recruitment of THP-1 monocytes under static conditions. Figure 3.4 shows that the number of adherent and transmigrated THP-1 is increased when THP-1 are co-cultured with EC transfected with a GFP adenovirus compared to a KLF2 adenovirus. This suggests that KLF2 expression drives protective mechanisms involved in the adhesion and transmigration of monocytes. This adds to the "physical" protective effects of elevated hemodynamic forces applied by atheroprotective flow on monocytes that may adhere to the endothelium compared lower forces applied by atheroprone flow.

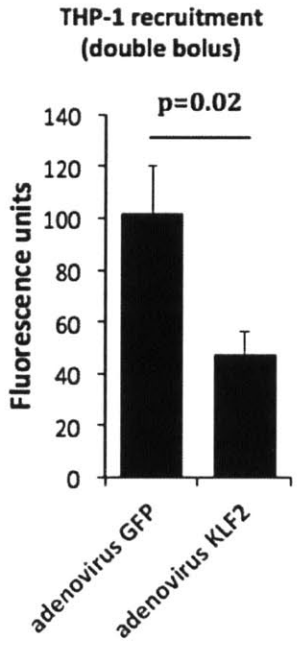

Figure 3.4: KLF2 expression protects the endothelium from THP-1 monocyte recruitment in the absence of hemodynamic forces.

Fluorescence in cell lysates containing orange-labeled THP-1 cells. The intensity of the fluorescence correlates with the number of recruited THP-1 cells. We observed that endothelium transfected with KLF2 allows greater recruitment of THP-1 cells in static condition compared to cells transfected with and empty vector. This suggests

that KLF2 expression limits the availability or activity of molecules involved in monocyte adhesion or transmigration.

3.6 Gene analysis of THP-1

Since previous data indicate that monocyte accumulate on endothelial cultures exposed to atheroprone flow, we decided to primarily work with this waveform. Our hypothesis stipulates that transmigration of monocytes through flow-mediated dysfunctional endothelium promotes a pro-inflammatory phenotype for the monocyte. We tested this hypothesis by collecting the free floating, adherent and transmigrated THP-1 cells in a co-culture exposed to atheroprone flow. We exposed endothelial cells alone to flow for 24h, then the co-culture for another 24h. We decided to change the time points of the experiment compared to the previous one because of the technical complexity of the experiment. As we were probing the system, we realized that the success rate of the experiments made on a 48h/48h scheme would not be reasonable and privileged increasing the data output. Disappointingly, we were not able to make a definitive conclusion based on this experiment. We performed the experiment many times and we able to conduct several gene expression analyses but at the end, we could not overcome the variability of the system (Figure 3.5). We assessed the expression of many genes related to the inflammatory cascade but we only present data on the genes IL-1β and IL6. Although some experiments incriminate transmigration as the driver for the expression of IL-1β and IL6, others completely argue against this proposition.

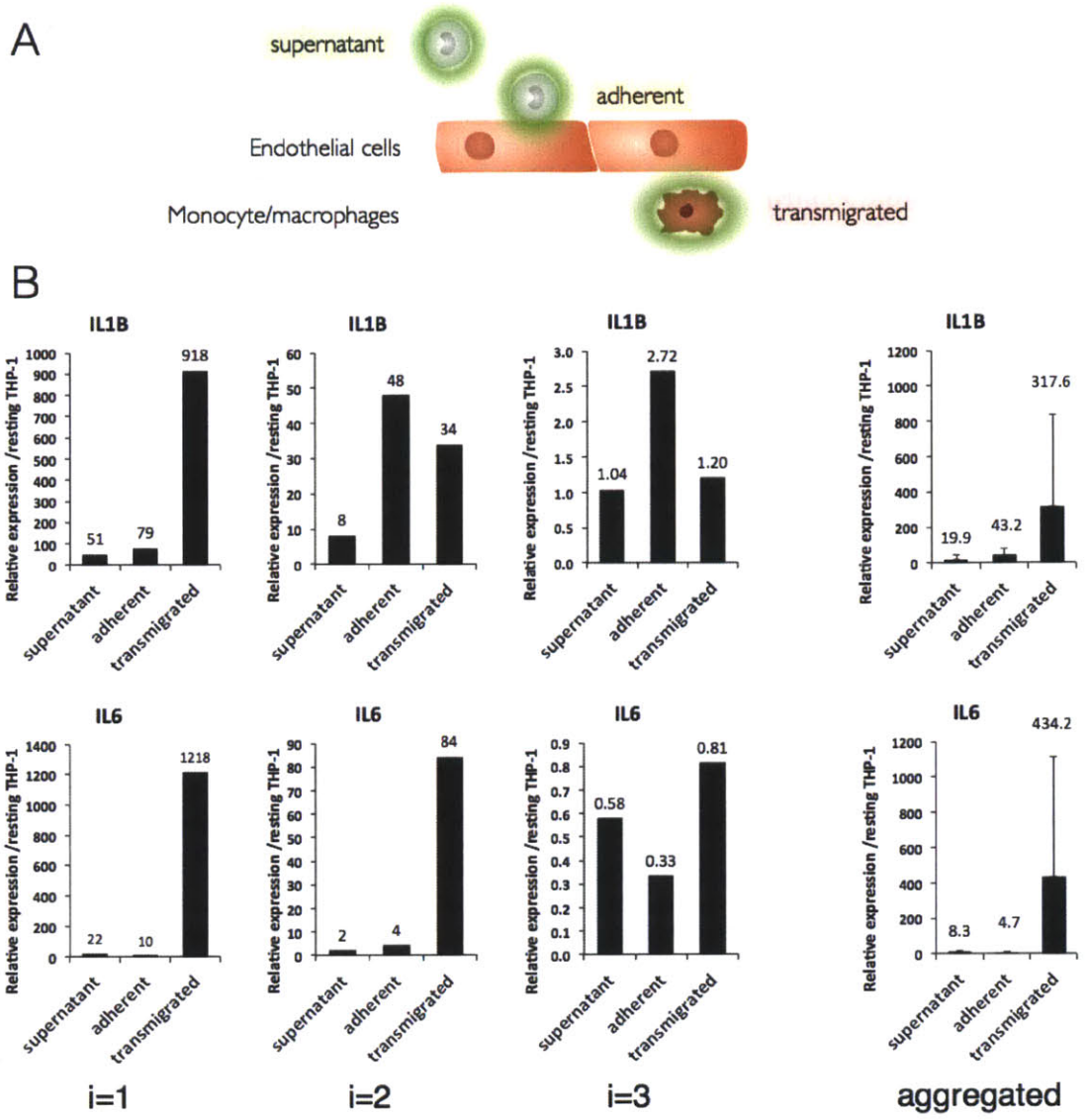

Figure 3.5: Gene expression of free floating, adherent and transmigrated THP-1 monocytes.

A. Cartoon illustrating the different isolated fractions of THP-1 monocytes: the free-floating ones in the supernatant, the adherent ones and the transmigrated one. Monocytes pre-treated with a green dye were FACS sorted based on there intensity in the green channel. B. Expression of IL-1β and IL6 genes in the fractions described above. The results of individual experiments show the variability of the system also captured by the size of the standard deviation in the plots of aggregated data.

We were disappointed with this conclusion, yet we realized that the variability of the results might lie within the THP-1 cells themselves or their maintenance. For all subsequent experiments, we expanded THP-1 to a lower passage, aliquoted and stored the cells at -196°C. For each experiment, we defrosted a new vial of THP-1 rather than keeping culturing these cells. The variability of system will be discussed in Chapter 4. Regardless, we continued to search for some biological insight and flipped the question one its head. Rather than investigating the influence of the endothelial state on the monocyte fate, we asked the question: "what is the influence of the monocytes on the atheroprone endothelium?"

3.7 Hypothesis 2

In the second part of this Chapter, we examined the role of monocytes on the endothelial states. We surmised that the presence of monocytes in the vicinity of atheroprone endothelium would exacerbate the already dysfunctional state. Thus indirectly, we impute to the monocytes with part of the responsibility for the chronic nature of atherogenesis. The graphical hypothesis (Figure 3.6) illustrates our proposition: atheroprone endothelium (orange) becomes more and more inflamed as monocytes aggregate and interact with it.

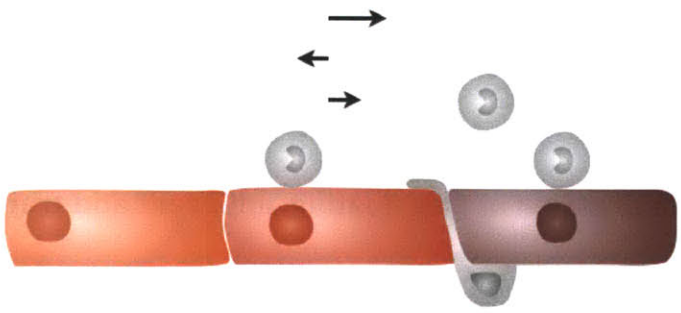

Figure 3.6: Graphical hypothesis: monocytes exacerbate the atheroprone endothelial phenotype.

We postulate that the presence of monocytes is deleterious to the already beset monolayer. Implicitly, we also assume that there exists a continuum of dysfunctional state rather than a duality between healthy:diseased states.

3.8 Results

3.8.1 Gene analysis of EC

Generally, the gene expression pattern of endothelial cells exposed to atheroprone flow is similar to endothelial:monocyte co-cultures exposed to the same flow, apart for IL-1β, which is expressed in endothelial cells from co-cultures but not alone. This is a novel an interesting finding since inflammation is at the heart of pathogenesis of atherosclerosis (Figure 3.7).

We selected four categories of genes that are representative of inflammation (IL-1β and IL6), vasoprotection (KLF2 and SIRT1), vascular stability (ANGPT2) and Endothelial-to-Mesenchymal Transition (EMT; SNAI1 and VIM1). We observed that IL1 is not statistically upregulated in endothelial co-cultured with monocytes compared to endothelium alone ($p=0.18$). Although each individual experiment showed upregulation of IL1 in endothelial cells sorted from co-cultures versus endothelium alone, the variability of the results does not allow us to make a definitive statement. Yet, we observed a robust upregulation ranging form 30 to ~300 times between the two conditions so we speculate was that there may be some interactions between endothelial cells and monocytes under atheroprone flow that mediate the inflammatory cascade.

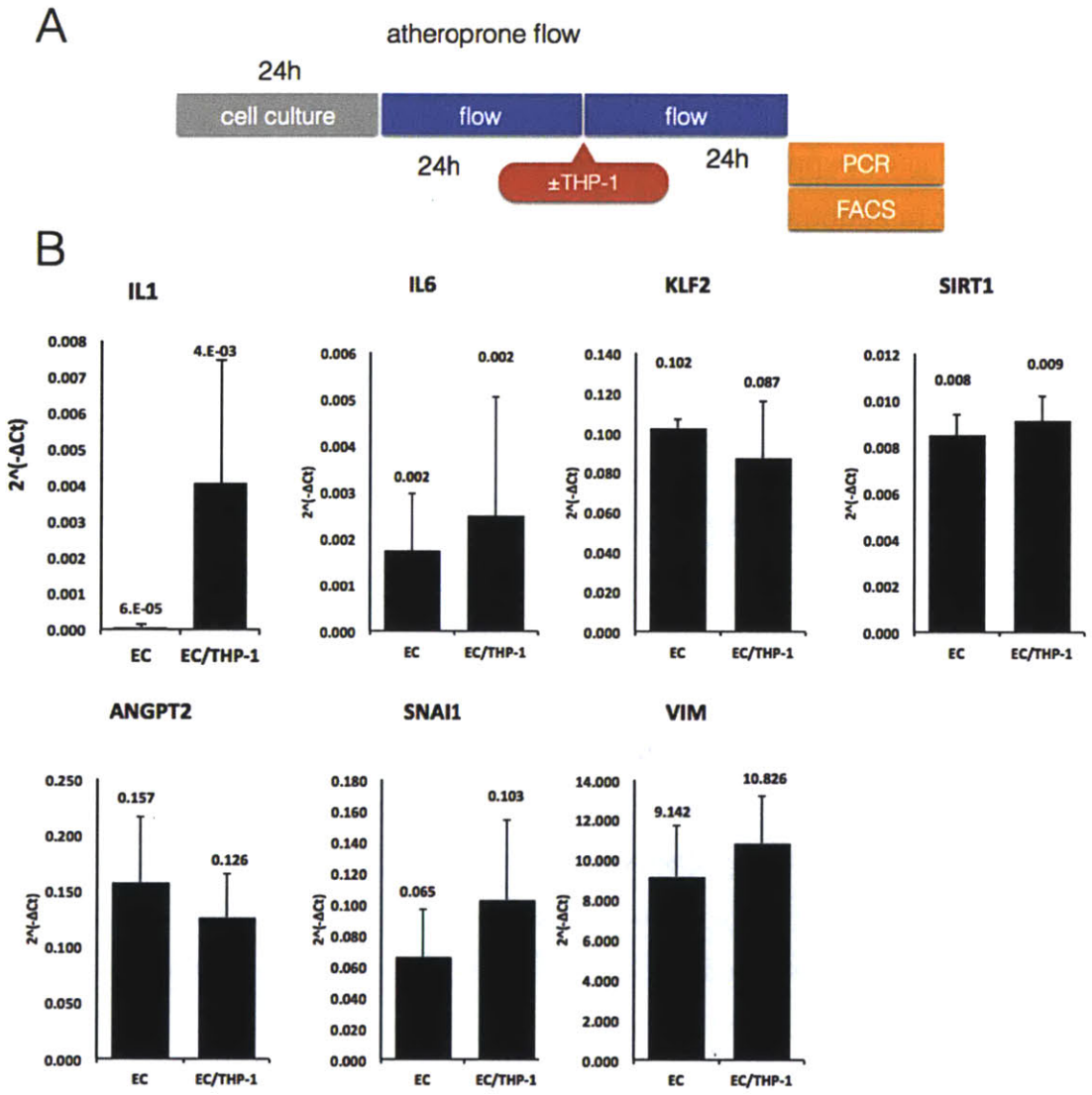

Figure 3.7: Gene expression analysis of endothelial cells exposed to atheroprone flow cultured with or without THP-1 monocytes.

A. Timeline of the experiment; we primed endothelial cells for 24h with atheroprone flow, then either added or not THP-1 monocytes and resumed flow for 24h. Endothelial cells were sorted through their VE-Cadherin expression. B. Gene expression analysis of endothelial cells alone (EC) or endothelial cells as part of a co-culture system (EC/THP-1). Notice that IL-1β is not statistically upregulated in endothelial co-cultured with monocytes compared to endothelium alone.

3.8.2 Expression of cell adhesion molecules

The expression of cell adhesion molecules in endothelial cells exposed to atheroprone flow either alone or as part of a co-culture is similar. In our scheme, atheroprone endothelium becomes even more dysfunctional following the introduction of monocyte. Hence, we expected that the cell adhesion molecule profile of endothelial cells from co-cultures would increase their expression of VCAM-1, ICAM-1 and E-Selectin. This belief was reinforced by upregulation expression of IL-1β, a potent "pro-inflammatory" cytokine able to trigger the surface expression of adhesion molecules, observed in the previous section. However, this was not verified by experimental data with these specific time points, since none of the three adhesion molecules we probed were upregulated (Figure 3.8).

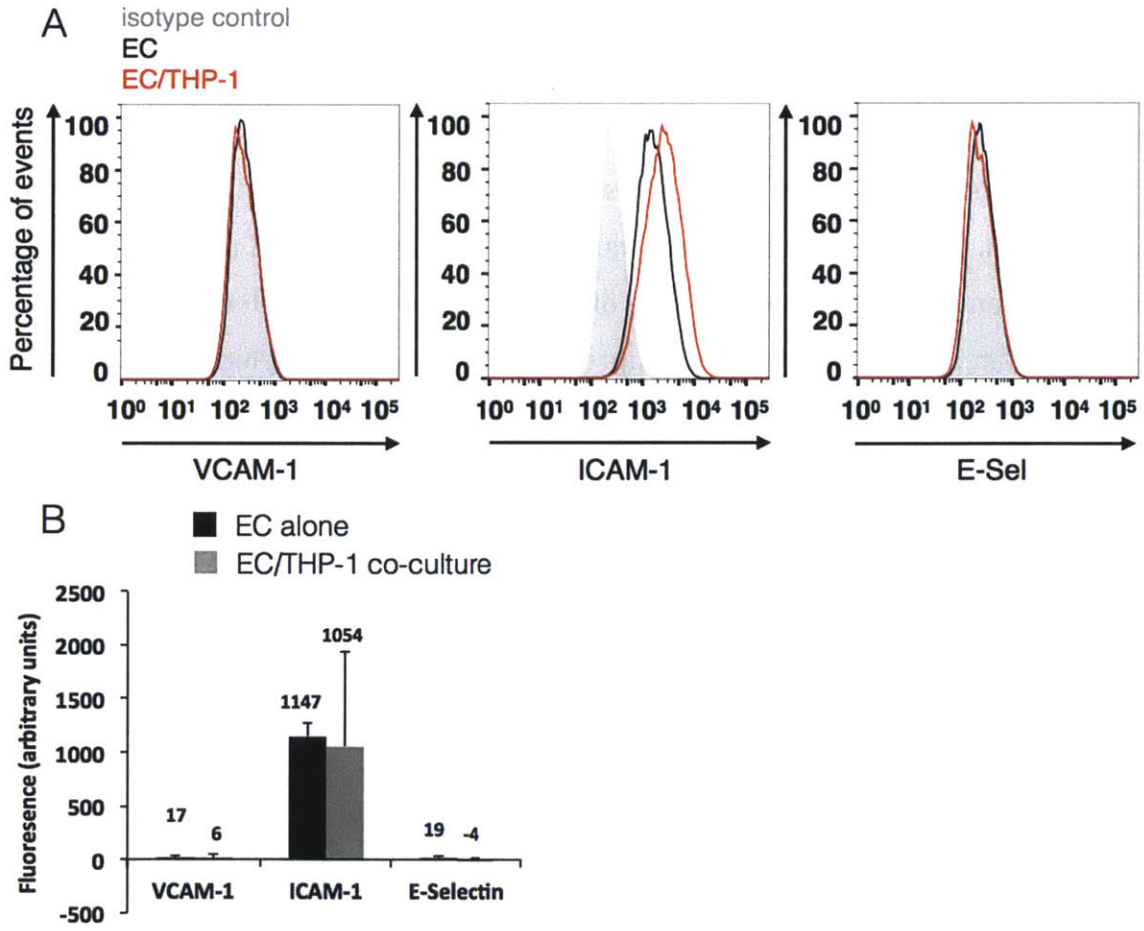

Figure 3.8: Expression of CAM in endothelial cells exposed to atheroprone flow cultured with or without THP-1 monocytes.

A. FACS plots of the expression levels of VCAM-1, ICAM-1 and E-selectin in VE-Cadherin positive cells. B. Aggregated results show identical levels in endothelial cells alone or endothelial cells from co-cultures. Notice that there was excellent separation of VE-cadherin positive events compared to the matching isotype; in addition there was no bleeding between the fluorophores used to stain adhesion molecules (Alexa 488) and VE-Cadherin (Alexa 647).

3.9 Partial conclusion 2

In this Chapter, our objective was to draw some biological insight from the well-characterized *in vitro* model that we build. We first compared the recruitment of THP-1 monocytes by endothelial cells exposed to atheroprone and atheroprone flow. Then, we successively examined the effects of endothelial cells on monocyte and the reverse interaction, the effect of monocytes on endothelial cells, both under atheroprone flow. While we were able to recapitulate critical aspects of atherogenesis and indict monocytes as inducers of IL-1β in atheroprone endothelium, our model suffers from variability, which precluded us from making a definitive conclusion on the influence of flow-mediated endothelial dysfunction on monocyte fate. We are left with the impression that this second objective is partially fulfilled and would benefit from further development of the model.

As previously reported by others *in vivo* [94, 126-128] and *in vitro* [102, 129-131], we showed, through both imaging and quantification of the number of adherent and transmigrated monocytes by FACS, that monocytes are primarily recruited to atheroprone flow regions. This is an important observation because it recapitulates key events of atherogenesis and also adds to the current knowledge on atherosclerosis. Indeed there is accumulating evidence that disturbed flow is responsible for the localized recruitment of monocytes, yet our model is simple enough that we can ascribe to flow the primary responsibility for this localized event. These observations give us some confidence that our model is relevant because it mimics *in vivo* data.

We hypothesized that the dysfunctional state of the endothelium in atheroprone regions is communicated to recruited monocytes and sealed during their transmigration. To test this hypothesis, we separated free-floating, adherent and transmigrated monocytes to analyze their gene expression independently. Disappointingly, we were not able to make a definitive statement about our hypothesis because biological variability stood in the way of our analysis. The results from some experiments supported our view, while others did not. Together the data that we acquired were too variable to make a conclusion. We believe that variability could arise intrinsically from the THP-1 since some of their biology is unregulated. Other factors such as the maintenance or the passage of the THP-1 cells, potential activation during staining before the experiment or inadequate sorting could also be at fault. Lastly, although it is less likely, the variability could emanate from the endothelial cells, which could influence dramatically the biology of monocytes. Unfortunately, we could not isolate the source of this variability. We continued using THP-1 cells because during the development phase it was not technically feasible to isolate such a high number of primary cells and as we summarize in the next paragraph some valuable information was collected with THP-1 proxies. In the future however, we recommend that the system be used with primary blood monocytes instead of THP-1 cells.

The second half of our question investigated the effect of monocytes on atheroprone endothelium. We posited that monocytes exacerbate the already dysfunctional state of atheroprone endothelium, leading to the upregulation of inflammatory genes and genes responsible for vascular stability, decreased vasoprotection and a transition to a mesenchymal phenotype. We measured the expression of an array of genes representative of these categories and found that the presence of monocytes triggers a non-statistical upregulation of IL-1β expression, although the trend was similar in all three independent experiments. The variability observed prevents an assertive statement but suggests that monocytes may act as a promoter of inflammation in atheroprone endothelium. Surprisingly however, our other probes of inflammation, the pro-inflammatory cytokine IL6 (assessed for gene expression)

or VCAM-1, ICAM-1 and E-Selectin adhesion molecules (assessed by FACS) were not upregulated. This is unexpected since it is well documented that IL-1β stimulation triggers the expression of adhesion molecules and the secretion of IL6. We suppose this contradiction can be explained by the biology of IL-1β. Pro-IL-1β is translated as a 31-33kD protein that is only active when processed by Caspase-1 to its 17kD mature form, when the inflammasome is active. Hence pro-IL-1β can be produced in the cell without being active or even secreted. Recent work from Duewell et al. [119] has highlighted that cholesterol crystals accumulate at early stages of atherogenesis - as soon as two weeks in Apo-E-deficient mice - and their phagocytosis by macrophages activates the NLRP3 inflammasome. It is not excluded that a similar process could happen as well for endothelial cells.

Despite difficulties to demonstrate our first hypothesis due to high variability in THP-1 gene expression pattern, we believe that we have utilized our novel *in vitro* model to show interesting and important findings. We showed that atheroprone but not atheroprotective flow triggers the recruitment and accumulation of monocytes, in agreement with others [102]. We also showed that flow-mediated endothelial dysfunction may augment in the presence of monocyte as evidenced by the trend in upregulation of IL-1β, which however did not show statistical relevance. We put this result in perspective with two on-going clinical trials that aim at lowering cardiovascular risks by decreasing the inflammatory pressure. The first one, the Canakinumab Anti-inflammatory Thrombosis Outcomes Study (CANTOS) trial uses a human monoclonal antibody directly targeted at IL-1β; the second one, Cardiovascular Inflammation Reduction Trial (CIRT) uses methotrexate as an anti-inflammatory therapy. Both of these trials are considered pivotal for the field of atherosclerosis research since they will test whether anti-inflammatory therapies can globally decrease the rate of cardiovascular events such as myocardial infarction or stroke. Our modest finding indicts that IL-1β may be valuable target in atheroprone endothelium. Yet, Alexander et al. [132] showed that genetic deletion of IL1 signaling in mice results in increased plaque instability, which underlines the risks associated with manipulating of the inflammatory cascade at this stage of the

pathway. In the light of these findings and in line with the knowledge learned through my mentors, I consider that therapeutic targets against atherosclerosis should be directed at repairing the endothelial phenotype rather than focusing on the downstream secretions of cells. The *in vitro* model developed constitutes an outstanding platform to understand the deleterious interactions between the endothelium, and luminal elements and cells, and find new therapeutic avenues to mitigate atherogenesis.

4 Discussion

This thesis describes the development of a novel in vitro model of monocyte transmigration under defined shear stress relevant to atherogenesis: atheroprone and atheroprotected flow. It also presents data on the accumulation of monocytes and deleterious endothelial:monocyte interactions under atheroprone flow, notably through the upregulation of the potent pro-inflammatory cytokine IL-1β in endothelial cells. The motivation for this work came from the preponderant role of the endothelium as a global regulator of tissue homeostasis and in particular its orchestration of the inflammatory cascade and leukocyte recruitment during atherogenesis. The development of a novel model also responds to the pressing need for a model that accounts for all the canonical components of the atherogenesis triad: the regulator (the endothelium), the effector (the monocytes), and the trigger (aberrant flow). We surmised that endothelial dysfunction, specifically mediated by disturbed flow from atherosusceptible regions of the vasculature, is communicated to recruited monocytes and profoundly impacts their fate and polarization as they reside in the subendothelial matrix. We further hypothesized that the presence of monocytes exacerbates the dysfunctional state of atheroprone endothelium under flow. Globally, this work examined communication between endothelial cell and monocytes in flow-mediated diseased states.

We successfully built and integrated our *in vitro* model to a unique flow apparatus previously developed in the Gimbrone and García-Cardeña laboratories that can precisely replicate any shear stress waveform. The model relies on a fibronectin-coated collagenous matrix seeded with a confluent monolayer of endothelial cells co-cultured with THP-1 monocytes under flow. We sequentially measured the mechanical properties of the matrix and established the profiles of the three key adhesions molecules VCAM-1, ICAM-1 and E-Selectin before and after exposure to flow. Although the different flows did not elicit significant changes in the adhesion molecule landscape of endothelial cells, we observed responsiveness to flow through the morphological changes of the monolayer and differential expression of

endothelial KLF2, which is a critical integrator of flow-mediated vasoprotection. We also showed that our THP-1 monocytes constitute a homogeneous population of "classical" $CD14^{++}$ $CD16^{-}$ monocytes. Observations with confocal microscopy of the transmigration of monocytes under atheroprone and atheroprotective flow constitutes the highlight of the second Chapter and echoes electron micrographs of monocyte transmigration and early differentiation in static conditions.

The third Chapter is dedicated to understanding atherogenesis through the lens of endothelial:monocyte interactions under flow. In our studies, we found that atheroprone but not atheroprotective flow promotes the recruitment and accumulation of clusters of monocytes onto endothelial monolayers. This central finding exquisitely corroborates in vivo data in animal model of atherogenesis. Jongstra-Bilen et al. reported that CD68+ cells aggregate in the lower but not in the upper curvature of the aortic arch [94]. Our immunofluorescence pictures strikingly mirror their observations. Others have found that leukocytes, in particular monocytes' differentiated progeny, the macrophages and the dendritic cells, accumulate in regions of disturbed flow in animals and humans [133, 134], including in young adults [135]. In vitro vascular constructs fed by peristaltic pumps have also been used to show that atherosusceptible endothelium triggers monocyte recruitment [102, 106]. It is difficult to put in perspective our results with the work of Robert et al. since their construct was a straight tube, thus the attributes of flow were not the triggering event to adhesion and transmigrating, instead they used TNF-α or oxidized-LDL to activate the endothelium. It is equally hard to confront our results with Martorell et al. since they compared monocyte adhesion from distinct, yet vast regions of arteries rather than regions of phenotypically-homogeneous cells driven by flow such as atheroprone and atherosusceptible regions. They seeded smooth muscle cells and endothelial cells on polydimethylsiloxane (PDMS) replicas of the parts of the human common carotid bifurcation. The constructs were exposed to flow using peristaltic pumps. Analysis of cells was performed on the three distinct segments of the construct, namely the common (CCA), the external (ECA) and the internal (ICA) branch of the carotid. They

observed a ~1.5-fold increase in monocyte adhesion between the ECA and CCA, and ~2-fold increase between the ICA and CCA. This results is difficult to interpret since atherogenesis only proceed in a narrow region of the base of the ICA, the sinus of the carotid bulb, as well as another confined region of bifurcation, namely the crux of the bifurcation. As shown by Lipinski and colleagues [136] and others [64, 137], the region of atherosusceptibility is narrow. Thus endothelium in regions millimeters away from disturbed flow regions must interact differently with monocytes than atherosusceptible endothelium does. Our model provides a clear advantage on these constructs since flow is quasi-identical throughout the monolayer. Thus, we are not restricted to a meager atheroprone region to conduct biological assays of cells of the atheroprone regions.

We formulated and tested two hypotheses about the interactions of dysfunctional endothelium and monocytes. The first one derives from the established paradigms in vascular biology that postulate that healthy endothelium is vasoprotective while dysfunctional endothelial cells propagates the disease. Along this line of thought, we proposed that diseased endothelium induced by flow signals and disseminates inflammation to the transmigrating monocytes. Disappointingly, we were not able to provide a definitive answer to this question because high variability in the gene expression of THP-1 cells blurred our judgment. Although we could not use primary monocytes during the development phase of this model because of the limited availability of primary monocytes with respect to our needs, and neither could we pinpoint the exact causes of the variability, we believe that intrinsically THP-1 cells may not be suited for experiments that rely on gene expression analyses. An important area of future work is to overcome the variability in gene expression of monocytes in our system and examine the phenotypic modulation of transmigrated monocytes through both athero-protective and -prone endothelium. Now that the development of the model is complete, we believe that using primary blood monocytes is feasible and recommended. We also realized that the M1/M2 paradigm might not be an appropriate framework to reason about the propagation of a disease state from endothelium to monocyte. We reason that macrophage lipid

loading and defective efferocytosis are central to atherogenesis. Thus, we revise our initial hypothesis and suggest to test whether atheroprone endothelium renders transmigrating monocytes susceptible to foam cells transformation and/or become dysfunctional phagocytes, in comparison to cells that transmigrate through atheroprotective endothelium. We surmise that the secretions, surface receptors or even direct delivery of vesicles from dysfunctional endothelium to transmigrating monocytes may condition their propensity to become dysfunctional themselves. This would be best tested through a comparative proteomics study of the atheroprone and atheroprotective endothelium's secretome (under flow) as well as their respective secretome in the presence of monocytes (and flow).

The last part of this work focused on the study of the reverse question: what is the influence of monocyte on atheroprone endothelium? We showed that monocytes exacerbate dysfunction in atheroprone endothelium under flow. We measured a non-statistical upregulation of IL-1β (gene expression) in endothelial cells co-cultured with THP-1 monocytes and exposed to atheroprone flow compared to endothelial cells alone under flow. This process is distinct from the angiogenic [105] or proliferative [103, 104] properties described before. As a result, we suggest that atheroprone flow may be responsible for a potential distinct endothelial:monocyte interaction.

Here, we reflect on the shortcomings of our findings and suggest future axes of research for the continuation of this work. Evidently, much of the inflammatory response of endothelial cells to monocytes remains to be established and explained. Our primary data indicate that although IL-1β is transcribed in all three replicates of endothelial cells in co-cultures compared endothelium alone, we did not detected it in the supernatant of the co-cultures. Thus, the first experiment that we would pursue is to consolidate these data. If confirmed, we speculate that pro-IL-1β accumulates in endothelial cells; therefore we propose to measure the presence of pro-IL-1β in atheroprone endothelium exposed to monocytes and flow. Macrophages can engulf cholesterol crystals present in early atherogenic lesions

and activates the NLRP3 inflammasome [119] due to lyosomal damage during degradation of the crystals. Similarly, several groups have reported the activation of the inflammasome in the endothelial cells, through IL-18 secretion in lupus erythematosus [138], caused by hemorrhage shock in lung EC [139] or following acetaminophen-induced liver injury in sinusoidal endothelium [140]. In addition, Liu et al. [141] showed that silica particles elicit an inflammatory response in endothelial:monocyte cultures via the NF-κB pathway. We propose to assess the activity of the inflammasome in atheroprone endothelium in our model seeded with cholesterol crystals in the matrix. We anticipate that endothelial cells would be stimulated by their atherosusceptible milieu and their inflammasome activated.

We are particularly intrigued by the transfer of microparticles and macromolecules during monocyte transmigration and consider that the potential increase in membrane porosity is a great avenue for the exchanges of cytosolic elements between endothelial cells and monocytes. Diapedesis consists of monocytes "squeezing" through the endothelium to enter the vascular tissue, either between of through the endothelial cells themselves. It is already known that a rapid mechanical deformation of the cell's membrane is traumatic and produces transient pores at its surface [142]. We posit that endothelial molecules shuttled by diffusion inside the monocytes could affect the activation state of the monocytes. We also put this hypothesis in perspective with the updated cascade of transmigration proposed by Dr. William Müller, who introduced the concept of Lateral Border Compartment Recycling (LBRC) [143]. Platelet Endothelial Cell Adhesion Molecule (PECAM)-enriched vesicles create guiding channels for leukocytes throughout transendothelial migration. In our view, the recycling of junctional molecules during transmigration may exceed the simple creation of a passageway for the leukocyte, but also foster the transfer of endothelial molecules.

Another avenue that we have begun to explore but still constitutes an interesting axis for future research is the EMT. We have probed the expression of SNAI1 and VIM – overexpressed during EMT – in our system, in endothelium exposed to atheroprone flow and co-cultures exposed to flow too, but we did not find

significant differences. In 2012, Chen et al. [144] from the Simons laboratory, showed that the transplantation of a human segment of coronary artery into the aorta of immunodeficient mice receiving injections of primary blood mononuclear cells to induce rejection of the graft, showed extensive expression of the smooth muscle cell marker, Notch3, in neointimal endothelial cells. They went on to show how inflammation, especially IL-1β-mediated, caused the suppression of Fibroblast Growth Factor (FGF) signaling and in turn the reduction of let-7 miRNA, activation of the TGF-β signaling and finally the induction of EMT, as evidenced by mesenchymal markers on endothelial cells. This groundbreaking finding is tied to our study in two different ways. First, we speculate that IL-1β may be upregulated at the mRNA level in endothelial cells co-cultured with monocytes exposed to atheroprone flow. Thus if a stimulus from the atherosusceptible milieu, such as cholesterol crystals, were to activate the inflammasome in endothelial cells and IL-1β was upregulated at the transcription level, then IL-1β protein would potentially be secreted and could stimulate EMT. Regardless, of whether it is secreted by the endothelium, the monocytes or the mixture of M1/M2 macrophages present in nascent lesion [145-147], IL-1β is present in atherosclerotic lesions [148]. Second, let-7, the miRNA responsible for increase TGF-β ligands and receptor and ultimately EMT, is upregulated by atheroprone but not atheroprotective flow [81]. Thus atheroprone endothelium, which expresses high levels of KLF2, may be protected from EMT, but not atheroprone endothelium. Therefore, we surmise that monocytes and endothelial cells co-cultures under prone but not protective flow in the presence of an endothelial inflammasome inducer such as cholesterol crystals, may display characteristics of EMT.

Given the long-lasting interest of our laboratories in the biology of KLF2, its anti-inflammatory properties and its induction of let-7 [81], we suggest gain and loss of function experiments for both the recruitment of monocytes and potential EMT. We anticipate that endothelial KLF2 expression curtails the recruitment of monocytes and inhibits EMT through the induction of let-7. We propose to induce the expression of KLF2 in endothelial cells under atheroprone flow via adenoviral-

mediated transduction, or repress KLF2 expression using shRNA in endothelium exposed to atheroprotective flow. These "pre-conditioned cells" will be co-cultured with monocytes under flow. Although, we predict that endothelial cells transduced with KLF2 and exposed to prone flow will be partially protected to monocyte accumulation, we do not foresee that the loss of KLF2 would increase the monocyte recruitment. We support this view in light our data that did not show changes in the expression of adhesion molecule flowing priming with flow. We think that in this case, high hemodynamic forces prevail on the adhesion properties of the endothelial surface. For EMT, although we believe that these experiment are worth performing, we cannot formulate speculations without further data.

Lastly, we hope that this model can be used to identify new molecular pathways involved in interactions between the endothelium and the monocytes under flow that are relevant to atherogenesis and pave the way to the testing and discovery of novel therapeutic strategies to curb the pathogenesis of atherosclerosis.

5 References

1. Carmeliet, P. and R.K. Jain, *Angiogenesis in cancer and other diseases.* Nature, 2000. **407**(6801): p. 249-57.
2. Rouwkema, J., N.C. Rivron, and C.A. van Blitterswijk, *Vascularization in tissue engineering.* Trends Biotechnol, 2008. **26**(8): p. 434-41.
3. Bergman, R.A. and A.K. Afifi, *Atlas of microscopic anatomy; a companion to histology and neuroanatomy.* 1974, Philadelphia,: Saunders. vi, 426 p.
4. Bathe, K.-J. and K.-J. Bathe, *Finite element procedures.* New ed. 2006, S.l.: s.n. xiv, 1037 p.
5. Kim, S., et al., *Determination of rheological properties of whole blood with a scanning capillary-tube rheometer using constitutive models.* Journal of Mechanical Science and Technology, 2009. **23**(6): p. 1718-1726.
6. Basombrio, F.G., et al., *Numerical experiments in complex haemodynamic flows. Non-Newtonian effects.* International Journal of Computational Fluid Dynamics, 2002. **16**(4): p. 231-246.
7. Suo, J., et al., *Hemodynamic shear stresses in mouse aortas: implications for atherogenesis.* Arterioscler Thromb Vasc Biol, 2007. **27**(2): p. 346-51.
8. Dai, G., et al., *Distinct endothelial phenotypes evoked by arterial waveforms derived from atherosclerosis-susceptible and -resistant regions of human vasculature.* Proc Natl Acad Sci U S A, 2004. **101**(41): p. 14871-6.
9. Moncada, S., A. Higgs, and SpringerLink (Online service), *The vascular endothelium. I,* in *Handbook of experimental pharmacology,*. 2006, Springer,: Berlin ; New York. p. viii, 339 p.
10. Campbell, G.J. and M.R. Roach, *Fenestrations in the internal elastic lamina at bifurcations of human cerebral arteries.* Stroke, 1981. **12**(4): p. 489-96.
11. Cunningham, K.S. and A.I. Gotlieb, *The role of shear stress in the pathogenesis of atherosclerosis.* Lab Invest, 2005. **85**(1): p. 9-23.
12. Pries, A.R., T.W. Secomb, and P. Gaehtgens, *The endothelial surface layer.* Pflugers Arch, 2000. **440**(5): p. 653-66.
13. Florey, *The endothelial cell.* Br Med J, 1966. **2**(5512): p. 487-90.
14. Jaffe, E.A., et al., *Culture of human endothelial cells derived from umbilical veins. Identification by morphologic and immunologic criteria.* J Clin Invest, 1973. **52**(11): p. 2745-56.
15. Gimbrone, M.A., Jr., R.S. Cotran, and J. Folkman, *Endothelial regeneration: studies with human endothelial cells in culture.* Ser Haematol, 1973. **6**(4): p. 453-5.
16. Aird, W.C., *Endothelial biomedicine.* 2007, Cambridge ; New York: Cambridge University Press. xl, 1856 p., 24 p. of plates.
17. Aird, W.C., *Endothelial cell heterogeneity.* Cold Spring Harb Perspect Med, 2012. **2**(1): p. a006429.
18. Starling, E.H., *On the Absorption of Fluids from the Connective Tissue Spaces.* J Physiol, 1896. **19**(4): p. 312-26.

19. Pappenheimer, J.R., *Passage of molecules through capillary wals.* Physiol Rev, 1953. **33**(3): p. 387-423.
20. Graham, R.C., Jr. and M.J. Karnovsky, *The early stages of absorption of injected horseradish peroxidase in the proximal tubules of mouse kidney: ultrastructural cytochemistry by a new technique.* J Histochem Cytochem, 1966. **14**(4): p. 291-302.
21. Karnovsky, M.J., *The Localization of Cholinesterase Activity in Rat Cardiac Muscle by Electron Microscopy.* J Cell Biol, 1964. **23**: p. 217-32.
22. Fukuhara, S., et al., *Cyclic AMP potentiates vascular endothelial cadherin-mediated cell-cell contact to enhance endothelial barrier function through an Epac-Rap1 signaling pathway.* Mol Cell Biol, 2005. **25**(1): p. 136-46.
23. Gimbrone, M.A., Jr. and R.W. Alexander, *Angiotensin II stimulation of prostaglandin production in cultured human vascular endothelium.* Science, 1975. **189**(4198): p. 219-20.
24. Moncada, S., et al., *An enzyme isolated from arteries transforms prostaglandin endoperoxides to an unstable substance that inhibits platelet aggregation.* Nature, 1976. **263**(5579): p. 663-5.
25. Moncada, S., J.R. Vane, and B.J. Whittle, *Relative potency of prostacyclin, prostaglandin E1 and D2 as inhibitors of platelet aggregation in several species [proceedings].* J Physiol, 1977. **273**(2): p. 2P-4P.
26. Furchgott, R.F. and J.V. Zawadzki, *The obligatory role of endothelial cells in the relaxation of arterial smooth muscle by acetylcholine.* Nature, 1980. **288**(5789): p. 373-6.
27. Palmer, R.M., A.G. Ferrige, and S. Moncada, *Nitric oxide release accounts for the biological activity of endothelium-derived relaxing factor.* Nature, 1987. **327**(6122): p. 524-6.
28. Palmer, R.M., D.S. Ashton, and S. Moncada, *Vascular endothelial cells synthesize nitric oxide from L-arginine.* Nature, 1988. **333**(6174): p. 664-6.
29. Valentijn, K.M. and J. Eikenboom, *Weibel-Palade bodies: a window to von Willebrand disease.* J Thromb Haemost, 2013. **11**(4): p. 581-92.
30. Carmeliet, P. and R.K. Jain, *Molecular mechanisms and clinical applications of angiogenesis.* Nature, 2011. **473**(7347): p. 298-307.
31. Pober, J.S. and W.C. Sessa, *Evolving functions of endothelial cells in inflammation.* Nat Rev Immunol, 2007. **7**(10): p. 803-15.
32. Libby, P., *Inflammation in atherosclerosis.* Nature, 2002. **420**(6917): p. 868-74.
33. Kleemann, R., S. Zadelaar, and T. Kooistra, *Cytokines and atherosclerosis: a comprehensive review of studies in mice.* Cardiovasc Res, 2008. **79**(3): p. 360-76.
34. Ley, K., et al., *Getting to the site of inflammation: the leukocyte adhesion cascade updated.* Nat Rev Immunol, 2007. **7**(9): p. 678-89.
35. Chen, C.S., et al., *Geometric control of cell life and death.* Science, 1997. **276**(5317): p. 1425-8.
36. Geiger, B. and A. Bershadsky, *Exploring the neighborhood: adhesion-coupled cell mechanosensors.* Cell, 2002. **110**(2): p. 139-42.

37. Nerem, R.M., et al., *Hemodynamics and vascular endothelial biology.* J Cardiovasc Pharmacol, 1993. **21 Suppl 1**: p. S6-10.
38. Burridge, K. and M. Chrzanowska-Wodnicka, *Focal adhesions, contractility, and signaling.* Annu Rev Cell Dev Biol, 1996. **12**: p. 463-518.
39. Wang, N., J.D. Tytell, and D.E. Ingber, *Mechanotransduction at a distance: mechanically coupling the extracellular matrix with the nucleus.* Nat Rev Mol Cell Biol, 2009. **10**(1): p. 75-82.
40. Takeichi, M., *The cadherins: cell-cell adhesion molecules controlling animal morphogenesis.* Development, 1988. **102**(4): p. 639-55.
41. Brown, A.E. and D.E. Discher, *Conformational changes and signaling in cell and matrix physics.* Curr Biol, 2009. **19**(17): p. R781-9.
42. Discher, D.E., P. Janmey, and Y.L. Wang, *Tissue cells feel and respond to the stiffness of their substrate.* Science, 2005. **310**(5751): p. 1139-43.
43. Olesen, S.P., D.E. Clapham, and P.F. Davies, *Haemodynamic shear stress activates a K+ current in vascular endothelial cells.* Nature, 1988. **331**(6152): p. 168-70.
44. Tzima, E., et al., *Activation of integrins in endothelial cells by fluid shear stress mediates Rho-dependent cytoskeletal alignment.* EMBO J, 2001. **20**(17): p. 4639-47.
45. Tzima, E., et al., *A mechanosensory complex that mediates the endothelial cell response to fluid shear stress.* Nature, 2005. **437**(7057): p. 426-31.
46. Chachisvilis, M., Y.L. Zhang, and J.A. Frangos, *G protein-coupled receptors sense fluid shear stress in endothelial cells.* Proc Natl Acad Sci U S A, 2006. **103**(42): p. 15463-8.
47. Weinbaum, S., J.M. Tarbell, and E.R. Damiano, *The structure and function of the endothelial glycocalyx layer.* Annu Rev Biomed Eng, 2007. **9**: p. 121-67.
48. Davies, P.F., *Flow-mediated endothelial mechanotransduction.* Physiol Rev, 1995. **75**(3): p. 519-60.
49. Lopez, A.D., et al., *Global and regional burden of disease and risk factors, 2001: systematic analysis of population health data.* Lancet, 2006. **367**(9524): p. 1747-57.
50. Davies, M.J., *Anatomic features in victims of sudden coronary death. Coronary artery pathology.* Circulation, 1992. **85**(1 Suppl): p. I19-24.
51. Davies, M.J. and A.C. Thomas, *Plaque fissuring--the cause of acute myocardial infarction, sudden ischaemic death, and crescendo angina.* Br Heart J, 1985. **53**(4): p. 363-73.
52. Feigin, V.L., et al., *Stroke epidemiology: a review of population-based studies of incidence, prevalence, and case-fatality in the late 20th century.* Lancet Neurol, 2003. **2**(1): p. 43-53.
53. Go, A.S., et al., *Heart disease and stroke statistics--2014 update: a report from the American Heart Association.* Circulation, 2014. **129**(3): p. e28-e292.
54. Go, A.S., et al., *Executive summary: heart disease and stroke statistics--2014 update: a report from the American Heart Association.* Circulation, 2014. **129**(3): p. 399-410.

55. Rayer, P., *Mémoire sur l'ossification morbide , considérée comme une terminaison des phlegmasies.* Archives Générales de Médecine. Vol. Tome I. 1823, Paris, France.
56. Virchow, R., *Thrombose und Embolie. Gefässentzündung und septische Infektion.* Gesammelte Abhandlungen zur wissenschaftlichen Medicin. Vol. 8. 1856, Frankfurt, Germany: Verlag von Meidinger Sohn & Comp.
57. Brotman, D.J., et al., *Virchow's triad revisited.* South Med J, 2004. **97**(2): p. 213-4.
58. Virchow, R., *Cellular pathology as based upon physiological and pathological histology : twenty lectures delivered in the Pathological Institute of Berlin during the months of February, March and April, 1858.* 1860, New York, USA: Robert M. De Witt.
59. Anitschkow, N., *Über die Veränderungen der Kaninchenaorta bei experimenteller Cholesterinsteatose.* Beitr Pathol Anat, 1913. **56**: p. 379-404.
60. Anitschkow, N. and S. Chatalov, *Über experimentelle Cholesterinsteatose und ihre Bedeutung für die Entstehung einiger pathologischer Prozesse.* Zentralbl Allg Pathol 1913. **24**: p. 1-9.
61. Galkina, E. and K. Ley, *Immune and inflammatory mechanisms of atherosclerosis (*).* Annu Rev Immunol, 2009. **27**: p. 165-97.
62. Hansson, G.K. and P. Libby, *The immune response in atherosclerosis: a double-edged sword.* Nat Rev Immunol, 2006. **6**(7): p. 508-19.
63. Gimbrone, M.A., Jr. and G. Garcia-Cardena, *Vascular endothelium, hemodynamics, and the pathobiology of atherosclerosis.* Cardiovasc Pathol, 2013. **22**(1): p. 9-15.
64. Won, D., et al., *Relative reduction of endothelial nitric-oxide synthase expression and transcription in atherosclerosis-prone regions of the mouse aorta and in an in vitro model of disturbed flow.* Am J Pathol, 2007. **171**(5): p. 1691-704.
65. Duguid, J.B. and W.B. Robertson, *Mechanical factors in atherosclerosis.* Lancet, 1957. **272**(6981): p. 1205-9.
66. Fry, D.L., *Acute vascular endothelial changes associated with increased blood velocity gradients.* Circ Res, 1968. **22**(2): p. 165-97.
67. Fox, J.A. and A.E. Hugh, *Localization of atheroma: a theory based on boundary layer separation.* Br Heart J, 1966. **28**(3): p. 388-99.
68. Caro, C.G., J.M. Fitz-Gerald, and R.C. Schroter, *Arterial wall shear and distribution of early atheroma in man.* Nature, 1969. **223**(5211): p. 1159-60.
69. Orr, A.W., et al., *The subendothelial extracellular matrix modulates NF-kappaB activation by flow: a potential role in atherosclerosis.* J Cell Biol, 2005. **169**(1): p. 191-202.
70. Bell, F.P., A.S. Gallus, and C.J. Schwartz, *Focal and regional patterns of uptake and the transmural distribution of 131-I-fibrinogen in the pig aorta in vivo.* Exp Mol Pathol, 1974. **20**(2): p. 281-92.
71. Ross, R. and L. Harker, *Hyperlipidemia and atherosclerosis.* Science, 1976. **193**(4258): p. 1094-100.
72. Moore, K.J. and I. Tabas, *Macrophages in the pathogenesis of atherosclerosis.* Cell, 2011. **145**(3): p. 341-55.

73. Akira, S., S. Uematsu, and O. Takeuchi, *Pathogen recognition and innate immunity.* Cell, 2006. **124**(4): p. 783-801.
74. Hajra, L., et al., *The NF-kappa B signal transduction pathway in aortic endothelial cells is primed for activation in regions predisposed to atherosclerotic lesion formation.* Proc Natl Acad Sci U S A, 2000. **97**(16): p. 9052-7.
75. Mullick, A.E., et al., *Increased endothelial expression of Toll-like receptor 2 at sites of disturbed blood flow exacerbates early atherogenic events.* J Exp Med, 2008. **205**(2): p. 373-83.
76. Goode, T.B., et al., *Aortic endothelial cell morphology observed in situ by scanning electron microscopy during atherogenesis in the rabbit.* Atherosclerosis, 1977. **27**(2): p. 235-51.
77. Collins, T. and M.I. Cybulsky, *NF-kappaB: pivotal mediator or innocent bystander in atherogenesis?* J Clin Invest, 2001. **107**(3): p. 255-64.
78. Civelek, M., et al., *Chronic endoplasmic reticulum stress activates unfolded protein response in arterial endothelium in regions of susceptibility to atherosclerosis.* Circ Res, 2009. **105**(5): p. 453-61.
79. Zhou, A.X. and I. Tabas, *The UPR in atherosclerosis.* Semin Immunopathol, 2013. **35**(3): p. 321-32.
80. Wu, W., et al., *Flow-Dependent Regulation of Kruppel-Like Factor 2 Is Mediated by MicroRNA-92a.* Circulation, 2011. **124**(5): p. 633-41.
81. Marin, T., et al., *Mechanosensitive microRNAs-role in endothelial responses to shear stress and redox state.* Free Radic Biol Med, 2013. **64**: p. 61-8.
82. Lovren, F. and S. Verma, *Evolving role of microparticles in the pathophysiology of endothelial dysfunction.* Clin Chem, 2013. **59**(8): p. 1166-74.
83. Kumar, S., et al., *Role of Flow-Sensitive microRNAs in Endothelial Dysfunction and Atherosclerosis: Mechanosensitive Athero-miRs.* Arterioscler Thromb Vasc Biol, 2014.
84. Sun, X., N. Belkin, and M.W. Feinberg, *Endothelial microRNAs and atherosclerosis.* Curr Atheroscler Rep, 2013. **15**(12): p. 372.
85. Vion, A.C., et al., *Shear stress regulates endothelial microparticle release.* Circ Res, 2013. **112**(10): p. 1323-33.
86. Hergenreider, E., et al., *Atheroprotective communication between endothelial cells and smooth muscle cells through miRNAs.* Nat Cell Biol, 2012. **14**(3): p. 249-56.
87. Feaver, R.E., B.D. Gelfand, and B.R. Blackman, *Human haemodynamic frequency harmonics regulate the inflammatory phenotype of vascular endothelial cells.* Nat Commun, 2013. **4**: p. 1525.
88. Choy, J.S., et al., *Endothelial actin depolymerization mediates NADPH oxidase-superoxide production during flow reversal.* Am J Physiol Heart Circ Physiol, 2014. **306**(1): p. H69-77.
89. Xiao, H., et al., *Sterol regulatory element binding protein 2 activation of NLRP3 inflammasome in endothelium mediates hemodynamic-induced atherosclerosis susceptibility.* Circulation, 2013. **128**(6): p. 632-42.
90. Koo, A., C.F. Dewey, Jr., and G. Garcia-Cardena, *Hemodynamic shear stress characteristic of atherosclerosis-resistant regions promotes glycocalyx*

formation in cultured endothelial cells. Am J Physiol Cell Physiol, 2013. **304**(2): p. C137-46.
91. Swirski, F.K., et al., *Identification of splenic reservoir monocytes and their deployment to inflammatory sites.* Science, 2009. **325**(5940): p. 612-6.
92. Ziegler-Heitbrock, L., et al., *Nomenclature of monocytes and dendritic cells in blood.* Blood, 2010. **116**(16): p. e74-80.
93. Cros, J., et al., *Human CD14dim monocytes patrol and sense nucleic acids and viruses via TLR7 and TLR8 receptors.* Immunity, 2010. **33**(3): p. 375-86.
94. Jongstra-Bilen, J., et al., *Low-grade chronic inflammation in regions of the normal mouse arterial intima predisposed to atherosclerosis.* J Exp Med, 2006. **203**(9): p. 2073-83.
95. Cybulsky, M.I. and M.A. Gimbrone, Jr., *Endothelial expression of a mononuclear leukocyte adhesion molecule during atherogenesis.* Science, 1991. **251**(4995): p. 788-91.
96. Lawrence, T. and G. Natoli, *Transcriptional regulation of macrophage polarization: enabling diversity with identity.* Nat Rev Immunol, 2011. **11**(11): p. 750-61.
97. Mosser, D.M. and J.P. Edwards, *Exploring the full spectrum of macrophage activation.* Nat Rev Immunol, 2008. **8**(12): p. 958-69.
98. Beesley, J.E., et al., *Interaction of leukocytes with vascular cells in culture.* J Cell Sci, 1978. **33**: p. 85-101.
99. DiCorleto, P.E. and C.A. de la Motte, *Characterization of the adhesion of the human monocytic cell line U937 to cultured endothelial cells.* J Clin Invest, 1985. **75**(4): p. 1153-61.
100. Randolph, G.J., et al., *Differentiation of monocytes into dendritic cells in a model of transendothelial trafficking.* Science, 1998. **282**(5388): p. 480-3.
101. Gerszten, R.E., et al., *MCP-1 and IL-8 trigger firm adhesion of monocytes to vascular endothelium under flow conditions.* Nature, 1999. **398**(6729): p. 718-23.
102. Martorell, J., et al., *Extent of flow recirculation governs expression of atherosclerotic and thrombotic biomarkers in arterial bifurcations.* Cardiovasc Res, 2014. **103**(1): p. 37-46.
103. Polverini, P.J., et al., *Activated macrophages induce vascular proliferation.* Nature, 1977. **269**(5631): p. 804-6.
104. Schubert, S.Y., et al., *Monocyte activation state regulates monocyte-induced endothelial proliferation through Met signaling.* Blood, 2010. **115**(16): p. 3407-12.
105. Baer, C., et al., *Reciprocal interactions between endothelial cells and macrophages in angiogenic vascular niches.* Exp Cell Res, 2013.
106. Robert, J., et al., *A three-dimensional engineered artery model for in vitro atherosclerosis research.* PLoS One, 2013. **8**(11): p. e79821.
107. McDonald, D.A., *Blood flow in arteries.* Physiological Society Monograph,. 1960, London: Edward Arnold. x, 328 p.
108. Dewey, C.F., Jr., et al., *The dynamic response of vascular endothelial cells to fluid shear stress.* J Biomech Eng, 1981. **103**(3): p. 177-85.

109. Takaku, M., et al., *An in vitro coculture model of transmigrant monocytes and foam cell formation.* Arterioscler Thromb Vasc Biol, 1999. **19**(10): p. 2330-9.
110. Buton, X., et al., *Unique cellular events occurring during the initial interaction of macrophages with matrix-retained or methylated aggregated low density lipoprotein (LDL). Prolonged cell-surface contact during which ldl-cholesteryl ester hydrolysis exceeds ldl protein degradation.* J Biol Chem, 1999. **274**(45): p. 32112-21.
111. Shyy, Y.J., et al., *Fluid shear stress induces a biphasic response of human monocyte chemotactic protein 1 gene expression in vascular endothelium.* Proc Natl Acad Sci U S A, 1994. **91**(11): p. 4678-82.
112. Parmar, K.M., et al., *Integration of flow-dependent endothelial phenotypes by Kruppel-like factor 2.* J Clin Invest, 2006. **116**(1): p. 49-58.
113. Hudnall, S.D., *Hematology a pathophysiologic approach,* in *The Mosby physiology monograph series.* 2012, Mosby/Elsevier,: Philadelphia, Pa. p. 1 online resource (xiii, 171 p., 32 p.
114. Langstein, J., J. Michel, and H. Schwarz, *CD137 induces proliferation and endomitosis in monocytes.* Blood, 1999. **94**(9): p. 3161-8.
115. Suzuki, T., et al., *Comprehensive gene expression profile of LPS-stimulated human monocytes by SAGE.* Blood, 2000. **96**(7): p. 2584-91.
116. Auffray, C., M.H. Sieweke, and F. Geissmann, *Blood monocytes: development, heterogeneity, and relationship with dendritic cells.* Annu Rev Immunol, 2009. **27**: p. 669-92.
117. Tsuchiya, S., et al., *Establishment and characterization of a human acute monocytic leukemia cell line (THP-1).* Int J Cancer, 1980. **26**(2): p. 171-6.
118. Qin, Z., *The use of THP-1 cells as a model for mimicking the function and regulation of monocytes and macrophages in the vasculature.* Atherosclerosis, 2012. **221**(1): p. 2-11.
119. Duewell, P., et al., *NLRP3 inflammasomes are required for atherogenesis and activated by cholesterol crystals.* Nature, 2010. **464**(7293): p. 1357-61.
120. Gerrity, R.G., *The role of the monocyte in atherogenesis: I. Transition of blood-borne monocytes into foam cells in fatty lesions.* Am J Pathol, 1981. **103**(2): p. 181-90.
121. Boring, L., et al., *Decreased lesion formation in CCR2-/- mice reveals a role for chemokines in the initiation of atherosclerosis.* Nature, 1998. **394**(6696): p. 894-7.
122. Takahashi, M., et al., *Human monocyte-endothelial cell interaction induces synthesis of granulocyte-macrophage colony-stimulating factor.* Circulation, 1996. **93**(6): p. 1185-93.
123. Combe, C., et al., *Induction of intercellular adhesion molecule-1 by monocyte adhesion to endothelial cells in human culture system.* J Cell Physiol, 1995. **164**(2): p. 295-303.
124. Ikeda, U., M. Takahashi, and K. Shimada, *Monocyte-endothelial cell interaction in atherogenesis and thrombosis.* Clin Cardiol, 1998. **21**(1): p. 11-4.
125. Zhang, Y., et al., *Secreted monocytic miR-150 enhances targeted endothelial cell migration.* Mol Cell, 2010. **39**(1): p. 133-44.

126. Schwartz, C.J., et al., *Aortic intimal monocyte recruitment in the normo and hypercholesterolemic baboon (Papio cynocephalus). An ultrastructural study: implications in atherogenesis.* Virchows Arch A Pathol Anat Histopathol, 1985. **405**(2): p. 175-91.
127. Walker, L.N., M.A. Reidy, and D.E. Bowyer, *Morphology and cell kinetics of fatty streak lesion formation in the hypercholesterolemic rabbit.* Am J Pathol, 1986. **125**(3): p. 450-9.
128. Swirski, F.K., et al., *Monocyte accumulation in mouse atherogenesis is progressive and proportional to extent of disease.* Proc Natl Acad Sci U S A, 2006. **103**(27): p. 10340-5.
129. Chappell, D.C., et al., *Oscillatory shear stress stimulates adhesion molecule expression in cultured human endothelium.* Circ Res, 1998. **82**(5): p. 532-9.
130. Hsiai, T.K., et al., *Monocyte recruitment to endothelial cells in response to oscillatory shear stress.* FASEB J, 2003. **17**(12): p. 1648-57.
131. Conway, D.E., et al., *Endothelial cell responses to atheroprone flow are driven by two separate flow components: low time-average shear stress and fluid flow reversal.* Am J Physiol Heart Circ Physiol, 2010. **298**(2): p. H367-74.
132. Alexander, M.R., et al., *Genetic inactivation of IL-1 signaling enhances atherosclerotic plaque instability and reduces outward vessel remodeling in advanced atherosclerosis in mice.* J Clin Invest, 2012. **122**(1): p. 70-9.
133. Bobryshev, Y.V. and R.S. Lord, *Ultrastructural recognition of cells with dendritic cell morphology in human aortic intima. Contacting interactions of Vascular Dendritic Cells in athero-resistant and athero-prone areas of the normal aorta.* Arch Histol Cytol, 1995. **58**(3): p. 307-22.
134. Millonig, G., et al., *Network of vascular-associated dendritic cells in intima of healthy young individuals.* Arterioscler Thromb Vasc Biol, 2001. **21**(4): p. 503-8.
135. Millonig, G., G.T. Malcom, and G. Wick, *Early inflammatory-immunological lesions in juvenile atherosclerosis from the Pathobiological Determinants of Atherosclerosis in Youth (PDAY)-study.* Atherosclerosis, 2002. **160**(2): p. 441-8.
136. Lipinski, M.J., et al., *Technology insight: targeting of biological molecules for evaluation of high-risk atherosclerotic plaques with magnetic resonance imaging.* Nat Clin Pract Cardiovasc Med, 2004. **1**(1): p. 48-55.
137. Caro, C.G., *Discovery of the role of wall shear in atherosclerosis.* Arterioscler Thromb Vasc Biol, 2009. **29**(2): p. 158-61.
138. Kahlenberg, J.M., et al., *Inflammasome activation of IL-18 results in endothelial progenitor cell dysfunction in systemic lupus erythematosus.* J Immunol, 2011. **187**(11): p. 6143-56.
139. Xiang, M., et al., *Hemorrhagic shock activation of NLRP3 inflammasome in lung endothelial cells.* J Immunol, 2011. **187**(9): p. 4809-17.
140. Imaeda, A.B., et al., *Acetaminophen-induced hepatotoxicity in mice is dependent on Tlr9 and the Nalp3 inflammasome.* J Clin Invest, 2009. **119**(2): p. 305-14.

141. Liu, X., et al., *Enhancement of proinflammatory and procoagulant responses to silica particles by monocyte-endothelial cell interactions.* Part Fibre Toxicol, 2012. **9**: p. 36.
142. Sharei, A., et al., *A vector-free microfluidic platform for intracellular delivery.* Proc Natl Acad Sci U S A, 2013. **110**(6): p. 2082-7.
143. Muller, W.A., *Mechanisms of leukocyte transendothelial migration.* Annu Rev Pathol, 2011. **6**: p. 323-44.
144. Chen, P.Y., et al., *FGF regulates TGF-beta signaling and endothelial-to-mesenchymal transition via control of let-7 miRNA expression.* Cell Rep, 2012. **2**(6): p. 1684-96.
145. Khallou-Laschet, J., et al., *Macrophage plasticity in experimental atherosclerosis.* PLoS One, 2010. **5**(1): p. e8852.
146. Stoger, J.L., et al., *Distribution of macrophage polarization markers in human atherosclerosis.* Atherosclerosis, 2012. **225**(2): p. 461-8.
147. da Rocha, R.F., M.A. De Bastiani, and F. Klamt, *Bioinformatics Approach to Evaluate Differential Gene Expression of M1/M2 Macrophage Phenotypes and Antioxidant Genes in Atherosclerosis.* Cell Biochem Biophys, 2014.
148. Sheedy, F.J. and K.J. Moore, *IL-1 signaling in atherosclerosis: sibling rivalry.* Nat Immunol, 2013. **14**(10): p. 1030-2.